# Politecnico di Torino

Master's Degree Course in Mechanical Engineering

# Assessment and Analysis of Accidental and Ultimate Load Cases in the Design of Floating Offshore Wind Turbines

*Supervisor:*
Giuseppe Giorgi
Massimo Sirigu
Markel Penalba
Giovanni Bracco

*Candidate:*
Mauro Scalera

A.Y.2023/2024

# Abstract

Wind energy is increasingly becoming one of the most viable renewable energy sources. Recent developments have focused on offshore wind turbines, positioning them farther from the coast to access higher-quality wind resources with a reduced environmental footprint. However, as the distance from the shore increases, so does the sea depth, making fixed foundation installations prohibitively expensive. This challenge has led to the innovation of floating wind turbines.

Faults in wind turbines can emerge in various components, such as the pitch control system, gearbox, or electrical generator, among others. Existing mathematical models typically focus either on predicting dynamic behavior and energy generation under normal operating conditions or on analyzing faults and reliability issues. Yet, the dynamic behavior and energy generation potential of wind turbines are intricately connected to faults and reliability factors.

Therefore, the development of a health-informed mathematical model that can predict both energy generation during fault conditions and the degradation of specific components due to dynamic forces is of significant value.

This research focuses on a coupled, non-linear aero-hydro-servo-elastic mathematical model applied to two distinct floating offshore wind turbines: the IEA 15 MW offshore reference turbine and the NREL 5 MW reference turbine. Multiple fault scenarios are deliberately incorporated into this model, which is evaluated across a wide spectrum of environmental conditions using correlated wind and wave data from a defined location.

Firstly, an overview of global wind energy trends, with a particular focus on floating offshore wind, is provided. Recent trends and future projections are examined in the first chapter. The thesis then proceeds with a comprehensive literature review of the current "state of the art" in the second chapter.

Following the theoretical foundations, the third chapter introduces the two wind turbine systems alongside their respective platforms, leading into the methodology used in the research, which is outlined in the fourth chapter.

In the subsequent chapter, environmental conditions and failure scenarios are discussed to simulate a realistic power generation scenario at a specific site. These simulations are conducted using OpenFAST, a simulation tool.

This project aims to explore both accidental loads, caused by unexpected events or

accidents, and ultimate loads, which arise from extreme environmental conditions or rare occurrences. Simulation results focus on key variables, including maximum, minimum, and standard deviation values.

The impact of different failures is then assessed, and the final annual energy production is estimated based on failure statistics. These results are compared to ideal scenarios without failures. The thesis concludes by presenting the final findings and discussing the implications of the results.

# Contents

# List of Figures

# List of Tables

# Chapter 1

# Introduction to the offshore wind energy

The continuous expansion of the global population, along with human progress and the research of better living conditions, has contributed to a significant rise in global energy consumption over recent decades. The massive use of fossil fuels has given rise to numerous challenges, including climate change, air pollution, and the depletion of the Earth's natural resources.

As a result, it is crucial to explore renewable energy technologies that can fulfill the world's energy requirements in a sustainable way. Among these, wind energy seems one of the most promising options, due to its availability worldwide and its potential to meet human energy demands.

## 1.1 Wind energy overlook

Wind energy is the most advanced and developed among renewable energy sources. It has been used since ancient times to propel sailing vessels and operate windmills, utilizing the kinetic energy of air currents through rotating blades. Since the early 20th century, this same principle has been applied to electricity generation through wind turbines.

In these turbines, the rotor blades, driven by the wind, make a central shaft rotate. This rotational motion is transmitted through a gearbox to an electrical generator, which is connected to the power grid. Wind turbines exist in various designs, including vertical and horizontal axes, with different numbers of blades. However, the most commonly adopted configuration is the horizontal-axis turbine with three blades. Based on their location, wind turbines can be located either onshore or offshore [8].
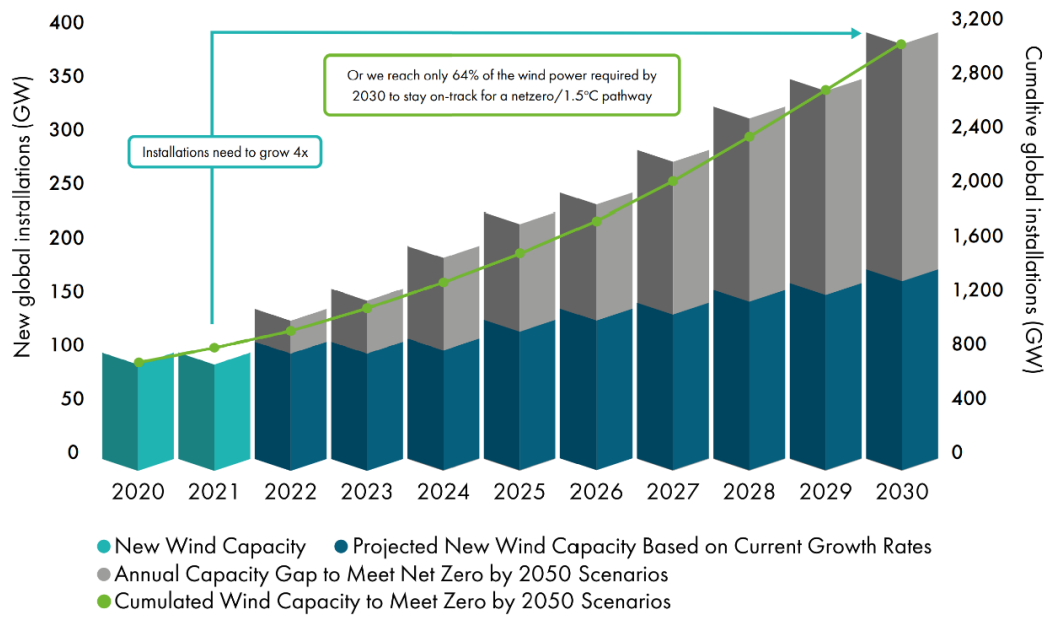
Figure 1.1: New worldwide wind capacity predictions(2020-2023)[1]

In 2022, Europe saw a total of 19.1 GW of new wind power installations, with 16.7 GW coming from onshore projects and 2.5 GW from offshore projects. Despite the economic challenges and supply chain disruptions, this was a record year for wind installations in Europe, reflecting a 4% increase compared to the previous year. However, this number was 12% lower than the realistic expectations from 2021 and fell short of the pace required to meet Europe's climate and energy targets.

To reach the EU's goal of 45% renewable energy by 2030, annual wind energy installations must average 31 GW between 2023 and 2030. This is based on a target of achieving a total wind power capacity of 440 GW.

Germany was the European leader in wind farm installations in 2022, with nearly 90% of the capacity installed being onshore, continuing its increasing trend in installation rates.

Offshore wind accounted for 13% of Europe's total installations, with 2.5 GW of new capacity added. The UK contributed almost half of this new offshore capacity (1.2 GW), followed by France (0.5 GW), the Netherlands (0.4 GW), Germany (0.3 GW), and Italy, which launched its first offshore wind project, Beleolico (30 MW).

Within the EU-27, 16.1 GW of new wind power installations were recorded in 2022, accounting for 84% of all wind installations in Europe. [2]

| | 2013 | 2014 | 2015 | 2016 | 2017 | 2018 | 2019 | 2020 | 2021 | 2022 |
|---|---|---|---|---|---|---|---|---|---|---|
| ● Onshore | 11.1 | 11.7 | 10.8 | 12.3 | 14.1 | 9.5 | 12.0 | 12.1 | 15.4 | 16.7 |
| ● Offshore | 1.6 | 1.5 | 3.0 | 1.5 | 3.2 | 2.7 | 3.7 | 2.9 | 2.9 | 2.5 |

Source: WindEurope

Figure 1.2: New onshore and offshore wind installations in Europe[2].

New wind installations in Europe per country in 2022

| | Germany | Sweden | Finland | France | UK | Spain | Poland | Netherlands | Turkey | Italy | Norway | Austria | Belgium | Ireland | Others |
|---|---|---|---|---|---|---|---|---|---|---|---|---|---|---|---|
| ● Onshore | 2,403 | 2,441 | 2,430 | 1,590 | 502 | 1,659 | 1,517 | 933 | 867 | 496 | 372 | 328 | 303 | 280 | 546 |
| ● Offshore | 342 | 0 | 0 | 480 | 1,179 | 0 | 0 | 369 | 0 | 30 | 60 | 0 | 0 | 0 | 0 |

Source: WindEurope
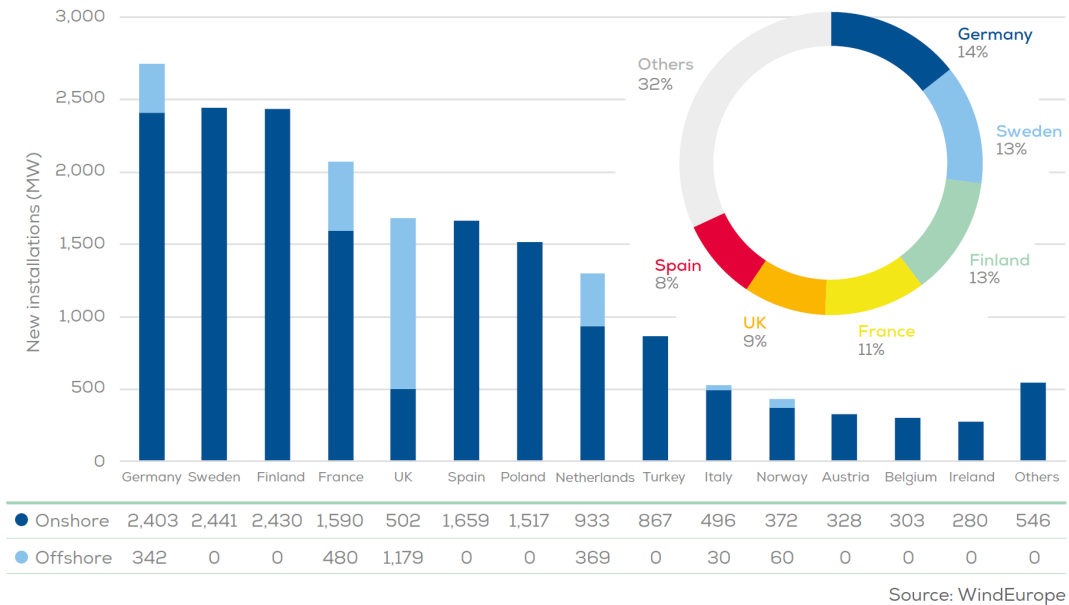
Figure 1.3: New wind installations in Europe in 2022 per country[2]

## 1.2 Offshore wind energy

Wind turbines can be classified as onshore or offshore, each presenting distinct advantages. Onshore turbines primarily benefit from economic and logistical factors: they are generally more affordable and accessible, making them easier to install, maintain, and repair.

In contrast, offshore wind turbines present two great advantages. First, they achieve higher capacity factors, which is the ratio of the actual energy generated over time to the energy that would have been generated if the turbine had operated at full capacity throughout the same period. This is due to the better quality of offshore wind resources compared to onshore. Offshore winds are less affected by orography and ground irregularities, resulting in higher wind speeds and enabling the use of larger and taller turbines that can capture more energy.

Secondly, offshore wind farms have a significantly reduced environmental impact compared to their onshore counterparts. The farther from the coast the turbines are installed, the lower the impact on the environment.

The first offshore wind turbine was installed in Denmark in 1991. Since then, there have been substantial advancements in turbine size and power. Technological developments and improved manufacturing processes have increased the tip height from 100 meters in 2003 (for a 3 MW turbine) to over 200 meters in 2016 (for an 8 MW turbine), and the swept area has expanded by 230%. Current development efforts are aimed at producing 15-20 MW turbines by 2030, as shown in (figure1.4). Larger blades increase the swept area of the turbine, thereby capturing more wind and extracting additional energy.

In this study, we focus on the International Energy Agency (IEA) 15-MW offshore reference turbine and the NREL 5-MW offshore reference turbine.



*Technology advances enabled offshore wind turbines to become much bigger in just a few years and are supporting ongoing increases in scale*
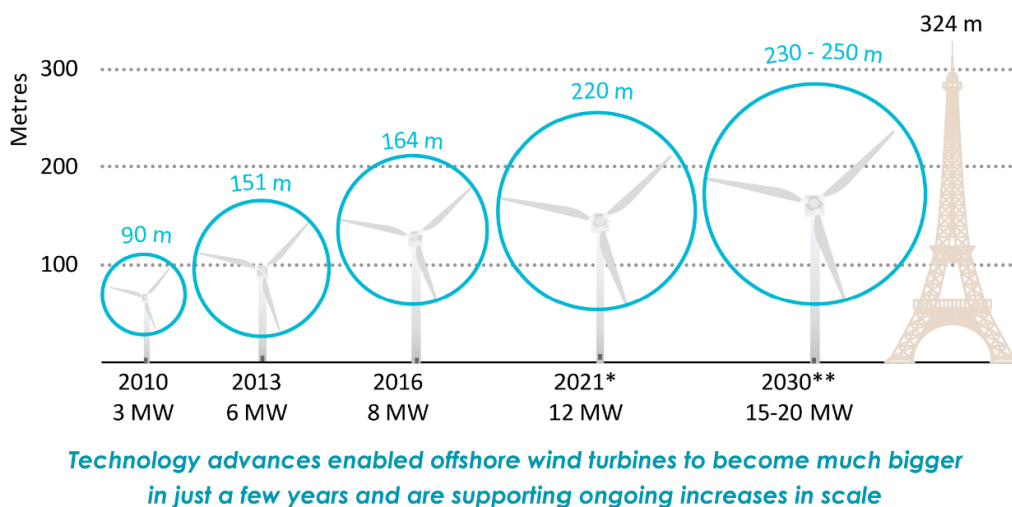
\* Announced expected year of commercial deployments. \*\* Further technology improvements through to 2030 could see bigger turbines sizes of 15-20 MW.

Figure 1.4: Evolution of the largest commercially available wind turbines.

The increase in the size of offshore wind turbines has posed challenges for construction and foundations, in addition to driving up capital costs. However, the operation and maintenance costs have decreased, which in turn lowers the levelized cost of energy (LCOE) over time, making offshore wind energy more competitive.

Another significant consequence of larger turbines is the improvement in the capacity factor. From 2010, when the average turbine size in offshore wind farms was 3 MW, to 2018, when the average size had increased to 5.5 MW, annual capacity factors rose from 38% to 43%. Currently, offshore wind turbines achieve capacity factors well above 50%. Given the same site conditions, a larger turbine may offer an increase in the capacity factor of between 2% and 7% compared to smaller turbines. However, the capacity factor is also dependent on wind quality and location, so not all new wind farm projects will necessarily exhibit higher capacity factors, although the general trend is towards continued improvement as suggested by recent data.

The average capacity factor is a valuable indicator of wind resource quality for energy production, as it translates wind speeds in a given area into average performance over a year. As shown in (figure1.5), wind resources are heavily influenced by geographical location, specifically latitude. According to the IEA Offshore Wind Outlook 2019: "In Europe, the North Sea, Baltic Sea, Bay of Biscay, Irish Sea, and Norwegian Sea have offshore wind with average annual capacity factors of around 45-65%, which is higher than comparable figures for the United States (40-55%), China (35-45%), and Japan (35-45%). Capacity factors are also high off the coast of South America and New Zealand (50-65%). Moderate wind speed resources in India result in a 30-40% average capacity factor. Generally, the average capacity factor is relatively low in regions closer to the equator, such as Southeast Asia and parts of Western Africa" [3].
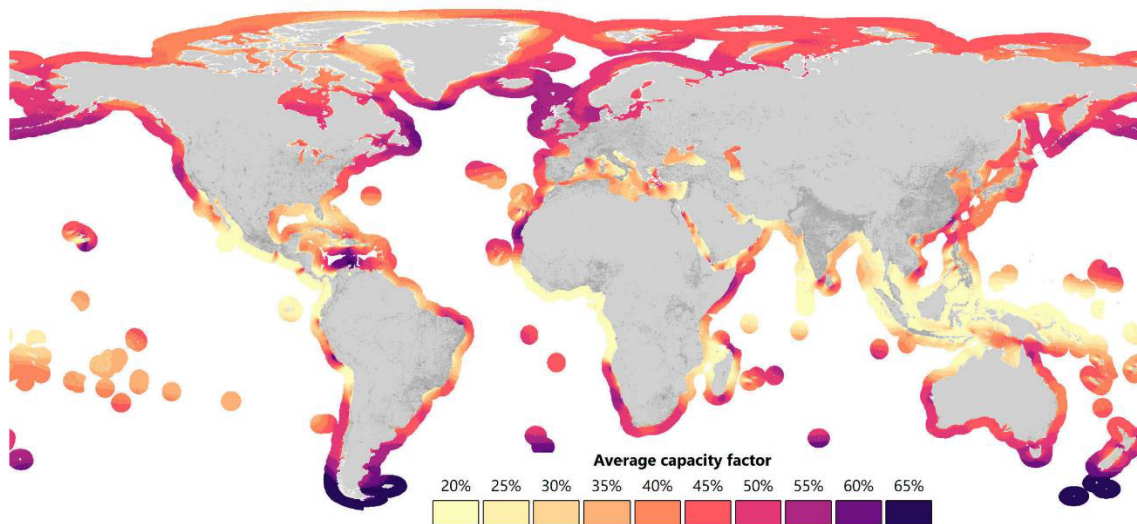


Figure 1.5: Average simulated capacity factors for offshore wind worldwide [3].

## 1.3 Floating offshore wind turbines

The primary drawback of offshore wind turbines is typically the high cost and complexity of installation and maintenance, as they are less accessible. As the distance from the coast increases and the depth of the seabed grows, the cost of bottom-fixed

structures becomes significantly higher.

It is estimated that 80% of the world's offshore wind resource potential is located in waters deeper than 60 meters. At depths of 50 meters or more, the cost of fixed structures becomes prohibitively expensive, making bottom-fixed options impractical for many countries with limited fixed offshore wind potential. Floating offshore wind turbines (FOWTs) provide a viable solution for these regions to harness their wind resources.

The first FOWT was installed in Norway in 2009. Following its success, the offshore industry launched the world's first commercial floating offshore wind project, Equinor/Masdar's Hywind Scotland wind farm, which deployed five SGRE 6 MW turbines, in the UK in 2017. The largest floating offshore wind site to date is the 50 MW Kincardine project in Scotland, utilizing the Principal Power Windfloat platform and five Vestas V164-9.5 MW turbines [9].

As depicted below, there are four predominant types of floating wind foundations either in use or under development. The case studies examined in this work include the semi-submersible UMaine VolturnUS-S Reference Platform, developed for the IEA Wind 15-MW Offshore Reference Wind Turbine, and the OC3Hywind spar-type Reference Platform for the NREL 5-MW Offshore Reference Wind Turbine.
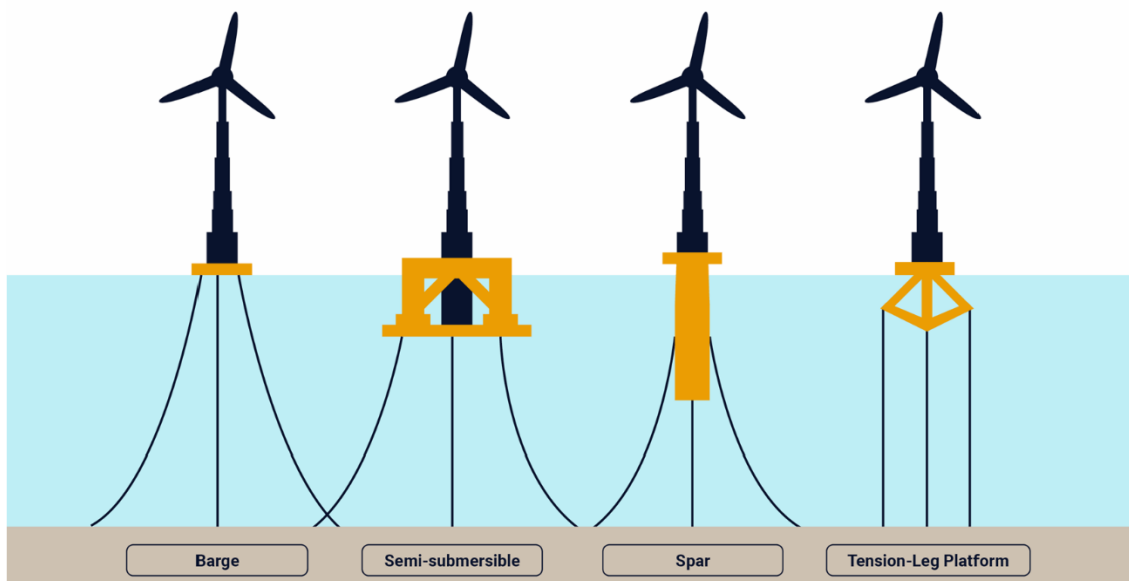


Figure 1.6: Floating offshore designs.

## 1.3.1 Semi-submersible platforms

Semi-submersible platforms for wind turbines are advanced offshore structures consisting of multiple columns and pontoons. Each component has a specific role: the columns primarily provide stability, while the pontoons offer additional buoyancy. The design achieves stability through the positioning of the center of gravity above the center of buoyancy, with stability ensured by the restoring moment generated by the columns.

To maintain its position, the floating structure uses a mooring system. This system typically includes catenary or taut spread mooring lines and drag or suction anchors. Over time, designers have developed various innovative semi-submersible designs aimed at optimizing the foundation structure and enhancing the stability of the wind turbines.

In these designs, the wind turbine may be placed at the center of the floating unit or on top of one column. The latter arrangement requires additional ballast to counterbalance the turbine's weight. This configuration is currently the most popular in the industry for several reasons:

1. *Versatility in Water Depth:* Semi-submersibles can be deployed in a broad range of water depths, typically starting from 40 meters and extending deeper, offering greater flexibility in site selection.

2. *Cost-Effectiveness:* The cost of the anchoring system is lower compared to Tension Leg Platforms (TLP), making it a more economically attractive option.

3. *Simplified Transportation and Installation:* The process of transportation and installation is relatively simpler compared to other concepts, making it more feasible for offshore wind farms.

4. *Dockside Installation:* Wind turbines can be installed on the semi-submersible at the dockside and then towed to the deployment site, eliminating the need for costly offshore installations.

## 1.3.2   Spar Foundation

The Spar foundation is an innovative offshore structure characterized by a large-diameter, vertical buoyant cylinder that is ballasted at its bottom end, resulting in a deep draft. This design provides increased stability, making the structure less susceptible to the effects of wind, waves, and currents. Like semi-submersibles, the Spar foundation is anchored using a mooring system with catenary or taut spread mooring lines and drag or suction anchors.

The Spar concept offers several key advantages:

1. *Enhanced Stability:* The deep draft design of the Spar foundation provides superior stability compared to semi-submersibles.

2. *Simplicity in Structure Configuration:* Spar structures generally have simpler designs compared to semi-submersibles and Tension Leg Platforms (TLP).

3. *Cost-Effectiveness:* The anchoring system of Spar foundations tends to be more economical than that of TLPs.

However, the Spar concept also faces some limitations:

1. *Minimum Water Depth Requirement:* Spar foundations require water depths greater than 100 meters for effective deployment, which may limit their applicability in shallower waters.

2. *Transportation Challenges:* The tall hull structure of Spar foundations presents challenges during transportation in shallow water zones, potentially complicating deployment in certain regions.

# Chapter 2

# Review of wind turbine failures in literature

## 2.1    Wind turbine failures in offshore wind turbine

Offshore wind turbines,like any complex engineering system,are not immune to failures and challenges that arise in their operation. This chapter will present a comprehensive literature overview that examines the failures experienced by offshore wind turbines.

By critically analyzing the existing body of research, this chapter aims to uncover the underlying causes, implications, and lessons learned from these failures. By understanding the vulnerabilities and limitations of offshore wind turbines, it's possible to improve design, maintenance, and operation of future installations, ensuring their reliability and longevity. The central focus of this literature review is to underscore the fundamental impact that failures of offshore wind turbines have on the global dynamic response of the system.

Recognizing that wind turbines operate as complex systems with interconnected components, it is crucial to understand how failures in one part can reverberate throughout the entire turbine, affecting its overall dynamic behavior. By understanding how failures propagate and manifest in the turbine's dynamic behavior, it's possible to identify key areas that require attention for improved reliability and operational efficiency.

Throughout the literature review, it's possible to explore studies that examine the repercussions of failures in various turbine components, such as the rotor, blades, gearbox, and electrical systems, on the global dynamic response. These failures can lead to changes in the turbine's response to wind loads, introduce additional vibrations and stresses, and impact the overall structural health and fatigue life of the turbine.

Additionally, this literature review also explores the context of ultimate load cases. Ultimate load cases refer to extreme conditions and events that wind turbines must withstand, such as severe storms, high winds, or rare gusts. Understanding how

failures impact the global dynamic response of the turbine under these extreme scenarios is crucial for ensuring their structural integrity and resilience.

## 2.2   Wind turbine component failure analysis

Several studies have been conducted to gather reliability data on wind turbines (WTs). This data is presented in various formats, such as failure distributions, downtime distributions (%), failure rates measured as the number of failures per turbine annually, and downtime recorded as hours lost per component per turbine per year. The data varies across different locations, weather conditions, types of WTs, and operational lifespan. It has been observed that both weather and location play crucial roles in WT reliability due to wind speed variations.

A study conducted in northern Germany [10] found that the most frequent failures were associated with the blades/pitch system, control system, and gearbox. In 2001, the onshore failure rate per turbine per year was reported to be 2.20. Another study [11] analyzed downtime distribution among WT components, revealing that more than 85% of the total downtime was attributed to failures in the blades, generator, and gearbox. The study further noted an average of 0.402 failures per turbine annually, with the electrical system, sensors, and blades/pitch system experiencing the highest failure rates. Additionally, larger and more modern WTs (greater than 1 MW) exhibited higher failure rates. Data collected in Germany between 2003 and 2005 from 865 WTs represented approximately 4% to 7% of the total turbine population.

The average failure rates for WT components are shown in (figure 2.1). The control system has the highest cumulative failure rate, followed by the blades/pitch system and the electrical system. Components such as gears, yaw systems, hydraulics, brakes, generators, sensors, and others exhibit medium failure rates, while hubs, drive trains, and structural components have lower failure rates. The components with the highest failure rates and downtimes are summarized in the table 2.1. Blades, control systems, and electrical systems have the highest failure rates, whereas gearboxes, generators, and blades account for the most downtime.

| Study | Source | Country | Average number of WTs | Study period | Top 3 failure rates | Top 3 downtime |
| --- | --- | --- | --- | --- | --- | --- |
| Bussel and Zaaijer | Estimation ofexpert judgement in DOWEC project | DEU | - | - | Blades<br>Control gearbox | Blades<br>Generator gearbox |
| Braams and Rademakers | CONMOW project | DEU | | | Electronic<br>Control hydraulics | - |
| Ribrant and Bertling | Elforsk and Felanalys | SWE | 625 | 2000-2004 | Electric<br>Sensors<br>Blades/pitch | Gears<br>Control<br>Electric |
| | VTT | FIN | 72 | 2000-2004 | Hydraulics<br>Blades/pitch<br>Gears | Gears<br>Blades/pitch<br>Hydraulics |
| | ISET | DEU | 865 | 2003-2005 | Electric<br>Control<br>Sensors | Generator<br>Gears<br>Drive train |
| McMillan and Ault | Windstats | DEU | | | - | Gears<br>Generator<br>Blades/pitch |
| Spinato et al. | Windstats (WSDK) | DNK | 851-2345 | 1993-2004 | Control(converter)<br>Blades/hub<br>Yaw system | - |
| | Windstats (WSD) | DEU | 1291-4285 | 1993-2004 | Electric<br>Blades/hub<br>Control(converter) | - |
| | LWK | DEU | 158-643 | 1993-2004 | Electric<br>Blades/pitch/hub<br>Control(converter) | Gearbox<br>Electric<br>Generator |

Table 2.1: Review of failure studies in WTs
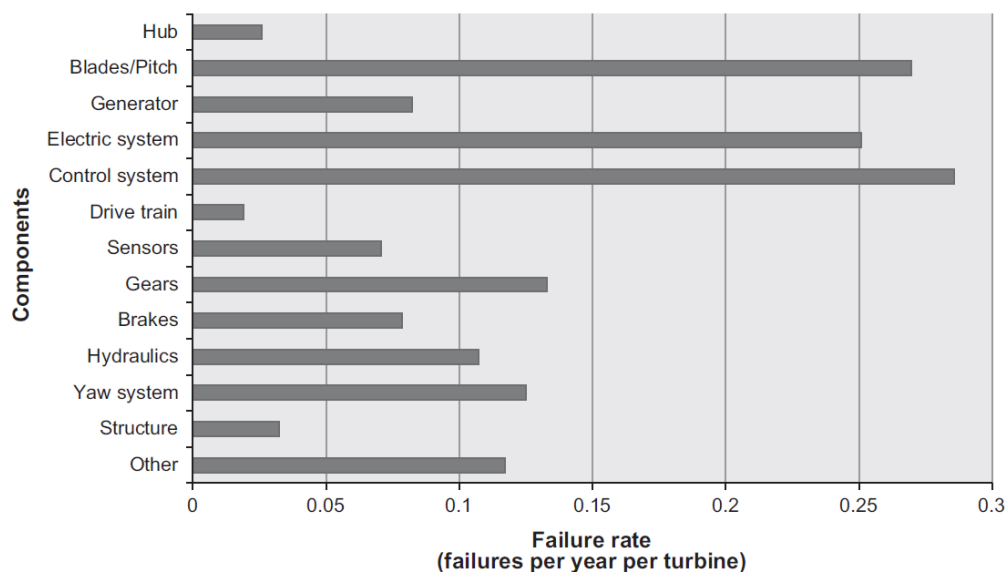


Figure 2.1: Average rate of failure vs WT components.

## 2.3 Example of fault cases - Accidental load cases

This section reviews a selection of some fault cases discussed in the existing literature, as well as the simulation techniques used to analyze their effects on the wind turbine's overall performance.

### 2.3.1 Blade Pitch Subsystem Faults

A common fault scenario involves the blade pitch system, as detailed, for istance, in the work of Peña-Sanchez, Penalba, and Nava [12] titled "Faulty wind farm simulation: An estimation/control-oriented model." In this study, only faults that allow the turbine to continue operating, albeit in a sub-optimal condition, are considered.

The faults identified in this study are classified into three main categories: sensor faults, actuator faults, and system faults. In the case of sensor faults, an incorrect reference signal may be generated, potentially damaging the turbine if left uncorrected. Specifically, the study examines three sensor fault types:

- *Stuck sensor*: The sensor's output remains constant and does not reflect the actual measured variable;

- *Constant offset*: The sensor output is consistently offset from the true signal;

- *Precision degradation*: Increased noise is present in the sensor's output signal.

Sensor faults are critical because they can affect key variables such as the pitch angle and rotor angular velocity, both of which are essential for the turbine's control system. An incorrect reading in either of these variables can lead to severe or even catastrophic consequences for the wind turbine's operation.

For actuator faults, the study identifies three types: stuck actuators, offset actuators, and reduced effectiveness. Reduced effectiveness refers to actuators deviating from expected performance, often resulting in slower response times to reach the target value. System faults, on the other hand, involve changes to the dynamics of specific subsystems, with the paper focusing on faults in the blade pitch system—specifically in both actuators and sensors—which affect multiple turbines in a wind farm.

The impact of actuator faults largely depends on the angle at which the blade actuator becomes stuck. This typically creates an imbalance in the forces acting on the three blades, leading to an uneven load distribution on the turbine. Such imbalances can significantly threaten the rotor's integrity and overall turbine operation. Therefore, early detection and resolution of these faults are essential for maintaining safe and efficient turbine operations.

In another paper, by Bae and Kim [13], titled "Influence of Failed Blade Pitch Control System to FOWT by Aero-Elastic-Control-Floater-Mooring Coupled Dynamic Analysis," the effects of a locked blade pitch angle on the NREL 5MW wind turbine were investigated. This study involved time-domain simulations with a total simulation time of 1,000 seconds, where the blade pitch control malfunction occurs at 100 seconds, and the pitch angle remains locked for the remainder of the simulation.

The study demonstrates that a partial failure in blade pitch control can have a significant impact, regardless of the final pitch angle at failure. In particular, notable changes are observed in the platform yaw response and the torsional moment at the tower base. Furthermore, turbine behaviors, including tower-base loads and blade-root shear forces, were examined under scenarios where the blade pitch control was partially compromised.

Due to the resulting imbalance in rotational forces, the 1P excitations and corresponding responses become more pronounced in both the tower and blade dynamics. In this context, 1P excitations refer to the periodic forces and responses associated with the rotation of the rotor blades at one revolution per minute (RPM). [13]. The term "1P" indicates the first harmonic of rotational motion, which corresponds to one complete cycle of the rotor as it completes one full rotation. One key finding is the variation in mean and peak blade-root shear forces across the two unaffected blades. This difference arises from the periodic inertial loading induced by platform yaw motion, which creates a cyclic pattern throughout the simulation. This loading pattern aligns with the overlap of 1P platform yaw motion and rotor rotation, causing the peak shear force on each blade to occur at different azimuth positions, depending on the rotor's orientation during each cycle.
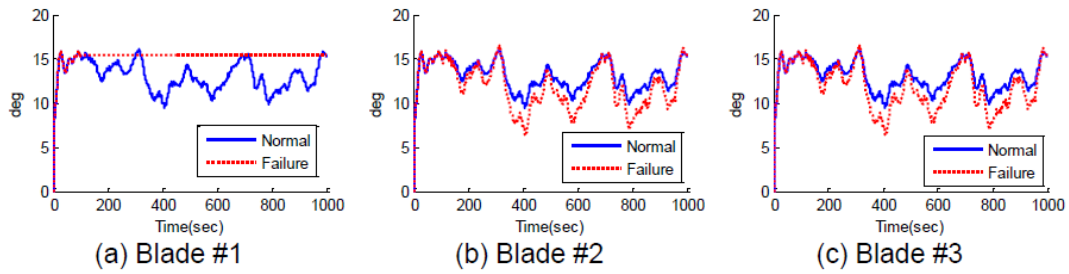


Figure 2.2: Blade pitch angle with failure after 100 seconds
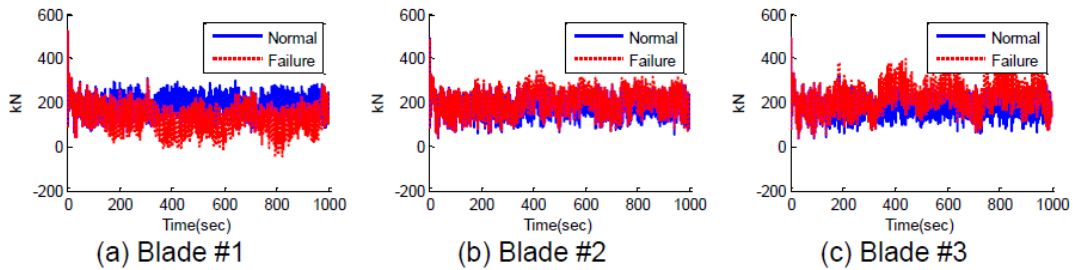


Figure 2.3: Blade flapwise shear force with failure after 100 seconds
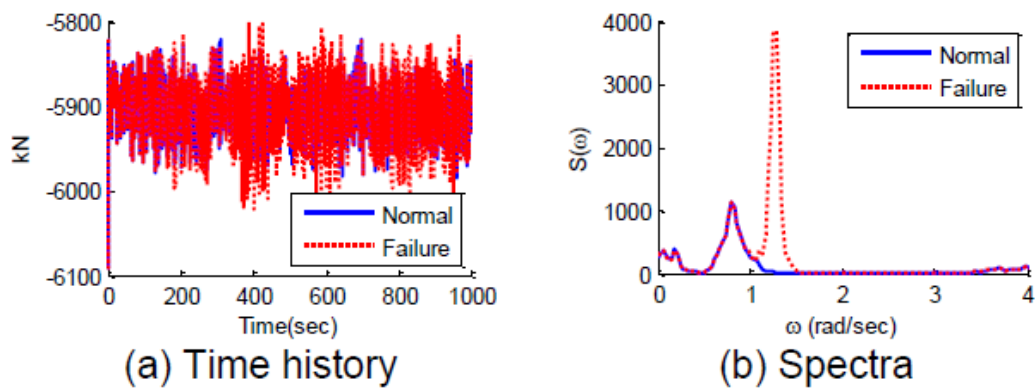
Figure 2.4: Tower base axial force .
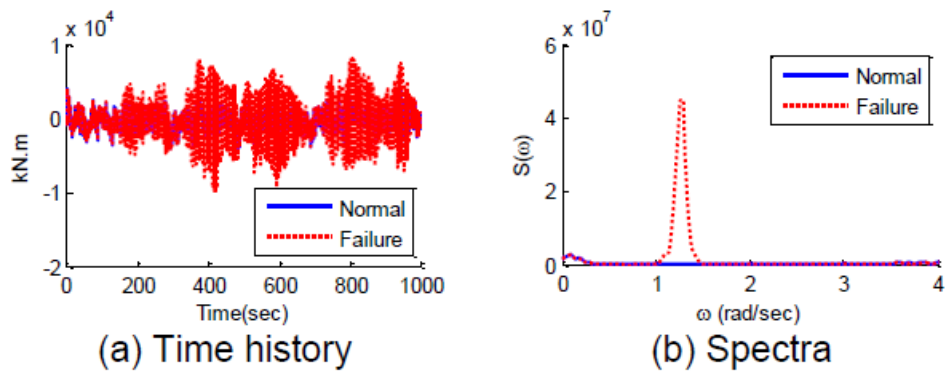


Figure 2.5: Tower base torsional moment .
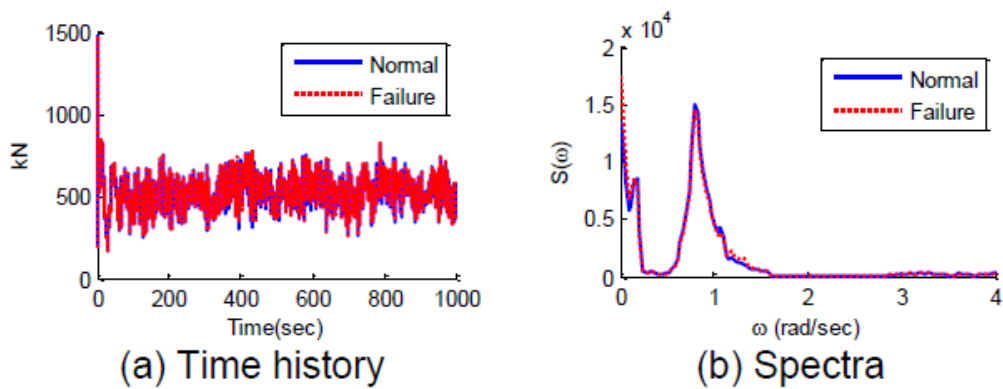


Figure 2.6: Rotor thrust force .
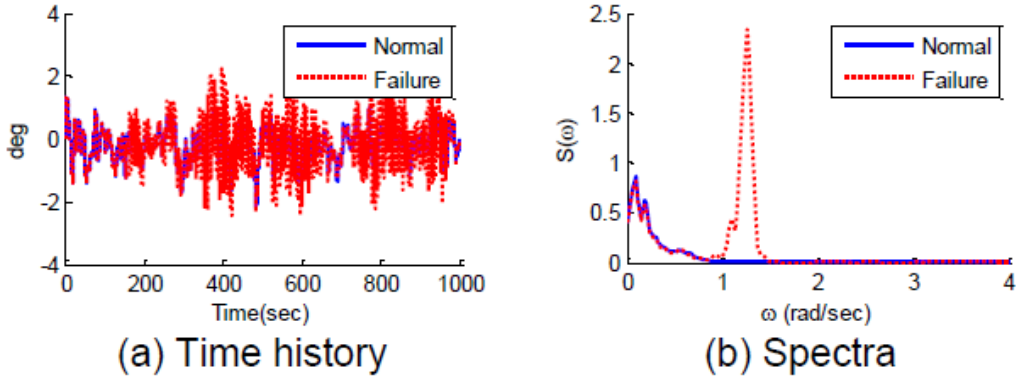
Figure 2.7: Platform yaw motion .

Bachynski and Etemaddar (2016) [14] carried out a case study examining the effects of a fixed blade pitch angle on the shutdown process of the NREL 5MW turbine. Initially, the turbine operated normally for about 395 seconds. However, an actuator malfunction caused blade 2 to become fixed in its pitch angle. The control system, after a brief delay of 0.1 seconds, responded by feathering the other two blades at a maximum rate of 8 degrees per second and disconnecting the generator. The study analyzed the turbine's performance under wind conditions of 14 m/s, incorporating varying wind speeds, shear, and directions using the normal turbulence model (NTM) of class A to assess turbulence intensity.

The primary investigation focused on the effects of the blade-pitch fault on the drivetrain system. The results indicated that the fault introduced a substantial axial force on the main bearing, which was transmitted through the gearbox and impacted other bearings, especially the carrier bearings in the first stage. This led to a significant increase in non-torque loads on the gearbox. Following the fault and emergency shutdown, a torque reversal occurred, which could cause gear rattle across all stages.

The study found that the main bearings (INP-A and INP-B) experienced the greatest impact during the fault and shutdown, with the carrier bearings in the first stage also significantly affected. This research underscores the critical need for prompt detection and resolution of blade-pitch faults, as their effects on the drivetrain system can lead to considerable mechanical stress and diminished turbine performance.

24
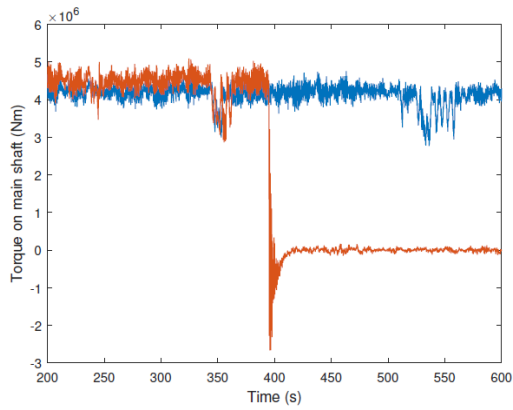
(a) Torque on the main shaft.
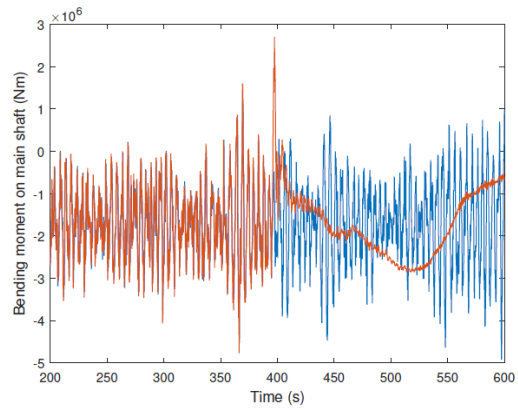


(b) Bending moment on the main shaft.

Figure 2.8: Input loadings on the main shaft without(blue) and with the fault(red) .
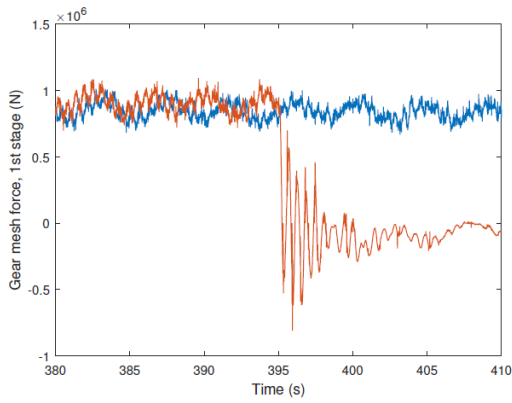


(a) Gear mesh force, 1st stage.
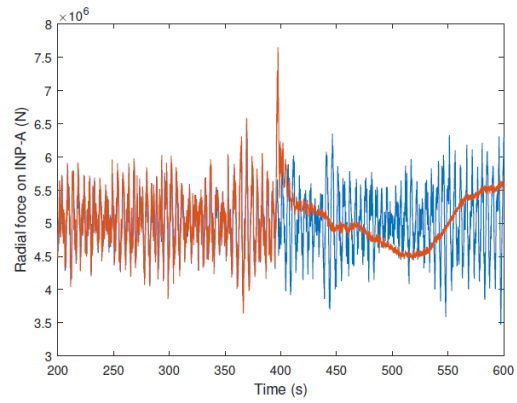


(b) Radial force on INP-A.

Figure 2.9: Radial force on INP-A and gear mesh force without(blue) and with the fault(red) .
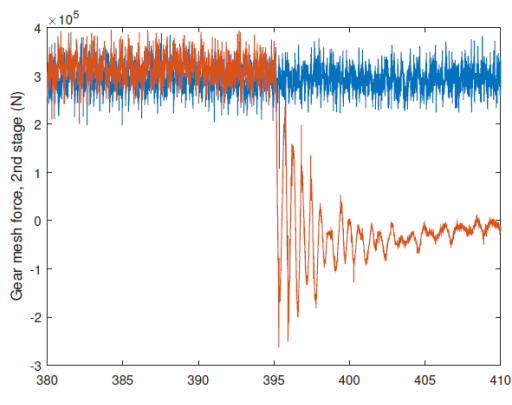


(a) Gear mesh force, 2nd stage.
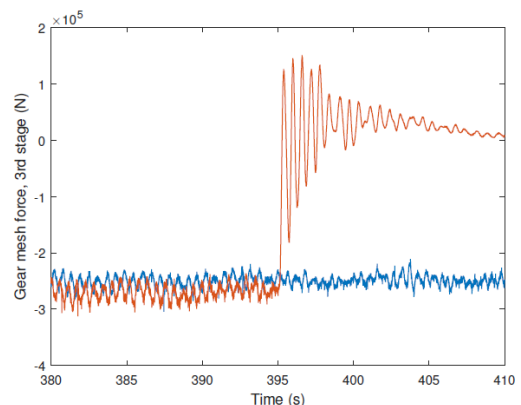


(b) Gear mesh force, 3rd stage.

Figure 2.10: Gear mesh force in 2nd and 3rd stages without(blue) and with the fault(red) .

In their 2013 study, Bachynski and Etemaddar [15] analyzed the impact of a grid

loss event followed by a subsequent shutdown on the NREL 5MW wind turbine, which is mounted on the OC3 Hywind spar platform. During the shutdown, the turbine experiences grid disconnection, and all blades with operational actuators are rotated to a feathered position (90 degrees) at a specified pitch rate (PR). In this particular study, the pitch rate during shutdown is set at PR = 8 degrees per second, which represents the maximum achievable rate.
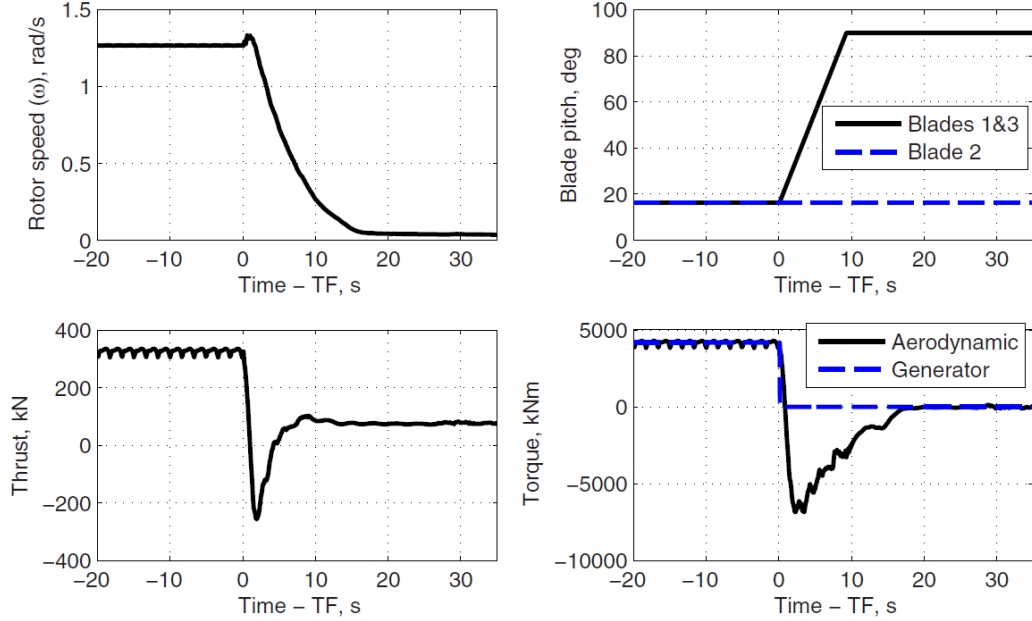


Figure 2.11: Fixed wind turbine: blade 2 seize followed by shutdown. Constant wind, 20 m/s.

In these cases, tower top and blade loads were critical. Specific platforms faced challenges with large yaw motions during faults and shutdown for spar and TLP, and significant pitch motions during shutdown for semi-sub platform.

## 2.3.2 Grid loss and electrical failures

In a study conducted by Roth, Röder, and Brimmers [16], two electrically-induced transient load events were examined with respect to the dynamic load magnitude and potential damage to the high-speed shaft (HSS) gears. The first event analyzed was a voltage drop in the power grid, which can be caused by the startup of external high loads. The second event was a short circuit of the generator windings, which could occur due to internal insulation failures.

For the first event, the grid voltage decreases linearly to 5% of its nominal value over a period of $\Delta t = 3$ ms. This reduced voltage level is maintained for $\Delta t = 97$ ms before the fault is cleared, at which point the voltage linearly increases back to the nominal value over another $\Delta t = 3$ ms.

As a result, the generator torque briefly exceeds the rated torque by a factor of two before rapidly dropping to zero. The mechanical torque in the HSS shows

oscillations shortly after the fault occurs, likely due to the excitation of a rotational natural frequency. At its peak, the HSS torque increases by approximately 19% compared to its nominal value. At $t = 10.1$ s, the voltage returns to its nominal value, causing the generator torque to rapidly rise, briefly exceeding the rated torque by a factor of 2.5 before returning to the rated value. This leads to a significant reduction in the HSS rotational speed and a sharp increase in the mechanical torque. The system control detects the restoration of normal grid operation and begins to ramp up the drive torque. Following this, the HSS torque shows oscillations around the nominal operating value, with decreasing amplitude due to damping effects. By $t = 11.5$ s, the wind turbine resumes normal operation.

As a consequence of this fault, the maximum flank pressure, $p_{H,\mathrm{max}} = 1,330$ MPa, was found to be slightly off-center on the tooth flank, due to micro-geometric corrections and the displacement of shafts and housing. The maximum flank pressure during the grid fault exceeded the nominal value by about $\Delta 7\%$. The microgeometry applied to the tooth flanks of the HSS compensates for system deformations at high torques, ensuring that the highest pressures remain nearly centered on the tooth flanks despite load-induced deformations. The study also considered all real tooth contact influences, including ideal microgeometry (design target specifications) and misalignments from the multi-body simulation (MBS). Regarding the load on the tooth root, the maximum stress, $\sigma_{\mathrm{max}} = 477$ MPa (tangential equivalent stress), was found to occur more centrally across the width of the tooth, exceeding the nominal value during the grid fault by approximately $\Delta 11\%$.
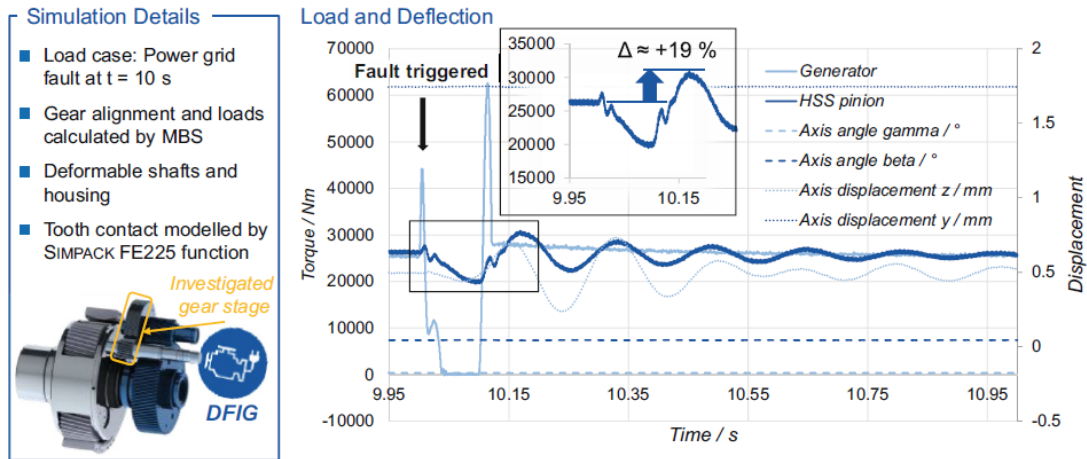


Figure 2.12: Load and deflection due to power grid fault (dip at 5% of nominal voltage) for a DFIG configuration.
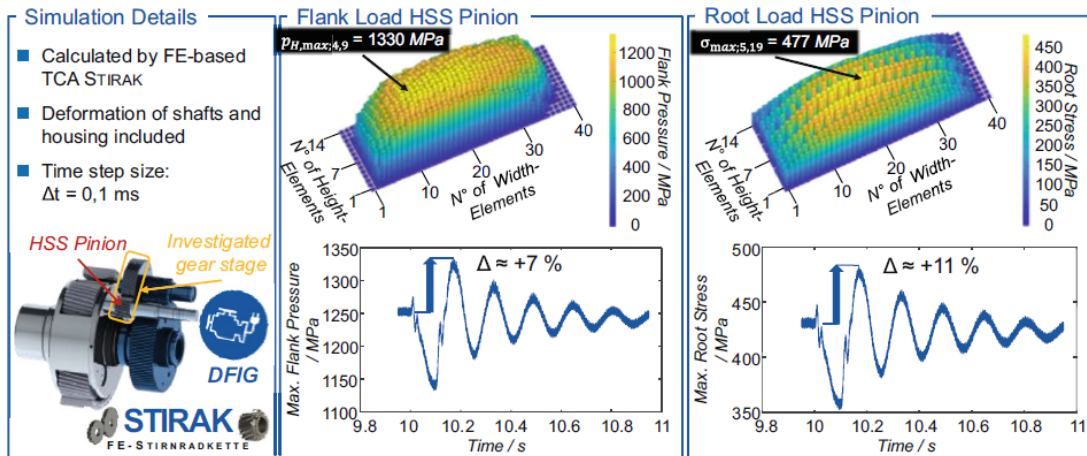
Figure 2.13: Flank pressure and root stress of the HSS pinion due to a power grid fault for a DFIG configuration.

Another load case analyzed in the study involved a short circuit between the phase windings of the generator, simulating the effects of damage in the machine-side phase module of the power converter, resulting in a permanent conducting state. This disturbance was introduced at time $t = 10$ s. Following the short circuit, high equalizing currents flowed between the phases due to potential differences in the lines. Consequently, the generator experienced a very high torque for a brief period immediately after the event, reaching approximately three times the nominal value after a delay of about $\Delta t \approx 4$ ms.

The control system quickly detected the malfunction and set the load-free state as the new target torque. However, due to the rotational inertia of the drive train, the torque on the high-speed shaft (HSS) followed the load increase with a time delay of approximately $\Delta t_{\text{Delay}} \approx 5$ ms. During the initial overshoot of the HSS torque, it exceeded the nominal value by roughly 13%.

The combination of the excited mechanical natural oscillation and the fluctuating torque of the generator led to a second overshoot, with a peak of approximately $\Delta 19\%$. Interestingly, similar maximum values for both tooth flank pressure and tooth root stress were observed, comparable to the results from the power grid fault scenario involving a Doubly Fed Induction Generator (DFIG).
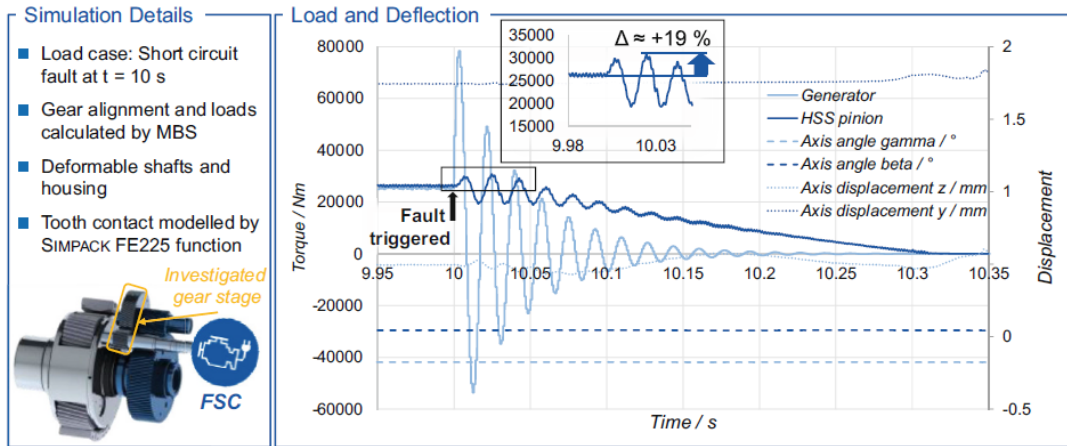
Figure 2.14: Load and deflection due to short circuit between the generator's phase windings for a FSC configuration.
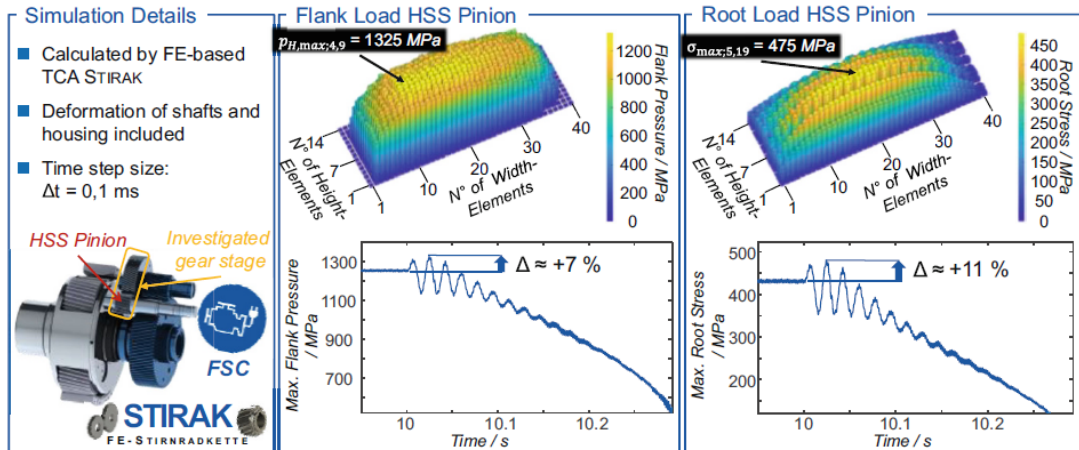


Figure 2.15: Flank pressure and root stress of the HSS pinion due to a short circuit for a FSC configuration.

## 2.4 Ultimate load analysis

This section provides a brief overview of ultimate load analysis. Ultimate loads refer to the maximum or extreme loads that a wind turbine may experience throughout its operational lifetime. These loads are designed to account for severe environmental conditions or unforeseen events that may occur. In the context of wind turbines, ultimate loads can be triggered by various factors, such as strong winds, gusts, turbulent atmospheric conditions, or even lightning strikes. The magnitude and characteristics of these loads are influenced by several factors, including the turbine's design, the specific site conditions, and the chosen safety standards and factors.

During extreme weather conditions or high wind speeds, wind turbines may be subjected to increased loads due to turbulence, sudden shifts in wind direction, or

elevated wind speeds. These ultimate loads can impact various components of the wind turbine, such as the rotor blades, the tower, the nacelle, and the foundation.

A study by Moratò and Sriramula (2016) [17] systematically analyzed a subset of ultimate limit state (ULS) load cases proposed by the IEC 61400-3 standard to evaluate their relative severity and identify the most critical among them. This study focused on power production and parked load cases using the NREL 5 MW prototype turbine model mounted on a monopile with a rigid foundation. The simulations were conducted using the aero-hydro-servo-elastic simulator FAST. Each Design Load Case (DLC) was analyzed individually, highlighting the key characteristics of the interaction between the environment and the structure.

Three response variables were selected as metrics for comparing the different DLCs: the flapwise (out-of-plane) moment and edgewise (in-plane) moment at the blade root, and the overturning moment at the seabed.

| DLC | WIND | | WAVES | | CONTROL |
|---|---|---|---|---|---|
| | Model | Speed | Model | Speed | |
| 1.1 | NTM | Vin <Vhub <Vout | NSS | Hs= E[Hs][V] | Extrapolation of loads |
| 1.3 | ETM | Vin <Vhub <Vout | NSS | Hs= E[Hs][V] | |
| 1.4 | ECD | Vhub = Vr±2m/s, Vr | NSS | Hs= E[Hs][V] | |
| 1.5 | EWS | Vin <Vhub <Vout | NSS | Hs= E[Hs][V] | |
| 1.6a | NTM | Vin <Vhub <Vout | SSS | Hs=Hs,sss | |
| 6.1a | EWM | Vhub=0.95*Vref | ESS | Hs= 1.09*Hs,50 | |
| 6.2a | EWM | Vhub=0.95*Vref | ESS | Hs= 1.09*Hs,50 | Loss of electrical network |
| 6.2b | EWM | V(zhub) = Ve50 | RWH | Hs=Hred50 | Loss of electrical network |

Table 2.2: List of Design Load cases

The study evaluates the structural responses across various ultimate limit states and ranks the Dynamic Load Cases (DLCs) based on three critical parameters. This ranking assists researchers and industry professionals in the design and optimization of these structures. The findings indicate that hydrodynamic loading is the primary factor influencing the design of the support structure, with the greatest overturning moment occurring in DLC 1.6a. Specifically, DLC 1.6 is categorized as an extreme operating gust (EOG) event combined with turbulent wind. The wind turbine is operating normally, but during this state, an extreme wind gust event (which lasts for a short duration) is superimposed on turbulent wind conditions. [17]. Conversely, the highest flapwise and edgewise moments are observed during scenarios involving wind gusts and changes in wind direction.
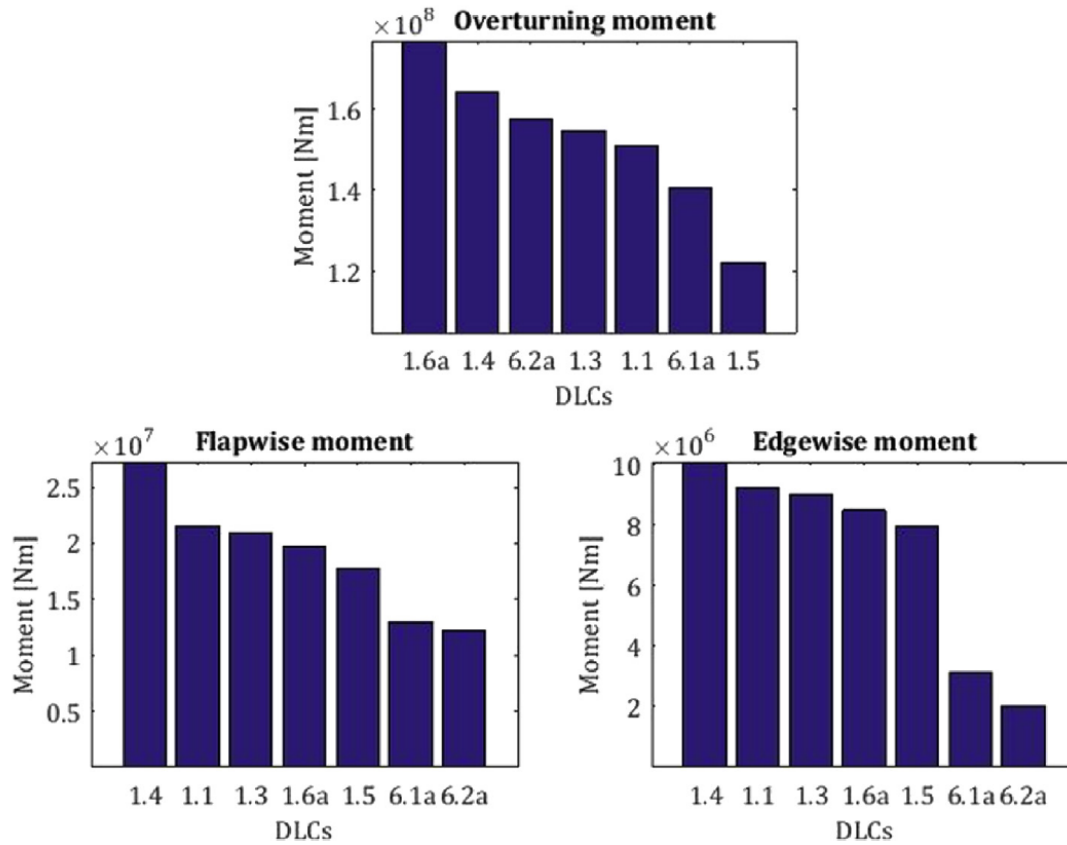
Figure 2.16: Ranking of all DLCs for the overturning moment at the seabed level and flapwise and DLC edgewise moment at the root of the blade.

This analysis underscores the importance of solid fault detection systems and advanced control mechanisms to reduce the impact of these failures on turbine longevity and performance. Additionally, the review reveals how external conditions, such as extreme wind and wave scenarios, play a vital role in the structural integrity and dynamic behavior of floating offshore wind turbines (FOWTs).

As the complexity of these systems grows, so does the need for comprehensive modeling that captures the aero-hydro-servo-elastic dynamics, especially under fault conditions. In the next chapter, we will introduce the technical details and configuration of the two wind turbine systems studied in this research: the IEA 15MW and the NREL 5MW reference turbines. A detailed description of the floating platforms supporting these turbines will also be provided, forming the foundation for the aeroelastic simulations conducted later in this thesis. This chapter will lay the groundwork for understanding the behavior of these systems in operational and fault conditions, setting the stage for the case studies to follow.

# Chapter 3

# System description

This case study focuses on two turbines: the IEA 15-MW Offshore Reference Wind Turbine supported by the VolturnUS-S Semisubmersible Reference Platform and the baseline NREL 5 MW turbine with the OC3-Hywind spar-type flotation system.

## 3.1 IEA 15-MW Offshore Reference Wind Turbine

In July 2020, the IEA published the technical report titled "Definition of the IEA Wind 15-Megawatt Offshore Reference Wind Turbine" [18], as an extension of IEA Wind Task 37 on Wind Energy Systems Engineering. The report details the design and performance characteristics of the IEA Wind 15-MW reference wind turbine, developed collaboratively by the National Renewable Energy Laboratory (NREL), the Technical University of Denmark (DTU), and the University of Maine (UMaine).

Subsequently, another technical report was released, which focused on the semisubmersible floating platform: "Definition of the UMaine VolturnUS-S Reference Platform Developed for the IEA Wind 15-Megawatt Offshore Reference Wind Turbine" [4].

The floating offshore wind turbine referenced in this study consists of a semisubmersible platform, a chain catenary mooring system, a floating-specific tower, and a rotor-nacelle assembly.

Figure 3.1: IEA-15-240 RWT and VolturnUS-S reference platform [4].

The 15 MW offshore reference turbine has a conventional three-bladed upwind design with a rotor diameter of 240 m; a 150-m hub height; a variable-speed, collective pitch controller; and a low-speed, direct-drive generator. The overall parameters of the turbine are shown in the table 3.1.

## 3.2   VolturnUS-S Reference Platform

The semisubmersible platform is engineered to accommodate the IEA-15-MW wind turbine and features a four-column structure, consisting of three radial columns and one central column, all made of steel. This structure is anchored to the seabed using a three-line chain catenary mooring system, which has a vertical pretension of 6,065 kN.

The tower is specifically crafted for floating applications: offshore wind turbine towers that float require greater stiffness compared to fixed-bottom configurations due to the increased inertial and gravitational forces resulting from the motion of the platform. In this case, the design employs an isotropic steel tube with a total weight of 1,263 tons.

The platform has a draft of 20 m with a 15-m freeboard to the upper deck of

| Parameter | Units | Value |
| --- | --- | --- |
| Power rating | MW | 15 |
| Turbine class | - | IEC Class 1B |
| Specific rating | W/m2 | 332 |
| Rotor orientation | - | Upwind |
| Number of blades | - | 3 |
| Control | - | Variable speed Collective pitch |
| Cut-in wind speed | m/s | 3 |
| Rated wind speed | m/s | 10.59 |
| Cut-out wind speed | m/s | 25 |
| Design tip-speed ratio | - | 9.0 |
| Minimum rotor speed | rpm | 5.0 |
| Maximum rotor speed | rpm | 7.56 |
| Maximum tip speed | m/s | 95 |
| Rotor diameter | m | 240 |
| Airfoil series | - | FFA-W3 |
| Hub height | m | 150 |
| Hub diameter | m | 7.94 |
| Hub overhang | m | 11.35 |
| Rotor precone angle | deg | -4.0 |
| Blade prebend | m | 4 |
| Blade mass | t | 65 |
| Drivetrain | - | Direct drive |
| Shaft tilt angle | deg | 6 |
| Rotor nacelle assembly mass | t | 1.017 |

Table 3.1: Key Parameters for the IEA Wind 15-MW Turbine

the columns and displaces 20,206 cubic meters of seawater. Figure 3.2 shows a representation of the whole assembly.
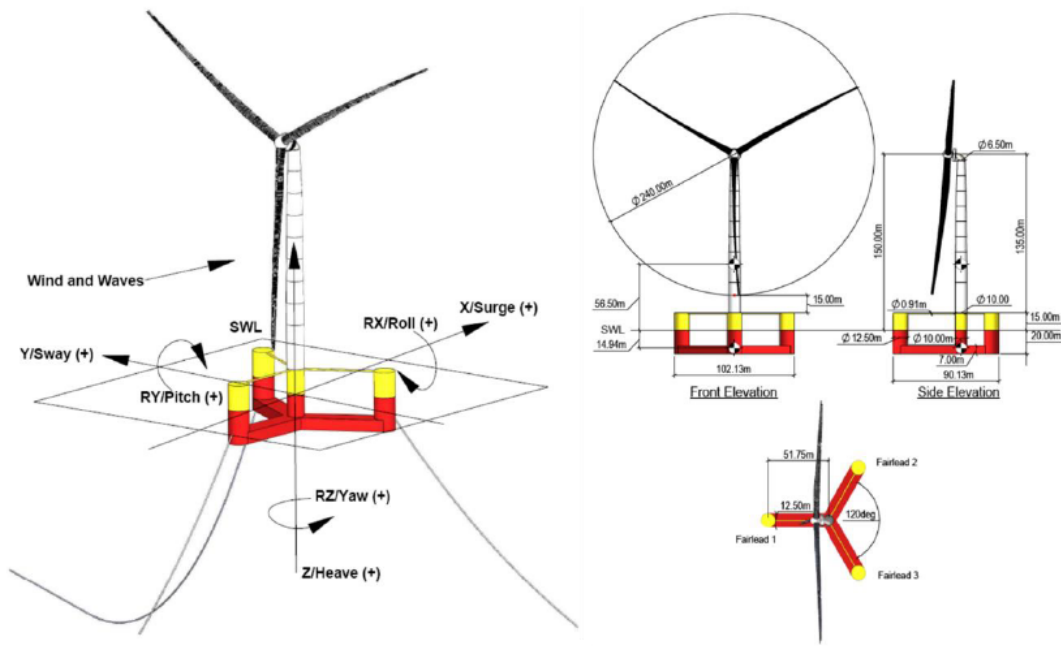


Figure 3.2: Platform view (left) and top-side view (right) [4].

## 3.3 NREL 5MW Offshore Reference Wind Turbine

The main characteristics of the baseline NREL 5 MW wind turbine modelled in OpenFAST are presented in the table 3.2. Additional characteristics of the wind turbine can be found in [19].

## 3.4 OC3-Hywind spar-type flotation system

The spar-type floating system is a design for offshore wind turbines that utilizes a large cylindrical component known as a spar buoy as the floating foundation. This spar buoy is a vertical structure that extends beneath the water surface and is secured to the seabed. The primary features of the OC3-Hywind spar-type floating system are detailed in Table 3.3. Additional information about the platform and the mooring of this wind turbine are presented in [5].

| Parameter | Units | Value |
|---|---|---|
| Power rating | MW | 5 |
| Turbine class | - | IEC Class 1B |
| Specific rating | W/m2 | 400 |
| Rotor orientation | - | Upwind |
| Number of blades | - | 3 |
| Control | - | Variable speed<br>Collective pitch |
| Cut-in wind speed | m/s | 3 |
| Rated wind speed | m/s | 11.4 |
| Cut-out wind speed | m/s | 25 |
| Design tip-speed ratio | - | 6.6 |
| Minimum rotor speed | rpm | 5.0 |
| Maximum rotor speed | rpm | 12.1 |
| Maximum tip speed | m/s | 80 |
| Rotor diameter | m | 126 |
| Hub height | m | 90 |
| Hub diameter | m | 3 |
| Hub overhang | m | 5 |
| Rotor precone angle | deg | 2.5 |
| Rotor mass | kg | 110.000 |
| Drivetrain | - | High speed<br>Multiple Stage Gearbox |
| Shaft tilt angle | deg | 5 |
| Nacelle mass | kg | 240.000 |
| Tower mass | kg | 347.460 |

Table 3.2: Key Parameters for the NREL 5MW Turbine

| | Value | Unit |
|---|---|---|
| Technology | Spar | – |
| Depth to platform base below SWL | 120 | m |
| Depth to anchors below SWL | 320 | m |
| Number of mooring lines | 3 | – |
| Platform mass, including ballast | 7466.33 | tonnes |
| Water displaced volume | 8029 | m3 |

Table 3.3: Main characteristics of the OC3-Hywind spar-type flotation system.

Figure 3.3: OC3-Hywind spar-type FOWT [5]

These descriptions set the technical foundation for the subsequent analysis, outlining the key parameters that will influence the behavior of the turbines in various fault and operational scenarios.

In the next chapter, we will explore the aeroelastic simulation methods used to model these turbines under different environmental and fault conditions, providing insights into their dynamic responses.

# Chapter 4

# Aeroelastic simulations

As discussed in Chapter 1, faults in wind turbines can occur in various components, including the pitch control system, gearbox, electrical generator, and others. Mathematical models typically focus on either the dynamic behavior and energy generation predictions under healthy conditions or the analysis of faults and reliability issues.

The primary aim of this project is to develop a coupled non-linear aero-hydro-servo-elastic mathematical model for the previously described wind turbines, incorporating several intentionally implemented fault scenarios. This model is assessed across a broad spectrum of environmental conditions, utilizing correlated wind and wave data from a specific location.

Consequently, the impact of different failures is analyzed, and the final annual energy generation is estimated based on failure statistics. These estimates are compared with ideal scenarios where no failures occur. The simulations are conducted using OpenFAST.

## 4.1   Introduction to OpenFAST

OpenFAST is an open-source, high-fidelity, multi-physics simulation environment that includes aerodynamics, hydrodynamics for offshore structures, control, and structural dynamics. It is designed to evaluate the coupled dynamic response of various wind turbine configurations, encompassing onshore, bottom-fixed offshore, and floating offshore topologies. An overview of the various components considered in an OpenFAST simulation is presented in 4.1.
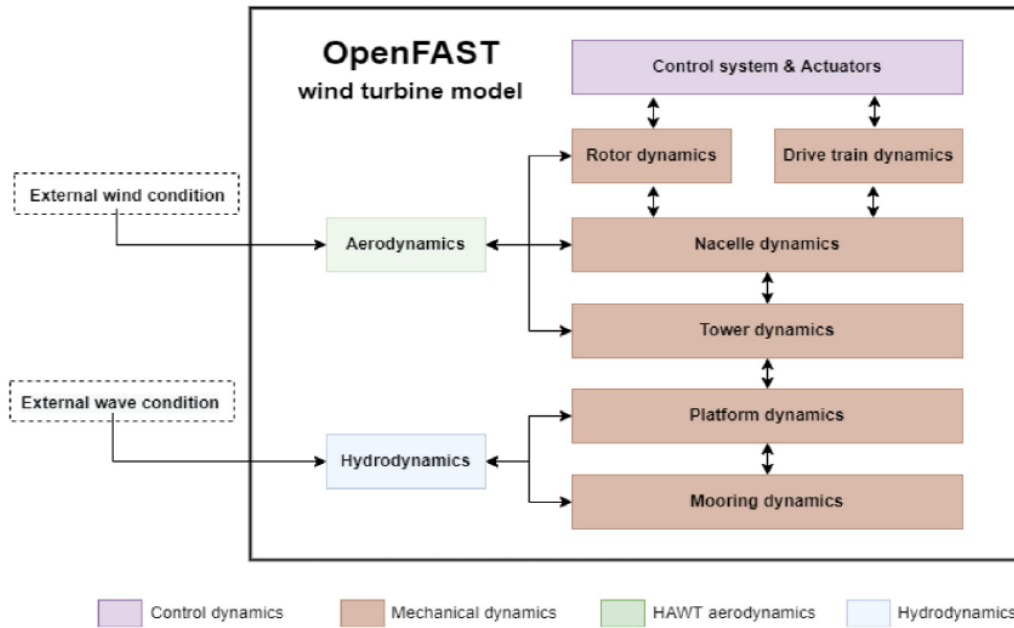
Figure 4.1: Overview of the multi-physic components involved in a FOWT simulation using OpenFAST.

It joins:

- Aerodynamics models, using wind-inflow data to compute the blade aerodynamic loads (AeroDyn module)

- Hydrodynamics models, which simulate the incident waves (HydroDyn module)

- Control and electrical system dynamics models, to simulate the controller logic

- Structural dynamics models, which simulate the elasticity of the blades and support structure applying the aerodynamic, hydrodynamic and gravitational loads (BeamDyn and ElastoDyn modules)

OpenFAST includes modules for various aspects of wind turbine simulation: MoorDyn for the mooring system, ElastoDyn for tower and structural motion, and TurbSim for generating wind distributions. The integration of these modules is facilitated through a glue code. By incorporating these elements, OpenFAST allows users to assess key performance metrics, such as power output, loads on turbine components, rotor speed, blade pitch angles, and turbine stability.

The OpenFAST v3.4.1 tool, along with its predecessors FAST, is extensively used in the literature for simulating and analyzing Horizontal Axis Wind Turbines (HAWTs), both onshore and offshore, with considerable detail and acceptance [20]. For example, [21] examined the impact of wind-wave misalignments on offshore wind turbine operation and mechanical loads using FAST. Similarly, studies on mechanical load reduction with passive structural elements [22] or active individual pitch actuation [23] have utilized this aeroelastic code.

In OpenFAST simulations, environmental conditions such as wind and wave characteristics can be defined externally (see Figure 4.1), depending on the analysis requirements. This flexibility allows for the simulation of various load cases under different wind speeds (primarily defined by the mean wind speed at hub height $U_{90}$) and sea states (defined by significant wave height $H_s$, peak period $T_p$, and wave direction $H_s, dir$). Turbulent wind speed fields are generated using the stochastic turbulence emulator TurbSim [24].

According to the standard IEC 61400-3 [25], the Kaimal spectrum, Normal Turbulence Model (NTM), and B wind class are used for simulating the Floating Offshore Wind Turbine (FOWT). Irregular waves are modeled based on the JONSWAP spectrum, with the peak enhancement factor calculated as per IEC 61400-3 Annex B, using the peak wave period $T_p$ and significant wave height $H_s$, as detailed in [26].

It is particularly noteworthy that OpenFAST simulations for implementing different failures are conducted using an external control system in Matlab-Simulink, which provides effective pitch and torque regulation to optimize wind turbine performance.

### 4.1.1 ElastoDyn

ElastoDyn specifically addresses the dynamic response of the turbine's structural components, including the blades, tower, and other flexible elements. It utilizes state-space representations and finite-element models to simulate the structural dynamics of the wind turbine.

The primary input file for ElastoDyn defines the modeling options and geometries for the OpenFAST structure, which includes the tower, nacelle, drivetrain, and blades (if BeamDyn is not employed). It also specifies the initial conditions for the structure.

The primary output file from ElastoDyn provides comprehensive information on the structural response of the wind turbine throughout the simulation. This output includes data on blade deflections, tower displacements, structural loads, and other pertinent quantities. Within this module, the degrees of freedom (DOF) of the platform can be controlled (either fixed or adjustable), as well as the initial blade pitch angle. The precone (-4°) and tilt (-6°) angles of the wind turbine are also fixed in this context. These parameters are managed through the OutList section, which contains quoted strings specifying one or more output parameter names.

ElastoDyn offers precise calculations of forces and moments, which is advantageous as it avoids the high computational costs associated with BeamDyn, which involves multiple degrees of freedom.

### 4.1.2 Hydrodyn

HydroDyn is specifically designed to simulate the hydrodynamic loads on offshore floating wind turbine platforms. This module is crucial for modeling the interactions between the wind turbine's support structure and the surrounding water environment, including waves and currents.

When coupled with OpenFAST, HydroDyn receives the position, orientation, velocities, and accelerations of the (rigid or flexible) substructure at each coupling time step, computes the hydrodynamic loads, and returns this data to OpenFAST. In this context, OpenFAST's ElastoDyn structural-dynamics module treats the substructure (floating platform) as a six-degree-of-freedom (DOF) rigid body. For fixed-bottom offshore wind turbines, OpenFAST's SubDyn module allows for structural flexibility in multi-member substructures, with HydroDyn's coupling including hydro-elastic effects.

The primary input file for HydroDyn specifies the substructure geometry, hydrodynamic coefficients, incident wave kinematics and currents, potential-flow solution options, flooding/ballasting, marine growth, and other auxiliary parameters.

The WAVES section of the input file determines whether first-order waves are generated internally or if externally generated waves are used, applicable to both strip-theory and potential-flow solutions. The wave spectrum settings in this section are relevant only for the first-order wave frequency components.

In this study, the kinematics model for the waves is "Irregular (stochastic) waves based on the JONSWAP or Pierson-Moskowitz frequency spectrum." The primary parameters that vary with wind speed are *WaveHs*, the significant wave height of incident waves, and *WaveTp*, the peak spectral period of incident waves.

### 4.1.3  Turbsim

TurbSim is a stochastic, full-field simulator for turbulent wind. It employs a statistical model, rather than a physics-based model, to numerically generate time series of three-component wind-speed vectors at points on a two-dimensional vertical rectangular grid that remains fixed in space.

Regarding input parameters, the first two parameters specify the number of grid points to generate in the vertical and horizontal directions, while the third parameter is the time step. Additional important parameters include the turbine's hub height and the dimensions of the grid. TurbSim assumes that the rotor disk diameter is the smaller of the grid height or width. If the grid height exceeds its width, TurbSim positions the top of the rotor disk at the top of the grid. Conversely, if the grid width is greater, the hub is centered both vertically and horizontally. The grid dimensions must be sufficiently large to ensure that no part of the blade extends beyond the grid boundaries.

Other inputs include turbulence intensity (TI), which can be specified using the IEC Kaimal or von Karman models. Input values of "A", "B", or "C" correspond to the standard IEC Normal Turbulence Model (NTM), with "A" representing the most turbulent conditions.

Alternatively, TI can be specified as a percentage rather than choosing standard turbulence characteristics. You can also select the type of IEC wind model to use, including "NTM" for the Normal Turbulence Model, "xETM" for the Extreme Turbulence Model (ETM), "xEWM1" for the Extreme Wind Speed Model (EWM) with

a 10-minute average wind speed and a recurrence period of 1 year, or "xEWM50" for the EWM with a 50-year recurrence period. The "x" in these extreme wind models should be replaced with the number 1, 2, or 3, denoting the respective wind turbine class.

Additionally, TurbSim allows for the specification of the reference wind speed height (in meters), which enables you to set the mean wind speed at a height other than the hub height. This reference height, combined with the wind profile type, is used by TurbSim to calculate the mean wind speed at hub height.

The final parameter is the power law exponent, used to determine the mean u-component wind speeds across the rotor disk for the power law wind profile (applicable to both "IEC" and "PL" wind profile types). A positive number should be entered to increase wind speed with height, or you can use the string "default" to allow TurbSim to apply a default value based on the specified spectral model.
The power-law mean velocity profile uses the PLExp input parameter to calculate the average wind speed at height z using the equation:

$$\bar{u}(z) = \bar{u}(z_{ref}) * (\frac{z}{z_{ref}})^{PLExp} \qquad (4.1)$$

where $\bar{u}(z)$ is the mean wind speed at z and zref is a reference height above ground where the mean wind speed $\bar{u}(z_{\text{ref}})$ is known.

TurbSim can generate eight different sets of output files, which use the root name of the TurbSim input file with extensions that specify the type of files produced. Notably, the Full-Field TurbSim Binary Files are of particular interest. These binary files, which have a ".bts" extension, are intended to be read by AeroDyn, the module responsible for simulating the aerodynamic behavior of the wind turbine blades.

TurbSim normalizes the data and encodes it into two-byte integers. The file begins with a header that provides information about the grid and instructions for AeroDyn on converting the integers to floating-point values. This is followed by the wind speeds for the grids and tower points (if specified).

In this study, these files are used to adjust wind conditions in relation to wave conditions. All simulations incorporate turbulent wind conditions to achieve more realistic results. Details of the wind speeds used are provided in the next chapter.

## 4.2   Controller

The wind turbine's control system is managed by the ROSCO controller [27] (Reference Open-Source Controller for fixed and floating offshore wind turbines), developed by Delft University of Technology. Unlike typical controllers that are designed for specific turbines and can be challenging to adapt for other models, the ROSCO controller serves as a reference model that is accessible even to non-control engineers.

The primary goal of the controller is to maximize power output by adjusting three control parameters: the rotor orientation (yaw system), the blade orientation (pitch

system), and the generated torque. This is achieved through two actuation methods: a variable-speed generator torque controller to manage generator power and a collective blade pitch controller to regulate rotor speed.

The control system's behavior can be categorized into four regions, as illustrated in the figure:

- **Region 1:** Below cut-in wind speed conditions. In this region, the wind speed is insufficient to generate power, and the generator torque is set to zero to allow the wind to accelerate the rotor for start-up.

- **Region 2:** Below rated wind speed conditions. The objective here is to maximize wind energy extraction.

- **Region 3:** Above rated wind speed conditions. In this region, power is capped to prevent damage to the components.

- **Region 4:** Above cut-out wind speed conditions. The turbine must be shut down because the wind speed is too high. The blades are pitched to reduce the thrust force to zero (feathering).
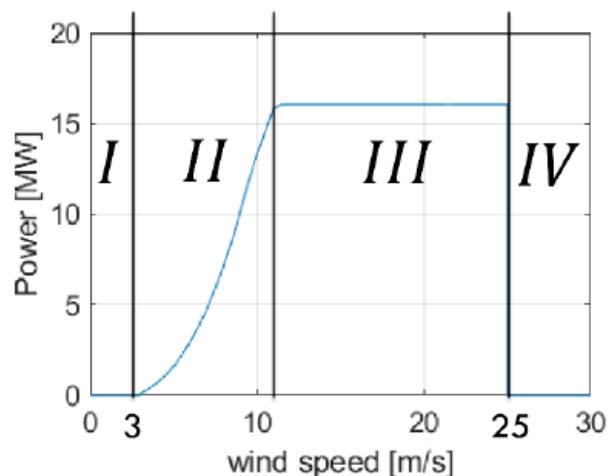


Figure 4.2: Controller zones [6]

Both generator torque and blade pitch controllers are PI controllers. Both modules vary according to the conditions in which the system is. This two modules plus some additional control modules are briefly discussed below.

## 4.2.1   Generator Torque Controller and blade pitch controller

For the generator torque controller, there are four distinct options available: two methods for operations below the rated wind speed and two methods for operations above it.

For below-rated conditions, one approach to optimize the extracted power at each wind speed is to apply a quadratic relationship between the generator torque and

the rotor angular speed. Alternatively, the tip speed ratio (TSR) can be tracked to maintain its optimal value, provided that the wind speed is accurately measured or estimated.

For above-rated conditions, the two methods include: the first method maintains a constant generator torque, while the second method keeps the extracted power constant at its rated value.

The primary objective of the blade pitch controller is to maintain the rotor angular speed at its rated value.

## 4.2.2 Additional Control Modules

In addition to the main modules, ROSCO includes several supplementary modules designed to enhance its performance:

- **Wind Speed Estimator**: This module estimates the wind speed used for tip speed ratio (TSR) tracking within the generator torque controller.

- **Set Point Smoothing**: During near-rated operations, conflicts may arise between the generator torque and blade pitch controllers due to differing reference rotor speeds. This module addresses this issue by adjusting the speed reference signal of the inactive controller while the active one operates.

- **Minimum Pitch Saturation**: At near-rated conditions, thrust force reaches its maximum values. Since the wind speed is lower below rated conditions and blade pitching reduces thrust force above rated conditions, this module sets a minimum blade pitch angle to limit the loads and prevent excessive forces during control operations.

- **Floating Offshore Wind Turbine Feedback**: This module introduces an additional term into the proportional-integral (PI) blade pitch controller. The goal is to determine a suitable gain value that minimizes rotor angular acceleration, thereby increasing the average extracted power and stabilizing the structure.

# Chapter 5

# Case study

As mentioned earlier, this work compares two turbines of different power: the IEA 15-MW Offshore Reference Wind Turbine supported by the VolturnUS-S Semisubmersible Reference Platform and the baseline NREL 5 MW turbine with OC3-Hywind spar-type flotation system. For each of these turbines, specific case studies are selected, which involve the following faults in the system:

- **Accidental load cases**:

  - **Blade pitch faults:**

    * *Blade pitch angle fixed*; where the pitch angle of one of the three blades is set at a specific value, and this value remains constant. This fixed blade position is usually set for optimal power production under normal operating conditions. As described in detail in [14] the other two blades are pitched to feather, which means they are rotated so that their angle of attack relative to the wind is minimal. This happens because the pitch safety system takes action; it's one of the most critical safety mechanisms in wind turbines, as it allows the blades to be pitched to a position that stops or significantly reduces the rotor's rotational speed in high winds or emergency situations.

    * *Offset in blade pitch angle*; where there is an abnormal deviation in the pitch angle of one or more blades from their position under normal conditions.

    * *Precision degradation*; where the white noise on the measurement of the blade pitch angle increases( with a standard deviation selected by the user)

  - **Simulation of disconnection from the grid**, where the torque of the electric generator instantly drop to zero, as the dynamics are very fast and the transient is neglected.

  - **Shutdown of the wind turbine**: when the wind speed exceeds a predetermined threshold, known as the cut-out wind speed,the turbine's control

system triggers an automatic shutdown to prevent potential damage and ensure the safety of the turbine and its surroundings.

- **Ultimate load cases**

  - *Extreme wind and waves conditions in shutdown state*, when the turbine structure and components are still exposed to the environmental forces like high winds and waves.

  - *Extreme wind shear*, that refers to a significant change in wind speed and direction over a short vertical distance in the atmosphere. During extreme wind shear events, the value of the exponent of the power law can significantly increase in comparison with the standard range. As a result, the wind turbine blades at higher heights experience significantly higher wind speeds than expected, which can lead to increased aerodynamic loads on the turbine.

## 5.1 Accidental load analysis

Significant values for wind and wave conditions under which simulations are conducted are shown in the table below. The real scatter of the wind, height and period of the waves is obtained from the shore of Pantelleria, Italy in ten years of data acquisition. [7]. The occurrence of the wind speed in Pantelleria based on these data is shown in (figure 5.1).

| Wind speed[m/s] | Significant height[m] | Peak period[s] |
|:---:|:---:|:---:|
| 11 | 1.89 | 6.24 |
| 14 | 2.22 | 6.38 |
| 17 | 3.19 | 7.06 |
| 20 | 4.31 | 7.85 |
| 23 | 4.71 | 7.95 |

Table 5.1: Scatter data for wind speed and sea states from Pantelleria used in the simulations
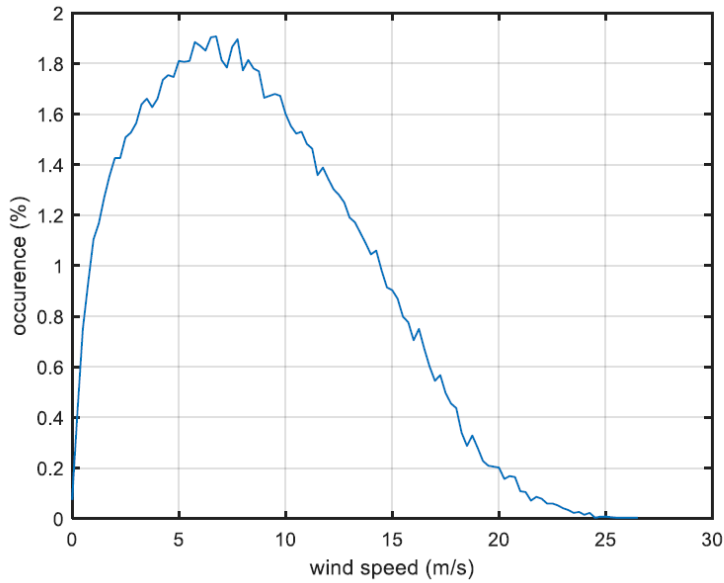
Figure 5.1: Occurrence of the wind speed in Pantelleria, Italy in ten years of data collection [6]

All of them are generated using 'Turbsim', which creates turbulent wind distributions with the mean values above mentioned, referred to the hub height. About the accidental load analysis ,the Normal Turbulence Model(NTM) with the turbulence characteristic "B" are selected. An average value of 0.14 for the exponent of the power law is chosen [28]. It's possible to run simulations using a Matlab script, where it's possible to load the Simulink controller each time, corresponding to the fault under consideration.

## 5.2 Ultimate load analysis

For the case of the extreme environmental conditions, this set of values for the site of Pantelleria [7] is chosen:

| wind speed[m/s] | Significant height[m] | Peak spectral period[s] |
|:---:|:---:|:---:|
| 26.14 | 7.33 | 9.89 |

Table 5.2: Set of extreme environmental conditions for Ultimate load analysis [7]

Simulations are conducted with the turbine switched off, and control is deactivated. The rotor speed is set to zero and the blade pitch angles to 90 degrees, in feathered position.

For the extreme wind shear case, a maximum value of 0.82 for the power law exponent is used. It's a significant value registered during extreme high-shear events in US mid-Atlantic offshore wind lease areas. [29] In this load case, in opposition to the previous case, the turbine is operational, and the control is through Simulink.

## 5.3    Setting the simulation parameters

The simulation time is set to 1500 seconds. This is a small amount of time and is not representative of real situations, but sufficient for testing purposes. In the glue code file, named for example "IEA-15-240-RWT-UMaineSemi.fst" for the 15MW wind turbine, the integration time step (DT) can be changed. The selected time step, denoted as *dt*, plays a critical role in obtaining accurate results while minimizing computational costs. A smaller time step allows for a more precise calculation but increases the computational time. It is necessary to find the balance between the two: in this case the integration time step is set to 0.02 seconds.

In the file "InflowFile.dat" it's possible to call up the "file.bts" corresponding to the wind speed considered in the simulation. In the module HydroDyn it is possible to set the model of the waves (in this case JONSWAP/Pierson-Moskowitz spectrum (irregular)) as well as the wave significant height (m) and peak period of the waves.

## 5.4    Simulation Results

In this section the results obtained in the simulation are presented. For each wind speed, sea state, and type of failure a structure in Matlab is created to store the results. To capture the effects of the wind speed variations, the results of five different ones, 11, 14, 17, 20 and 23 m/s are showed, using the turbulent wind files(.bts) generated by TurbSim. Each structure contains the following arrays of values in time related to the variables to be examined:

- Wind speed[m/s]
- Blade pitch angles[deg°]
- Generator speed[rad/s]
- Platform Pitch[deg°]
- Platform Heave[m]
- Tower base fore-aft shear force[kN]
- Tower base side-to-side shear force[kN]
- Tower base roll (or side-to-side) moment (i.e., the moment caused by side-to-side forces)[kN-m]
- Tower base pitching (or fore-aft) moment (i.e., the moment caused by fore-aft forces)[kN-m]
- Blade 1 flapwise shear force at the blade root[kN]
- Blade 1 edgewise shear force at the blade root[kN]
- Blade 1 edgewise moment (i.e., the moment caused by edgewise forces) at the blade root[kN-m]

- Blade 1 flapwise moment (i.e., the moment caused by flapwise forces) at the blade root[kN-m]

- Electrical generator torque

- Electrical generator power

- Low-speed shaft torque/Rotor Torque

- Fairlead tension of Line 1

For the ultimate load analysis with the turbine switched off, only static magnitudes are studied.

Each of them with a length of 75001 time-steps (corresponding to 1500s/0,02s). The results of the simulation are shown below, disregarding the first ten seconds of simulation to overcome the transient effects.
In order to obtain readable and at the same time meaningful results, the simulation period between 200 and 600 seconds is shown.
In order to make a meaningful comparison between the various results, maximum value, minimum value and standard deviation are taken into account.

### 5.4.1   IEA 15-MW - Blade pitch angle fixed

In the following figures, the main results for the failure "Blade pitch angle fixed" are presented, comparing the simulations with different wind speeds.



Figure 5.2: Main results for the simulation with wind speed=11 m/s

Figure 5.3: Main results for the simulation with wind speed=14 m/s



Figure 5.4: Main results for the simulation with wind speed=17 m/s

Figure 5.5: Main results for the simulation with wind speed=20 m/s



Figure 5.6: Main results for the simulation with wind speed=23 m/s

This scenario explores the impact of having one blade's pitch angle fixed while the others are pitched to feather.

As the wind speed increases, the differences in pitch angles between the blades become more pronounced. This results in an imbalance in the aerodynamic forces acting on the rotor, which can lead to increased vibrations and potential fatigue issues. The overall power generation is expected to decrease with the efficiency of the turbine that is compromised by the fixed blade, particularly at higher wind speeds, like the 23 m/s case. These fluctuations are critical as they could induce additional mechanical stress on the drivetrain, especially at higher wind speeds. The fixed blade pitch could cause asymmetric loading on the turbine, leading to changes

in the platform pitch motion. Indeed, he platform pitch is oscillatory in both cases without and with fault, but the amplitude is much higher with faults (up to $\pm 5$ degrees), indicating more instability in the platform during the fault scenario.

This behavior clearly shows the effect of the control system to mitigate damages. For instance, the sharp drop in generator power after around 200 seconds indicates that the turbine is shutting down or operating at reduced capacity. Once the turbine is no longer producing power, the forces acting on the structure such as moments in the blades, shaft, and tower—would reduce significantly because the turbine is no longer operating under load. This would explain why many of the moments (e.g., TwrBsMt, RootMb1) and forces (e.g., FAIRTEN1) decrease with the fault.

To better understand orders of magnitude, maximum, minimum and standard deviation are calculated for each simulation. The results are filtered for an interval of time between 100s and 600s, because the transient is not representative.
In all the following tables, the first column always represent the result for the faulty-free case, while the second is the result of the corresponding fault model.

| | | Maximum | Minimum | Standard deviation |
|---|---|---|---|---|
| **BldPitch1** | *11 m/s* | 8.7480 4.3219 | 0.0000 0.0000 | 1.8201 0.7950 |
| | *14 m/s* | 13.1576 12.0630 | 4.0350 4.9507 | 1.9338 1.3891 |
| | *17 m/s* | 17.0932 15.5488 | 9.1779 9.1776 | 1.5491 1.0912 |
| | *20 m/s* | 20.6196 18.9878 | 14.4363 14.4363 | 1.3296 0.9121 |
| | *23 m/s* | 24.1368 22.1142 | 17.7800 17.9695 | 1.2130 0.7686 |
| **BldPitch2** | *11 m/s* | 8.7480 90.1397 | 0.0000 0.0000 | 1.8201 35.2380 |
| | *14 m/s* | 13.1576 90.0614 | 4.0350 4.9507 | 1.9338 32.6738 |
| | *17 m/s* | 17.0932 90.0995 | 9.1779 9.1776 | 1.5491 30.8837 |
| | *20 m/s* | 20.6196 90.1051 | 14.4363 14.4363 | 1.3296 29.3630 |
| | *23 m/s* | 24.1368 90.0712 | 17.7800 17.9695 | 1.2130 28.0320 |
| **PtfmPitch** | *11 m/s* | 5.5299 5.5297 | 1.3302 -6.1136 | 0.7480 2.5599 |
| | *14 m/s* | 5.0145 4.3031 | 0.2663 -5.4197 | 1.0405 2.0568 |
| | *17 m/s* | 4.3746 4.3747 | 0.1953 -4.3917 | 0.7983 1.6450 |
| | *20 m/s* | 3.8224 3.8223 | 0.0888 -3.5435 | 0.6472 1.3063 |
| | *23 m/s* | 3.5466 3.5465 | -0.0360 -2.5949 | 0.6059 1.0996 |
| **LSShftMxa** | *11 m/s* | 21235.0684 21214.7129 | 12516.4678 0.0000 | 2196.6156 8203.5992 |
| | *14 m/s* | 21248.9316 21230.5645 | 21144.0117 0.0000 | 15.4488 8654.8113 |
| | *17 m/s* | 21257.1348 21239.0918 | 21131.3145 0.0000 | 17.8012 8687.9187 |
| | *20 m/s* | 21274.6465 21245.5176 | 21121.9023 0.0000 | 21.9140 8731.8737 |
| | *23 m/s* | 21286.2754 21282.0762 | 21096.2285 0.0000 | 25.7781 8774.2580 |

| | | | | |
|---|---|---|---|---|
| **TwrBsFt** | *11 m/s* | 4671.0334 4671.1118 | 1652.6445 1.3513 | 530.1272 1208.0639 |
| | *14 m/s* | 4291.3070 3861.9894 | 584.7426 6.4540 | 710.9212 959.7931 |
| | *17 m/s* | 4126.4401 4126.5421 | 159.1385 4.5902 | 641.8190 810.3658 |
| | *20 m/s* | 4097.6110 4097.5883 | 8.8075 6.4951 | 699.0689 735.2123 |
| | *23 m/s* | 4099.4283 4099.5588 | 17.8944 4.3285 | 716.0145 692.9817 |
| **TwrBsMt** | *11 m/s* | 439663.4950 439655.6989 | 160851.9008 248.1398 | 50389.7371 106675.8427 |
| | *14 m/s* | 410534.2799 364423.7819 | 37353.1484 466.9895 | 67464.2077 81559.0965 |
| | *17 m/s* | 385227.0383 385234.4773 | 22809.7752 643.6452 | 60124.0384 66348.8118 |
| | *20 m/s* | 393777.4953 393785.6455 | 15975.1307 438.5307 | 63780.3842 64687.8140 |
| | *23 m/s* | 387754.4633 387767.0749 | 9597.3486 299.7102 | 63965.3745 61382.4579 |
| **RootFb1** | *11 m/s* | 1306.1672 1306.1682 | 483.5387 94.6271 | 131.5086 248.9026 |
| | *14 m/s* | 1203.1547 1199.4182 | 338.6004 263.9323 | 144.9964 111.0690 |
| | *17 m/s* | 1149.8011 1108.0522 | 158.8869 8.1834 | 155.2612 197.6217 |
| | *20 m/s* | 1139.1564 1139.1668 | 125.9497 145.0195 | 167.0427 168.7657 |
| | *23 m/s* | 1130.2712 1064.3386 | 35.9176 111.4292 | 178.6648 161.7232 |
| **RootMb1** | *11 m/s* | 77515.0023 77520.1506 | 22052.1589 3772.9052 | 7757.4003 17311.2768 |
| | *14 m/s* | 70196.3611 68205.4107 | 12196.1216 8538.8016 | 8859.0997 10635.6179 |
| | *17 m/s* | 60119.0209 57348.5771 | 2211.2142 2209.5970 | 8997.9296 9421.4140 |
| | *20 m/s* | 53329.1239 50075.8730 | 70.9733 318.8383 | 9287.1560 7602.7292 |
| | *23 m/s* | 50926.9743 52587.0666 | 159.2206 387.6251 | 9302.4846 7278.0113 |
| **GenPwr** | *11 m/s* | 15939.0459 15534.0205 | 8314.3545 0.0000 | 1828.4364 5587.0031 |
| | *14 m/s* | 17584.6094 16851.4648 | 13479.9824 0.0000 | 746.1326 6401.7755 |
| | *17 m/s* | 17918.7012 17918.7715 | 14680.9307 0.0000 | 593.7853 6500.7721 |
| | *20 m/s* | 17655.9375 17647.2539 | 14449.3174 0.0000 | 620.8355 6493.9332 |
| | *23 m/s* | 17879.0840 17391.1074 | 14399.1465 0.0000 | 664.7399 6485.9932 |
| **FAIRTEN1** | *11 m/s* | 4175905.7500 4130368.5000 | 3217655.2500 2091546.6250 | 204321.6746 560074.3929 |
| | *14 m/s* | 4221720.5000 4123178.7500 | 2994581.5000 2174930.2500 | 275044.0517 467629.3444 |
| | *17 m/s* | 3885722.2500 3885710.0000 | 2922031.0000 2266522.0000 | 191405.7774 372453.6477 |
| | *20 m/s* | 3753333.0000 3753326.7500 | 2869060.5000 2325026.7500 | 156043.5705 311744.6000 |
| | *23 m/s* | 3664181.0000 3664190.5000 | 2825870.2500 2382466.2500 | 155616.6418 273463.1407 |

Table 5.3: Comparison of results for "No fault" and "Pitched to feather" models at different wind speeds

## 5.4.2   IEA 15-MW - Offset in blade pitch angle

In the following figures, the main results for the failure "Offset" are presented, comparing the simulations with different wind speeds.
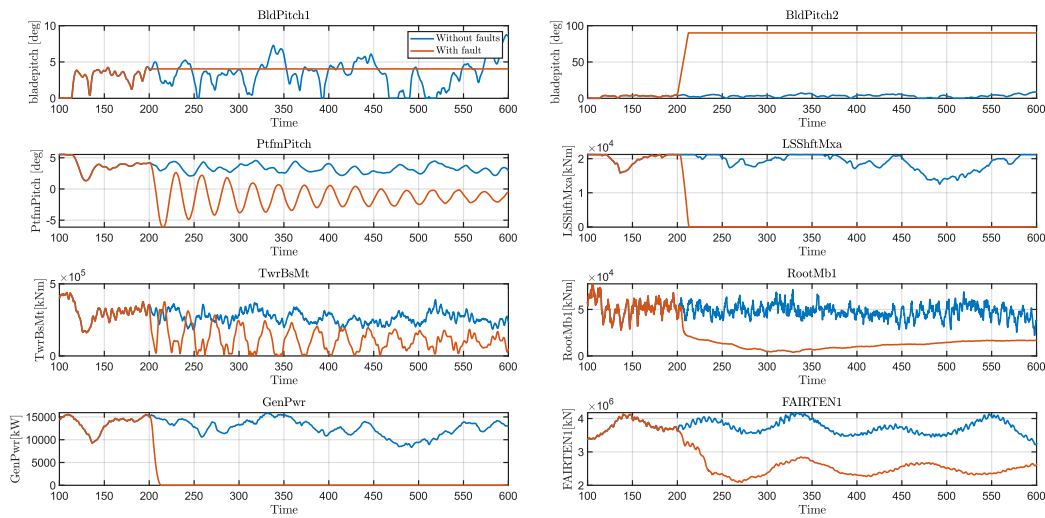


Figure 5.7: Main results for the simulation with wind speed=11 m/s
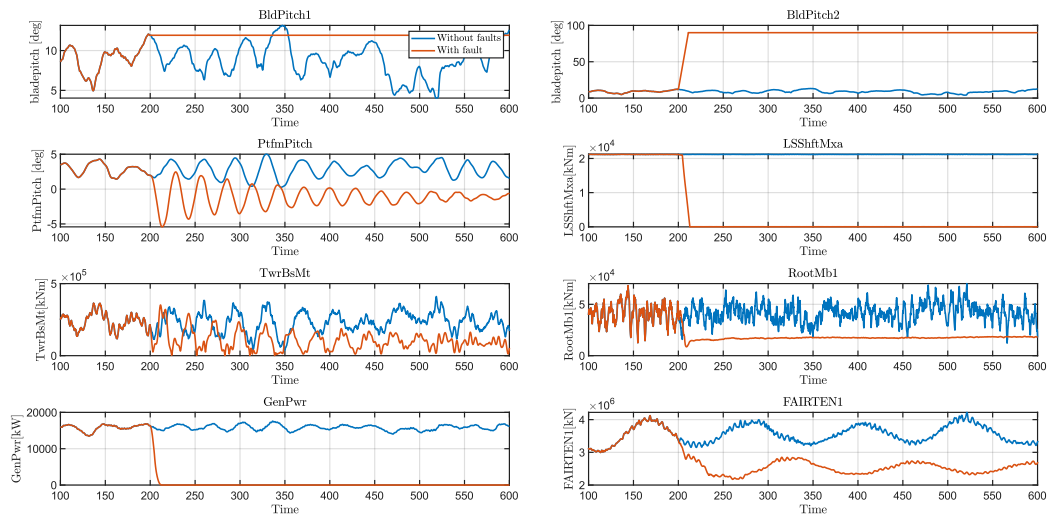


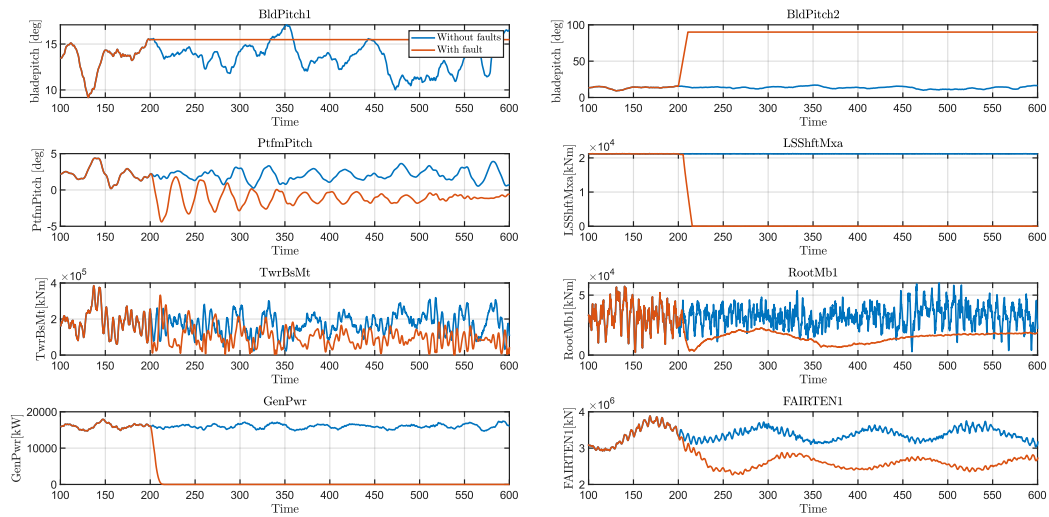Figure 5.8: Main results for the simulation with wind speed=14 m/s

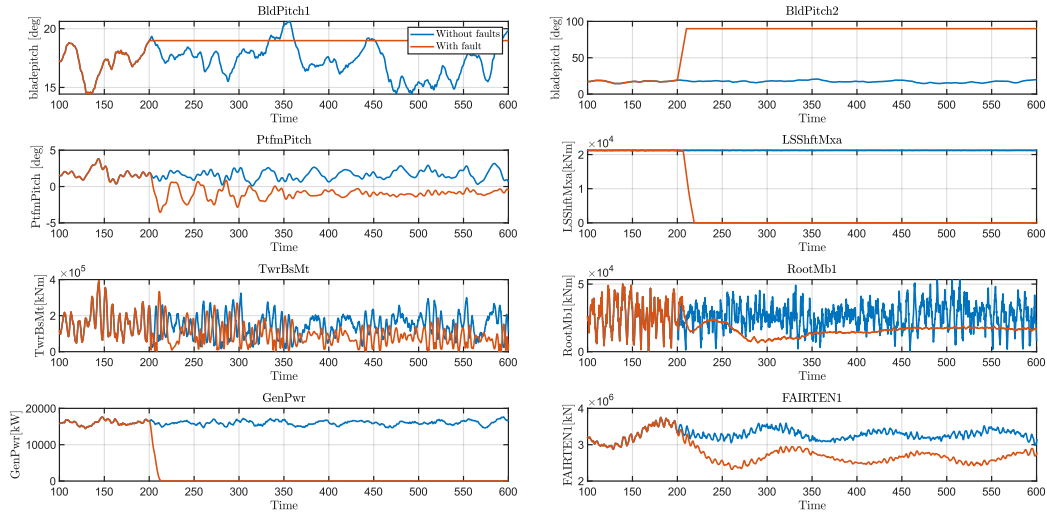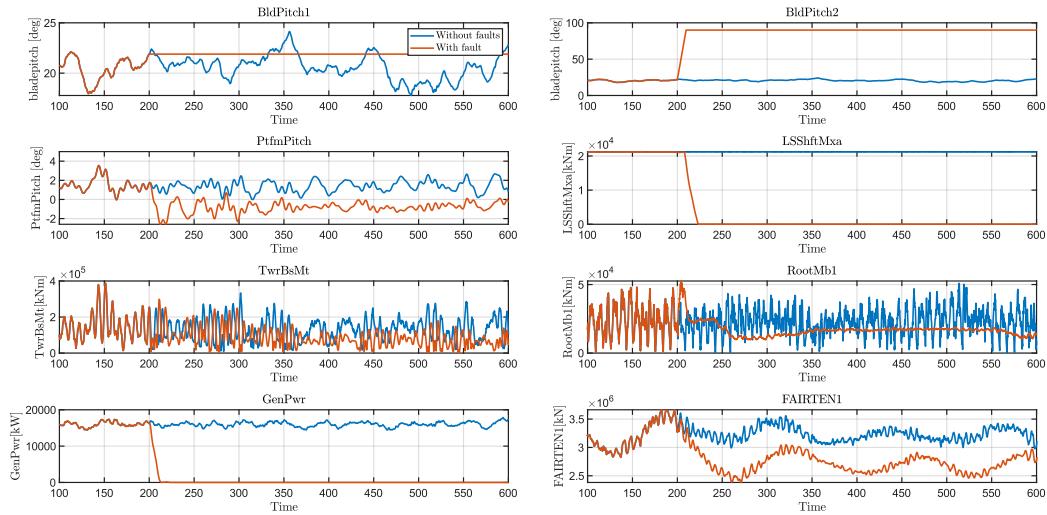Figure 5.9: Main results for the simulation with wind speed=17 m/s



Figure 5.10: Main results for the simulation with wind speed=20 m/s

Figure 5.11: Main results for the simulation with wind speed=23 m/s

| | | Maximum | Minimum | Standard deviation |
|---|---|---|---|---|
| **BldPitch1** | *11 m/s* | 8.7480 11.7480 | 0.0000 0.0000 | 1.8201 2.3197 |
| | *14 m/s* | 13.1576 15.5851 | 4.0350 4.9507 | 1.9338 1.9512 |
| | *17 m/s* | 17.0932 19.0334 | 9.1779 9.1779 | 1.5491 1.7908 |
| | *20 m/s* | 20.6196 22.6130 | 14.4363 14.4363 | 1.3296 1.6146 |
| | *23 m/s* | 24.1368 26.1848 | 17.7800 17.9694 | 1.2130 1.5236 |
| **BldPitch2** | *11 m/s* | 8.7480 8.7480 | 0.0000 0.0000 | 1.8201 1.8201 |
| | *14 m/s* | 13.1576 12.5851 | 4.0350 4.0350 | 1.9338 1.8273 |
| | *17 m/s* | 17.0932 16.0334 | 9.1779 8.8344 | 1.5491 1.6246 |
| | *20 m/s* | 20.6196 19.6130 | 14.4363 13.1534 | 1.3296 1.4159 |
| | *23 m/s* | 24.1368 23.1848 | 17.7800 16.7218 | 1.2130 1.3006 |
| **PtfmPitch** | *11 m/s* | 5.5299 5.5299 | 1.3302 1.3302 | 0.7480 0.8265 |
| | *14 m/s* | 5.0145 4.7350 | 0.2663 0.7548 | 1.0405 0.8458 |
| | *17 m/s* | 4.3746 4.3746 | 0.1953 0.1953 | 0.7983 0.8392 |
| | *20 m/s* | 3.8224 3.8224 | 0.0888 0.0931 | 0.6472 0.6593 |
| | *23 m/s* | 3.5466 3.5466 | -0.0360 -0.0360 | 0.6059 0.6061 |

56

| | | | | |
|---|---|---|---|---|
| **LSShftMxa** | *11 m/s* | 21235.0684 21223.3984 | 12516.4678 12218.2686 | 2196.6156 2330.8383 |
| | *14 m/s* | 21248.9316 21245.2930 | 21144.0117 21141.6289 | 15.4488 15.0063 |
| | *17 m/s* | 21257.1348 21263.3184 | 21131.3145 21133.6309 | 17.8012 18.1612 |
| | *20 m/s* | 21274.6465 21264.6582 | 21121.9023 21122.0527 | 21.9140 22.0654 |
| | *23 m/s* | 21286.2754 21285.2266 | 21096.2285 21096.2285 | 25.7781 25.7403 |
| **TwrBsFt** | *11 m/s* | 4671.0334 4671.0334 | 1652.6445 1616.1864 | 530.1272 581.0119 |
| | *14 m/s* | 4291.3070 4429.6643 | 584.7426 922.9856 | 710.9212 599.5237 |
| | *17 m/s* | 4126.4401 4126.4401 | 159.1385 159.4342 | 641.8190 663.4447 |
| | *20 m/s* | 4097.6110 4097.6110 | 8.8075 13.2226 | 699.0689 700.3473 |
| | *23 m/s* | 4099.4283 4099.4283 | 17.8944 4.5631 | 716.0145 710.7704 |
| **TwrBsMt** | *11 m/s* | 439663.4950 439663.4950 | 160851.9008 138295.0462 | 50389.7371 56231.8601 |
| | *14 m/s* | 410534.2799 377309.1576 | 37353.1484 56728.1948 | 67464.2077 56910.1404 |
| | *17 m/s* | 385227.0383 385227.0383 | 22809.7752 18418.8750 | 60124.0384 61958.8980 |
| | *20 m/s* | 393777.4953 393777.4953 | 15975.1307 11494.0457 | 63780.3842 64847.6372 |
| | *23 m/s* | 387754.4633 387754.4633 | 9597.3486 5588.0265 | 63965.3745 64825.3639 |
| **RootFb1** | *11 m/s* | 1306.1672 1306.1672 | 483.5387 373.1976 | 131.5086 149.5438 |
| | *14 m/s* | 1203.1547 1199.3977 | 338.6004 231.5881 | 144.9964 152.6692 |
| | *17 m/s* | 1149.8011 1108.0723 | 158.8869 96.0859 | 155.2612 166.6515 |
| | *20 m/s* | 1139.1564 1139.1564 | 125.9497 11.8773 | 167.0427 177.8627 |
| | *23 m/s* | 1130.2712 1064.3307 | 35.9176 21.0668 | 178.6648 186.5668 |
| **RootMb1** | *11 m/s* | 77515.0023 77515.0023 | 22052.1589 16877.0837 | 7757.4003 9415.3736 |
| | *14 m/s* | 70196.3611 68202.2382 | 12196.1216 3178.5137 | 8859.0997 9315.4974 |
| | *17 m/s* | 60119.0209 57348.0579 | 2211.2142 465.2633 | 8997.9296 9431.2454 |
| | *20 m/s* | 53329.1239 50076.0419 | 70.9733 314.5634 | 9287.1560 8635.5037 |
| | *23 m/s* | 50926.9743 48049.8502 | 159.2206 148.2003 | 9302.4846 7935.5424 |
| **GenPwr** | *11 m/s* | 15939.0459 15630.3340 | 8314.3545 8139.4668 | 1828.4364 1843.1247 |
| | *14 m/s* | 17584.6094 17050.3555 | 13479.9824 13186.8311 | 746.1326 841.9551 |
| | *17 m/s* | 17918.7012 17918.7012 | 14680.9307 14600.4629 | 593.7853 591.8628 |
| | *20 m/s* | 17655.9375 17647.2812 | 14449.3174 14449.3174 | 620.8355 604.4155 |
| | *23 m/s* | 17879.0840 17579.6660 | 14399.1465 14388.6494 | 664.7399 639.6189 |

| | | | | |
|---|---|---|---|---|
| | *11 m/s* | 4175905.7500 4130367.2500 | 3217655.2500 3115639.0000 | 204321.6746 213495.2096 |
| | *14 m/s* | 4221720.5000 4123180.2500 | 2994581.5000 2994581.5000 | 275044.0517 235388.3786 |
| **FAIRTEN1** | *17 m/s* | 3885722.2500 3885722.2500 | 2922031.0000 2922031.0000 | 191405.7774 192648.5986 |
| | *20 m/s* | 3753333.0000 3753333.0000 | 2869060.5000 2869060.5000 | 156043.5705 155971.9318 |
| | *23 m/s* | 3664181.0000 3664181.0000 | 2825870.2500 2825870.2500 | 155616.6418 156238.4041 |

Table 5.4: Comparison of results for "No fault" and "Offset" models at different wind speeds

The blade pitch variable follows a similar pattern in comparison with the offset fault-free case, but the oscillations appear slightly larger in magnitude. This suggests that the turbine's pitch control is still functional but may be experiencing less stability or increased oscillations due to the fault. In terms of platform motion, the oscillations are nearly identical to the fault-free case, with similar amplitude and frequency. This indicates that the fault has minimal impact on the platform pitch in this scenario. The moments are slightly higher, especially in the 250–450 second range, indicating that the fault is introducing higher dynamic loads on the tower, possibly due to less efficient blade pitch control, but the difference is not so severe. There is little to no impact of the fault on the root moment of the blades, suggesting that the blades are not experiencing significantly different forces. Despite the fault, the turbine continues to generate power at nearly the same rate. In this plots, the fault has minimal overall impact on the system. Most variables, including blade pitch, platform pitch, generator power, and fairlead tension, are nearly identical between the faulty and non-faulty cases.

### 5.4.3   IEA 15-MW - Precision degradation



Figure 5.12: Main results for the simulation with wind speed=11 m/s
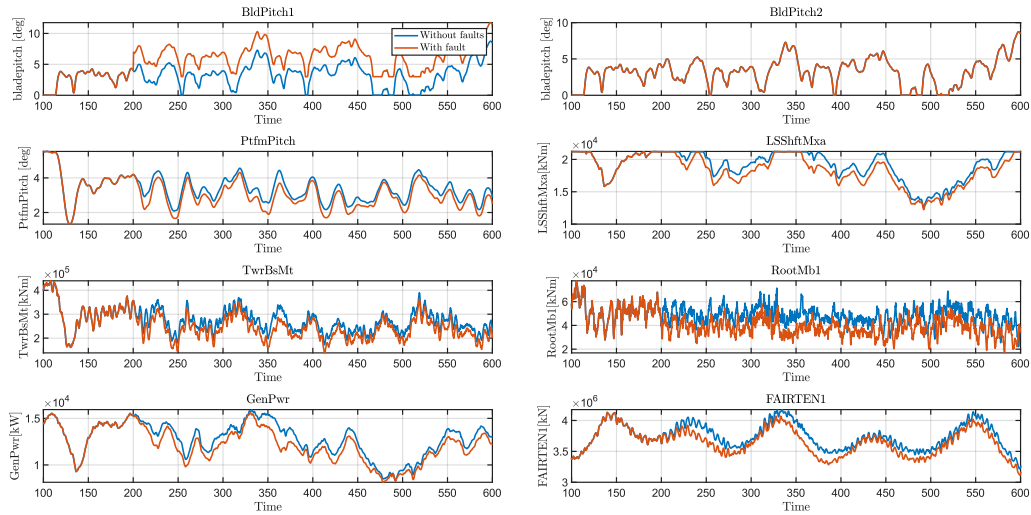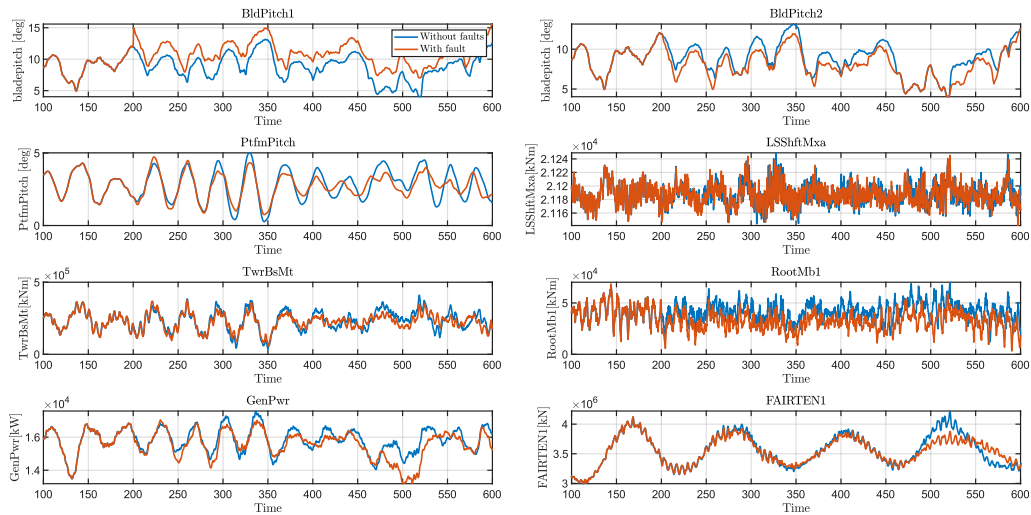
58

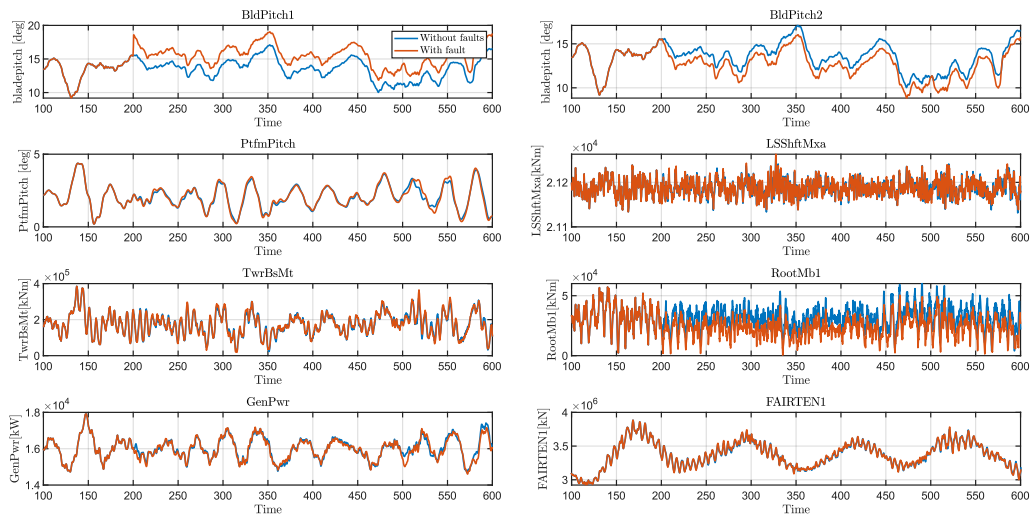Figure 5.13: Main results for the simulation with wind speed=14 m/s



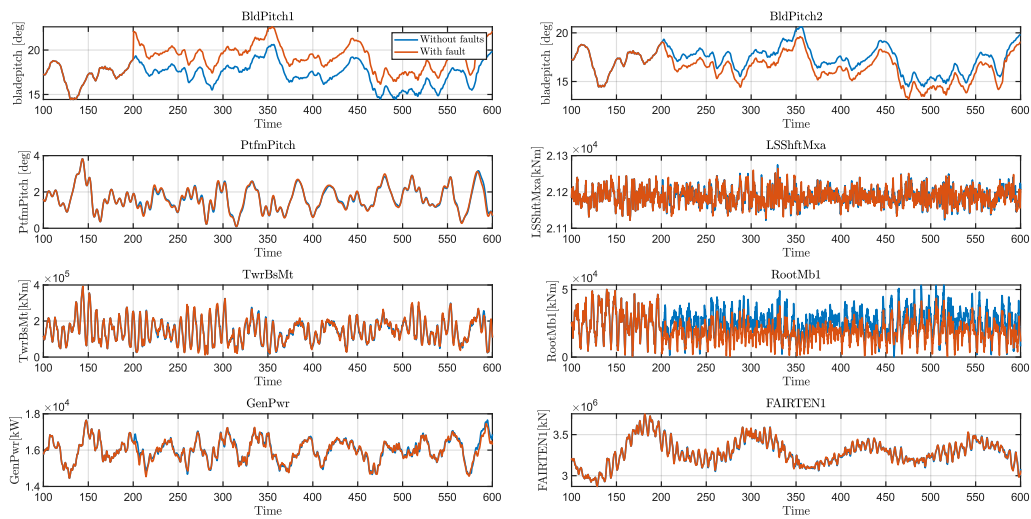Figure 5.14: Main results for the simulation with wind speed=17 m/s

Figure 5.15: Main results for the simulation with wind speed=20 m/s
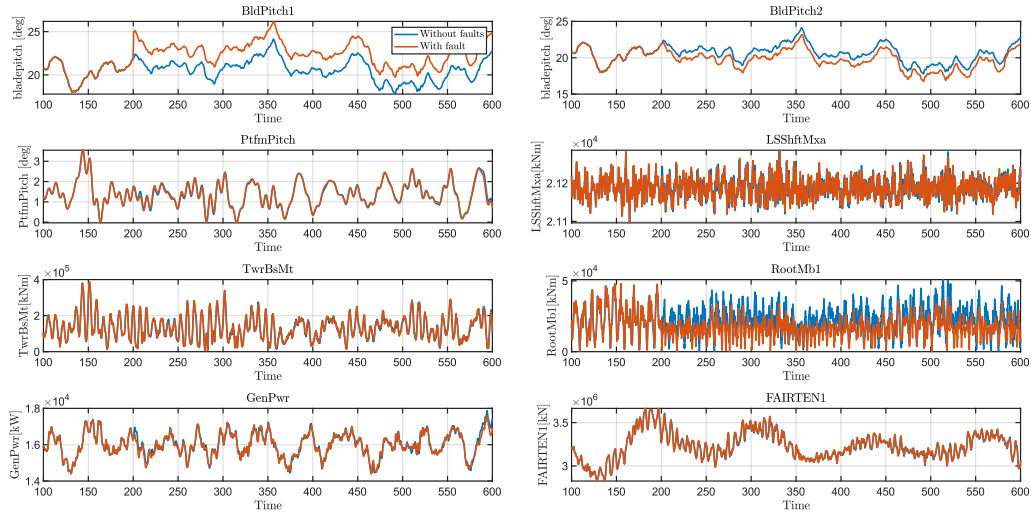


Figure 5.16: Main results for the simulation with wind speed=23 m/s

The fault appears to have minimal impact on the platform pitch, indicating that
the platform's tilt or rotation is not heavily affected by the fault. The fault has
a more important impact on the tower base moment, indicating that structural
loads may increase, possibly stressing the tower structure over time. While the fault
causes some increase in loads at the blade root, the difference is not extreme. The
turbine continues to generate power at a similar rate even under fault conditions,
showing the fault doesn't significantly affect energy production. The mooring lines
experience only minor increases in tension under fault conditions, showing that the
fault has minimal impact on mooring forces.

| | | Maximum | Minimum | Standard deviation |
|---|---|---|---|---|
| **BldPitch1** | *11 m/s* | 8.7480 12.9512 | 0.0000 0.0000 | 1.8201 2.3412 |
| | *14 m/s* | 13.1576 16.5178 | 4.0350 4.9507 | 1.9338 1.9838 |
| | *17 m/s* | 17.0932 19.8619 | 9.1779 9.1779 | 1.5491 1.8322 |
| | *20 m/s* | 20.6196 23.6336 | 14.4363 14.4363 | 1.3296 1.6612 |
| | *23 m/s* | 24.1368 27.0742 | 17.7800 17.9694 | 1.2130 1.5730 |
| **BldPitch2** | *11 m/s* | 8.7480 8.7480 | 0.0000 0.0000 | 1.8201 1.8201 |
| | *14 m/s* | 13.1576 12.5851 | 4.0350 4.0350 | 1.9338 1.8288 |
| | *17 m/s* | 17.0932 16.0422 | 9.1779 8.8490 | 1.5491 1.6257 |
| | *20 m/s* | 20.6196 19.5933 | 14.4363 13.1331 | 1.3296 1.4162 |
| | *23 m/s* | 24.1368 23.1504 | 17.7800 16.6715 | 1.2130 1.2996 |
| **PtfmPitch** | *11 m/s* | 5.5299 5.5299 | 1.3302 1.3302 | 0.7480 0.8255 |
| | *14 m/s* | 5.0145 4.7323 | 0.2663 0.7453 | 1.0405 0.8462 |
| | *17 m/s* | 4.3746 4.3746 | 0.1953 0.1953 | 0.7983 0.8425 |
| | *20 m/s* | 3.8224 3.8224 | 0.0888 0.0862 | 0.6472 0.6609 |
| | *23 m/s* | 3.5466 3.5466 | -0.0360 -0.0360 | 0.6059 0.6073 |
| **LSShftMxa** | *11 m/s* | 21235.0684 21226.6289 | 12516.4678 12219.8037 | 2196.6156 2328.2625 |
| | *14 m/s* | 21248.9316 21248.5000 | 21144.0117 21142.1270 | 15.4488 15.1166 |
| | *17 m/s* | 21257.1348 21264.6680 | 21131.3145 21133.6309 | 17.8012 18.3370 |
| | *20 m/s* | 21274.6465 21261.9121 | 21121.9023 21120.1797 | 21.9140 22.3405 |
| | *23 m/s* | 21286.2754 21286.5195 | 21096.2285 21096.2285 | 25.7781 25.9237 |
| **TwrBsFt** | *11 m/s* | 4671.0334 4671.0334 | 1652.6445 1606.9972 | 530.1272 580.2926 |
| | *14 m/s* | 4291.3070 4417.2639 | 584.7426 910.1873 | 710.9212 600.0478 |
| | *17 m/s* | 4126.4401 4126.4401 | 159.1385 158.7772 | 641.8190 665.1200 |
| | *20 m/s* | 4097.6110 4097.6110 | 8.8075 16.3035 | 699.0689 700.4977 |
| | *23 m/s* | 4099.4283 4099.4283 | 17.8944 12.2115 | 716.0145 710.8449 |
| **TwrBsMt** | *11 m/s* | 439663.4950 439663.4950 | 160851.9008 137285.3732 | 50389.7371 56143.4524 |
| | *14 m/s* | 410534.2799 378429.9660 | 37353.1484 54796.1906 | 67464.2077 56952.4534 |
| | *17 m/s* | 385227.0383 385227.0383 | 22809.7752 18610.0673 | 60124.0384 62136.4924 |
| | *20 m/s* | 393777.4953 393777.4953 | 15975.1307 12055.4950 | 63780.3842 64874.3596 |
| | *23 m/s* | 387754.4633 387754.4633 | 9597.3486 7214.2166 | 63965.3745 64817.7630 |

| | | | | |
|---|---|---|---|---|
| **RootFb1** | *11 m/s* | 1306.1672 1306.1672 | 483.5387 377.9200 | 131.5086 149.7341 |
| | *14 m/s* | 1203.1547 1199.3977 | 338.6004 199.0707 | 144.9964 152.6465 |
| | *17 m/s* | 1149.8011 1108.0723 | 158.8869 95.5626 | 155.2612 166.9599 |
| | *20 m/s* | 1139.1564 1139.1564 | 125.9497 9.3253 | 167.0427 178.0239 |
| | *23 m/s* | 1130.2712 1064.3307 | 35.9176 8.7608 | 178.6648 186.4837 |
| **RootMb1** | *11 m/s* | 77515.0023 77515.0023 | 22052.1589 18114.7888 | 7757.4003 9463.0232 |
| | *14 m/s* | 70196.3611 68202.2382 | 12196.1216 1680.6227 | 8859.0997 9356.3287 |
| | *17 m/s* | 60119.0209 57348.0579 | 2211.2142 101.4225 | 8997.9296 9481.3765 |
| | *20 m/s* | 53329.1239 50076.0419 | 70.9733 314.5634 | 9287.1560 8691.3482 |
| | *23 m/s* | 50926.9743 48049.8502 | 159.2206 225.6521 | 9302.4846 7982.6458 |
| **GenPwr** | *11 m/s* | 15939.0459 15620.8145 | 8314.3545 8116.4722 | 1828.4364 1841.1842 |
| | *14 m/s* | 17584.6094 17042.4805 | 13479.9824 13197.9336 | 746.1326 840.4468 |
| | *17 m/s* | 17918.7012 17918.7012 | 14680.9307 14587.7656 | 593.7853 594.1076 |
| | *20 m/s* | 17655.9375 17647.2812 | 14449.3174 14449.3174 | 620.8355 606.4560 |
| | *23 m/s* | 17879.0840 17599.2129 | 14399.1465 14398.6455 | 664.7399 640.9805 |
| **FAIRTEN1** | *11 m/s* | 4175905.7500 4130367.2500 | 3217655.2500 3112266.7500 | 204321.6746 213716.1744 |
| | *14 m/s* | 4221720.5000 4123180.2500 | 2994581.5000 2994581.5000 | 275044.0517 236233.1351 |
| | *17 m/s* | 3885722.2500 3885722.2500 | 2922031.0000 2922031.0000 | 191405.7774 192584.6538 |
| | *20 m/s* | 3753333.0000 3753333.0000 | 2869060.5000 2869060.5000 | 156043.5705 156032.2727 |
| | *23 m/s* | 3664181.0000 3664181.0000 | 2825870.2500 2825870.2500 | 155616.6418 156229.3569 |

Table 5.5: Comparison of results for "No fault" and "Precision degradation" models at different wind speeds

### 5.4.4   IEA 15-MW - Disconnection from the grid

In this section, the results of the grid disconnection simulation are presented. As this dynamic occurs in the order of milliseconds, the transient has been neglected.
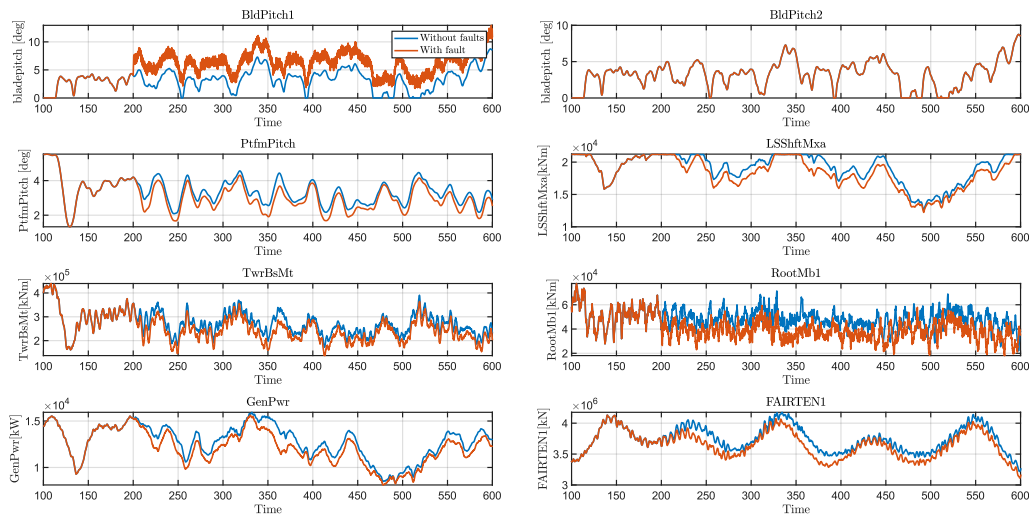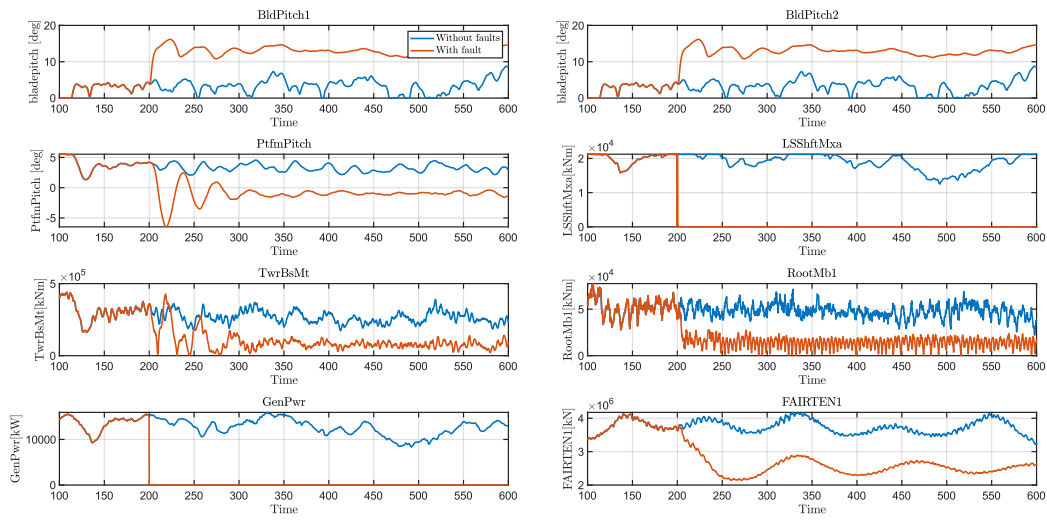
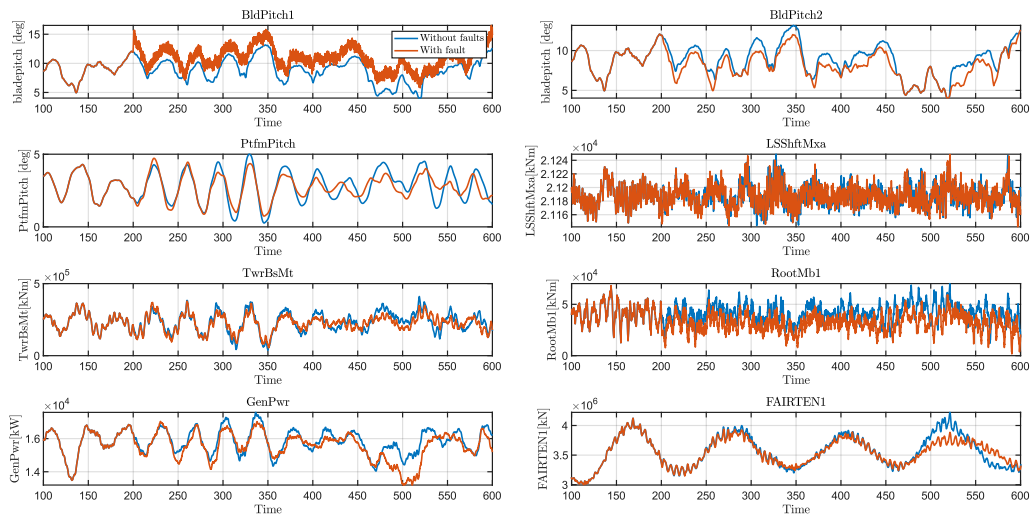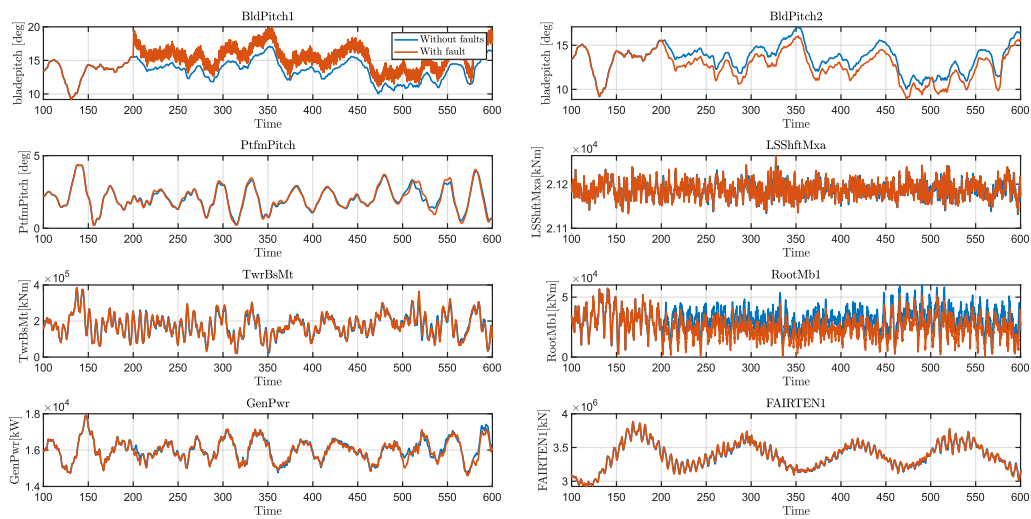Figure 5.17: Main results for the simulation with wind speed=11 m/s
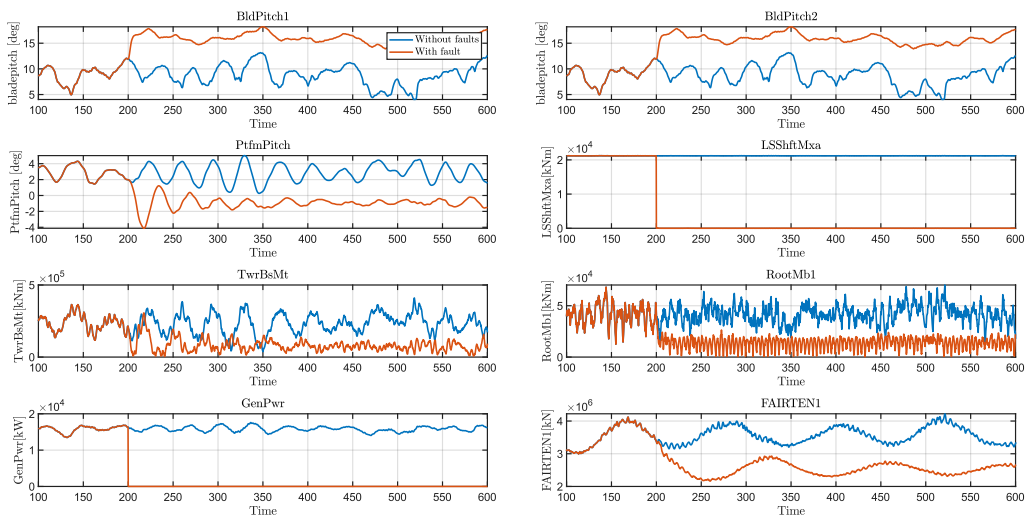


Figure 5.18: Main results for the simulation with wind speed=14 m/s
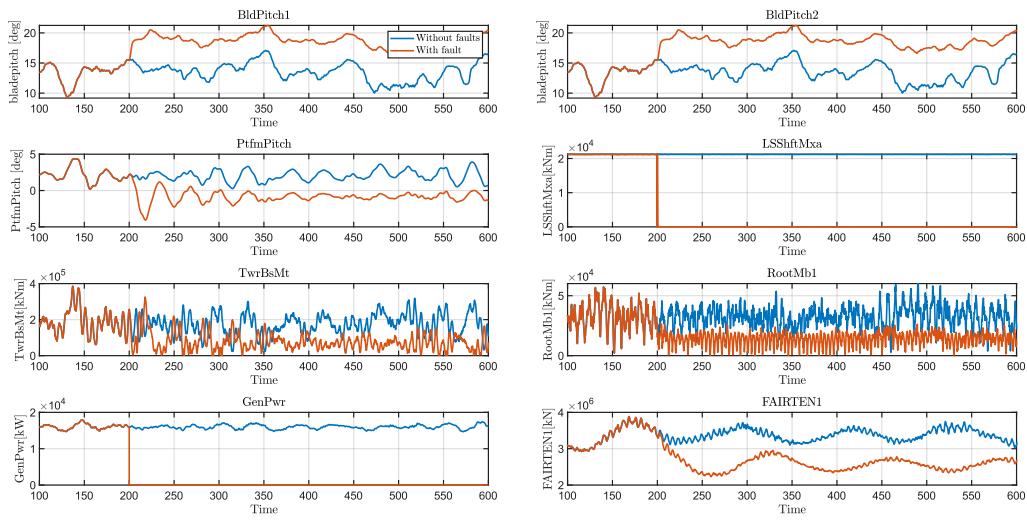
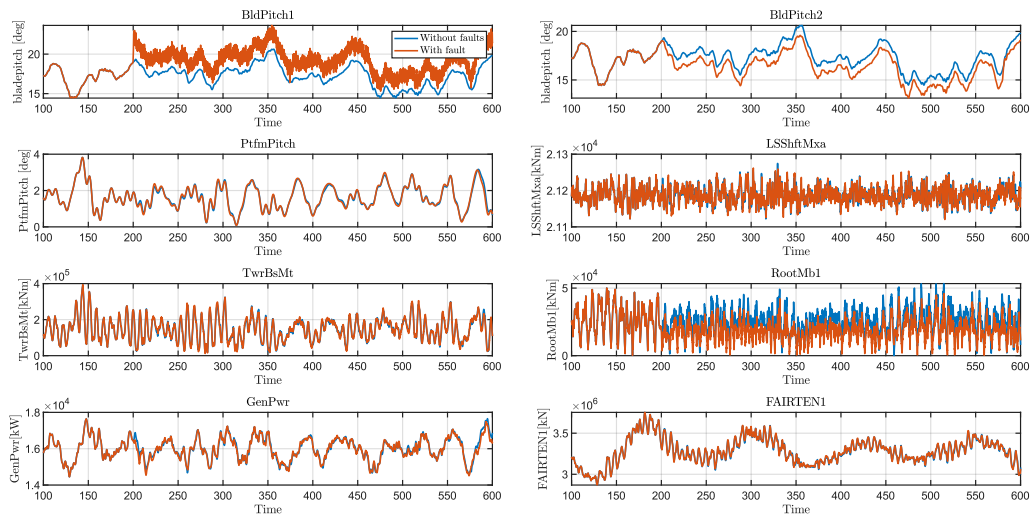Figure 5.19: Main results for the simulation with wind speed=17 m/s



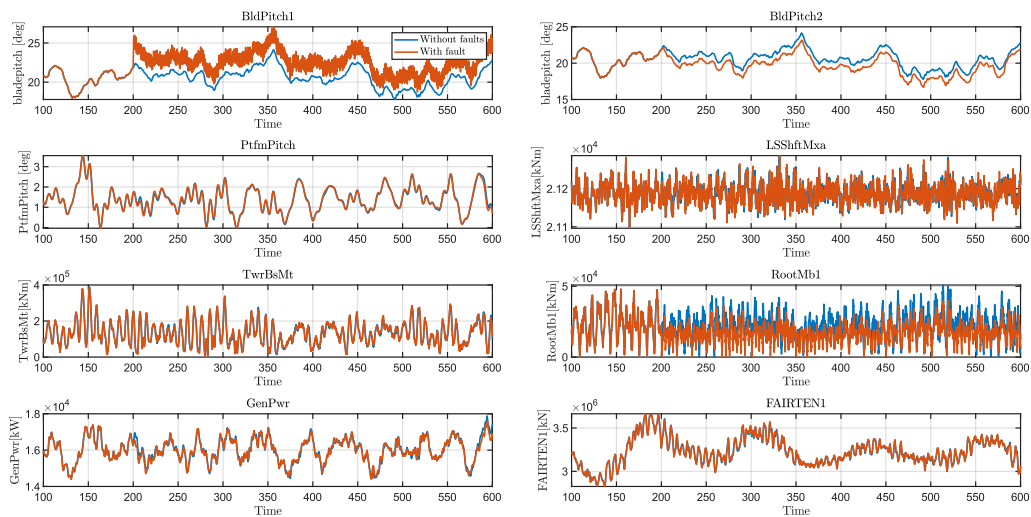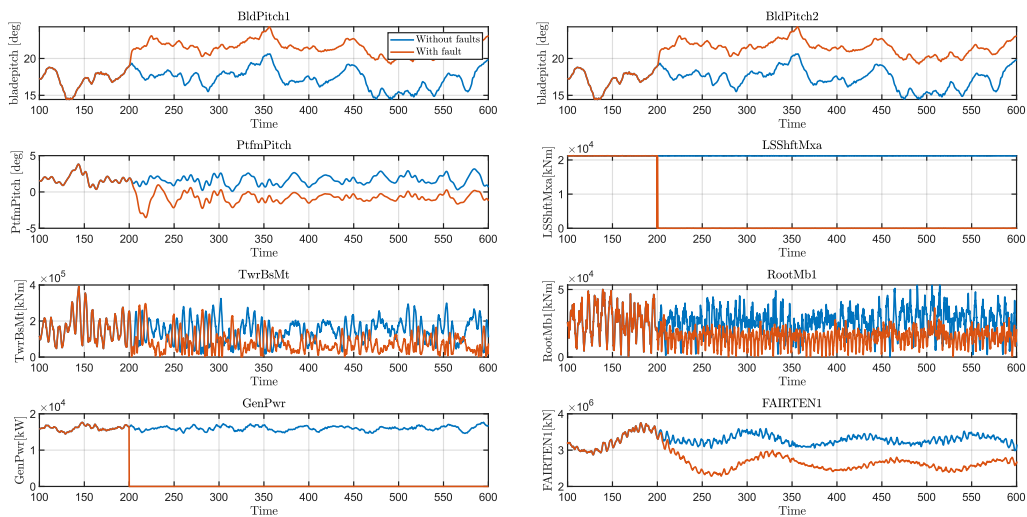Figure 5.20: Main results for the simulation with wind speed=20 m/s

64
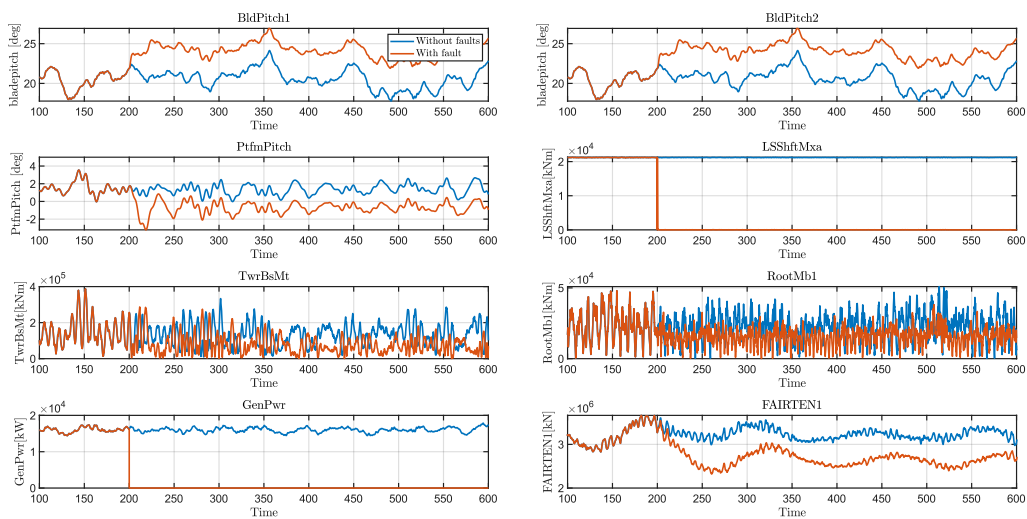
Figure 5.21: Main results for the simulation with wind speed=23 m/s

Faults are causing the turbine to hold the blade pitch at a higher angle for a longer time, and it could be an attempt to reduce loads on the turbine under abnormal conditions. The platform pitch experiences larger fluctuations, reaching extremes of -2 to 2 degrees. The fault significantly affects the drivetrain, losing totally torque or moment transmission to the low-speed shaft, showing the intervent of a safety mechanism to avoid further damage.

| | | Maximum | Minimum | Standard deviation |
|---|---|---|---|---|
| **BldPitch1** | *11 m/s* | 8.7480 16.1802 | 0.0000 0.0000 | 1.8201 4.2552 |
| | *14 m/s* | 13.1576 18.1944 | 4.0350 4.9507 | 1.9338 2.9781 |
| | *17 m/s* | 17.0932 21.2472 | 9.1779 9.1779 | 1.5491 2.3926 |
| | *20 m/s* | 20.6196 24.2943 | 14.4363 14.4363 | 1.3296 1.9912 |
| | *23 m/s* | 24.1368 26.9201 | 17.7800 17.9694 | 1.2130 1.7550 |
| **BldPitch2** | *11 m/s* | 8.7480 16.1802 | 0.0000 0.0000 | 1.8201 4.2552 |
| | *14 m/s* | 13.1576 18.1944 | 4.0350 4.9507 | 1.9338 2.9781 |
| | *17 m/s* | 17.0932 21.2472 | 9.1779 9.1779 | 1.5491 2.3926 |
| | *20 m/s* | 20.6196 24.2943 | 14.4363 14.4363 | 1.3296 1.9912 |
| | *23 m/s* | 24.1368 26.9201 | 17.7800 17.9694 | 1.2130 1.7550 |

| | | | | |
|---|---|---|---|---|
| **PtfmPitch** | *11 m/s* | 5.5299 5.5299 | 1.3302 -6.4718 | 0.7480 2.2803 |
| | *14 m/s* | 5.0145 4.3031 | 0.2663 -4.1231 | 1.0405 1.7093 |
| | *17 m/s* | 4.3746 4.3746 | 0.1953 -4.0562 | 0.7983 1.4701 |
| | *20 m/s* | 3.8224 3.8224 | 0.0888 -3.5218 | 0.6472 1.2532 |
| | *23 m/s* | 3.5466 3.5466 | -0.0360 -3.2135 | 0.6059 1.1193 |
| **LSShftMxa** | *11 m/s* | 21235.0684 21214.6934 | 12516.4678 0.0000 | 2196.6156 8006.8129 |
| | *14 m/s* | 21248.9316 21230.5625 | 21144.0117 0.0000 | 15.4488 8475.3367 |
| | *17 m/s* | 21257.1348 21239.0898 | 21131.3145 0.0000 | 17.8012 8474.6009 |
| | *20 m/s* | 21274.6465 21245.5195 | 21121.9023 0.0000 | 21.9140 8474.1122 |
| | *23 m/s* | 21286.2754 21282.0996 | 21096.2285 0.0000 | 25.7781 8473.4618 |
| **TwrBsFt** | *11 m/s* | 4671.0334 4671.0334 | 1652.6445 1.1828 | 530.1272 1298.9621 |
| | *14 m/s* | 4291.3070 3861.8848 | 584.7426 1.7199 | 710.9212 970.6731 |
| | *17 m/s* | 4126.4401 4126.4401 | 159.1385 3.7133 | 641.8190 819.8902 |
| | *20 m/s* | 4097.6110 4097.6110 | 8.8075 2.0652 | 699.0689 732.6317 |
| | *23 m/s* | 4099.4283 4099.4283 | 17.8944 0.9295 | 716.0145 691.8489 |
| **TwrBsMt** | *11 m/s* | 439663.4950 439663.4950 | 160851.9008 1127.6764 | 50389.7371 106493.2667 |
| | *14 m/s* | 410534.2799 364420.9088 | 37353.1484 4543.1540 | 67464.2077 77311.8930 |
| | *17 m/s* | 385227.0383 385227.0383 | 22809.7752 431.5933 | 60124.0384 68970.6754 |
| | *20 m/s* | 393777.4953 393777.4953 | 15975.1307 407.0038 | 63780.3842 65781.9165 |
| | *23 m/s* | 387754.4633 387754.4633 | 9597.3486 427.7371 | 63965.3745 63453.7835 |
| **RootFb1** | *11 m/s* | 1306.1672 1306.1672 | 483.5387 7.8124 | 131.5086 243.9168 |
| | *14 m/s* | 1203.1547 1199.3977 | 338.6004 2.2136 | 144.9964 219.1622 |
| | *17 m/s* | 1149.8011 1108.0723 | 158.8869 8.7074 | 155.2612 205.0436 |
| | *20 m/s* | 1139.1564 1139.1564 | 125.9497 4.3223 | 167.0427 199.5662 |
| | *23 m/s* | 1130.2712 1064.3307 | 35.9176 3.0644 | 178.6648 196.7071 |
| **RootMb1** | *11 m/s* | 77515.0023 77515.0023 | 22052.1589 111.0997 | 7757.4003 16542.1200 |
| | *14 m/s* | 70196.3611 68202.2382 | 12196.1216 285.2258 | 8859.0997 12592.0274 |
| | *17 m/s* | 60119.0209 57348.0579 | 2211.2142 131.2509 | 8997.9296 9814.1057 |
| | *20 m/s* | 53329.1239 50076.0419 | 70.9733 142.7948 | 9287.1560 8297.1049 |
| | *23 m/s* | 50926.9743 48049.8502 | 159.2206 108.1680 | 9302.4846 7824.0941 |

| | | | | | | |
|---|---|---|---|---|---|---|
| **GenPwr** | *11 m/s* | 15939.0459 | 15534.0781 | 8314.3545 | 0.0000 | 1828.4364 5495.9643 |
| | *14 m/s* | 17584.6094 | 16851.5527 | 13479.9824 | 0.0000 | 746.1326 6337.7881 |
| | *17 m/s* | 17918.7012 | 17918.7012 | 14680.9307 | 0.0000 | 593.7853 6442.0013 |
| | *20 m/s* | 17655.9375 | 17647.2812 | 14449.3174 | 0.0000 | 620.8355 6429.4134 |
| | *23 m/s* | 17879.0840 | 17390.9609 | 14399.1465 | 0.0000 | 664.7399 6418.7284 |
| **FAIRTEN1** | *11 m/s* | 4175905.7500 | 4130367.2500 | 3217655.2500 | 2139110.7500 | 204321.6746 553953.5104 |
| | *14 m/s* | 4221720.5000 | 4123180.2500 | 2994581.5000 | 2160943.7500 | 275044.0517 470250.8119 |
| | *17 m/s* | 3885722.2500 | 3885722.2500 | 2922031.0000 | 2229554.7500 | 191405.7774 383304.9873 |
| | *20 m/s* | 3753333.0000 | 3753333.0000 | 2869060.5000 | 2282296.5000 | 156043.5705 327128.7837 |
| | *23 m/s* | 3664181.0000 | 3664181.0000 | 2825870.2500 | 2324791.5000 | 155616.6418 293367.7749 |

Table 5.6: Comparison of results for "No fault" and "Disconnection from the grid" models at different wind speeds

## 5.4.5   IEA 15-MW - Shutdown of the wind turbine
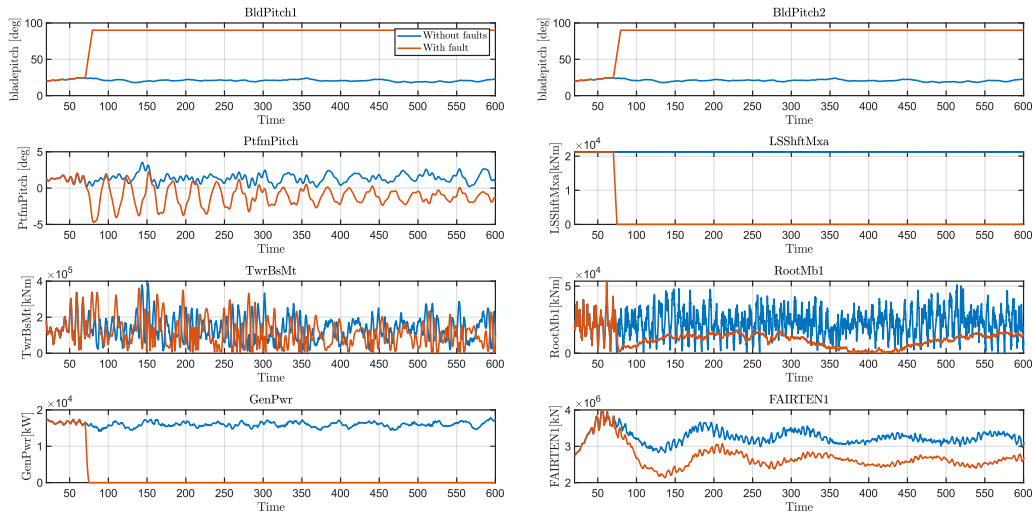


Figure 5.22: Main results for the simulation with wind speed=23 m/s

The results of the simulations shown in this section show that only in the case of a wind speed of 25 m/s the shutdown of the turbine occurs. At lower speeds, on the other hand, the speed never significantly exceeds the cut-out speed, allowing normal system operation.

| | | Maximum | Minimum | Standard deviation |
|---|---|---|---|---|
| **BldPitch1** | *23 m/s* | 24.5974 90.1228 | 17.7800 19.5906 | 1.4111 19.4389 |
| **BldPitch2** | *23 m/s* | 24.5974 90.1228 | 17.7800 19.5906 | 1.4111 19.4389 |
| **PtfmPitch** | *23 m/s* | 3.5466 2.2597 | -0.0360 -4.7241 | 0.5866 1.3869 |
| **LSShftMxa** | *23 m/s* | 21286.2754 21262.5469 | 21096.2285 0.0000 | 26.1210 6025.0732 |
| **TwrBsFt** | *23 m/s* | 4099.4283 3537.4196 | 17.8944 3.0833 | 716.5512 704.5224 |
| **TwrBsMt** | *23 m/s* | 387754.4633 361933.7108 | 9597.3486 368.5820 | 63874.4614 72233.7814 |
| **RootFb1** | *23 m/s* | 1130.2712 1061.5441 | 35.9176 0.8282 | 179.0306 207.8257 |
| **RootMb1** | *23 m/s* | 53722.1562 53722.1562 | 159.2206 11.5489 | 9202.1871 6420.3116 |
| **GenPwr** | *23 m/s* | 17879.0840 17501.4727 | 14126.1387 0.0000 | 684.4765 4710.1372 |
| **FAIRTEN1** | *23 m/s* | 4003869.0000 4003869.0000 | 2730644.5000 2132608.5000 | 197949.5542 323355.7794 |

Table 5.7: Comparison of results for "No fault" and "Shutdown" model at 23 m/s wind speed

## 5.4.6 IEA 15-MW - Extreme wind and waves conditions in shutdown state
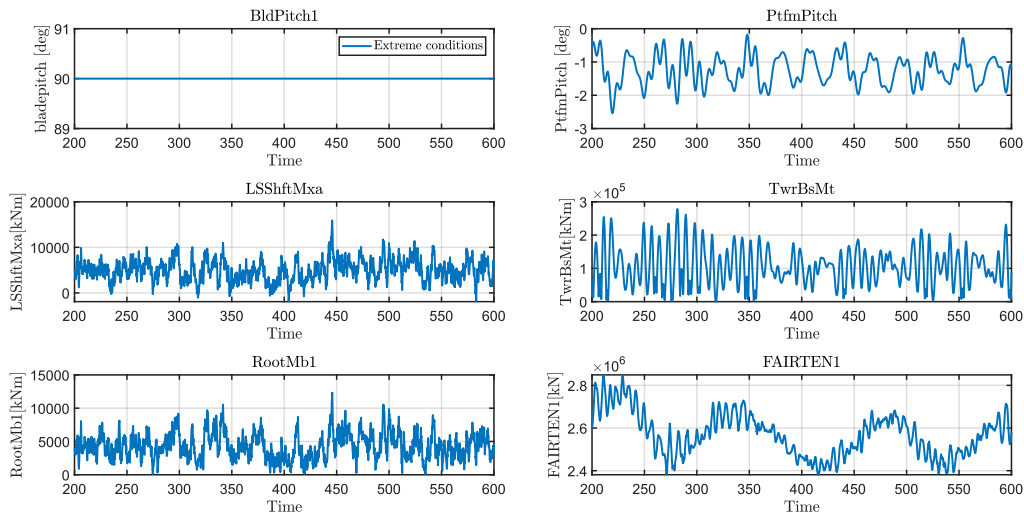


Figure 5.23: Main results for the simulation with extreme weather conditions

In extreme conditions, the blade pitch angles stabilize at higher values, which prevents the turbine from dangerous aerodynamic loads. The system shifts from energy

production mode to safety mode. The plot indicates that under extreme conditions, the platform pitch varies more dynamically. Across most variables (PtfmPitch, TwrBsMt, RootMb1, FAIRTEN1), the extreme wind and wave conditions introduce larger oscillations and variability, indicating the turbine is undergoing significant loading and dynamic movements. The turbine's control system will active shutdown when the wind exceeds the cut-out speed, leading to a drastic reduction in key parameters such as generator power, low-speed shaft moment, and tower base moment.

In this case, the comparison is between different wind speed conditions, with the considered "No fault" model representing the scenario at 23 m/s, while the middle wind speed for the extreme case that is 26.14 m/s. The same reasoning remains valid for the subsequent comparison for the 5MW turbine.

| | | Maximum | Minimum | Standard deviation |
|---|---|---|---|---|
| **BldPitch1** | *26.14 m/s* | 24.5974 90.0000 | 17.7800 90.0000 | 1.4111 0.0000 |
| **PtfmPitch** | *26.14 m/s* | 3.5466 0.7905 | -0.0360 -3.1350 | 0.5866 0.6226 |
| **LSShftMxa** | *26.14 m/s* | 21286.2754 15930.0000 | 21096.2285 0.0000 | 26.1210 2505.8483 |
| **TwrBsMt** | *26.14 m/s* | 387754.4633 325632.0201 | 9597.3486 216.2384 | 63874.4614 61797.4316 |
| **RootMb1** | *26.14 m/s* | 53722.1562 12426.8681 | 159.2206 26.2764 | 9202.1871 1994.9896 |
| **FAIRTEN1** | *26.14 m/s* | 4003869.0000 2881000.0000 | 2730644.5000 2311000.0000 | 197949.5542 113924.8015 |

Table 5.8: Comparison of results for "No fault" model at 23 m/s wind speed and "Extreme conditions" case

69

## 5.4.7 IEA 15-MW - Extreme wind shear
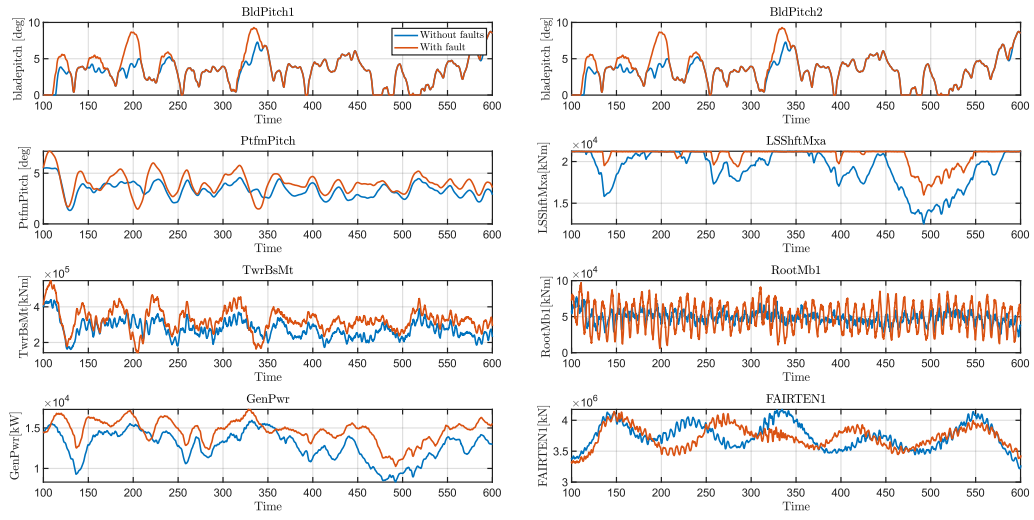


Figure 5.24: Main results for the simulation with wind speed=11 m/s
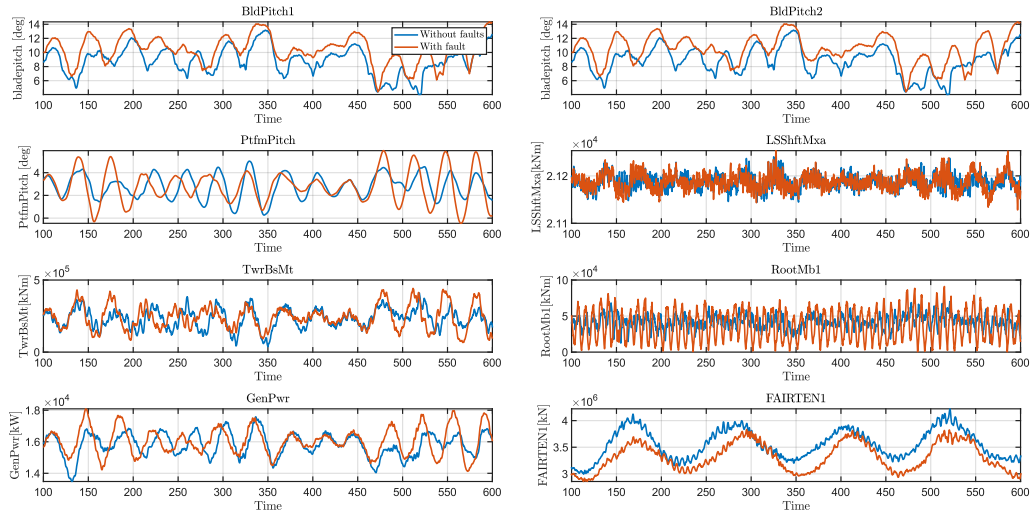


Figure 5.25: Main results for the simulation with wind speed=14 m/s
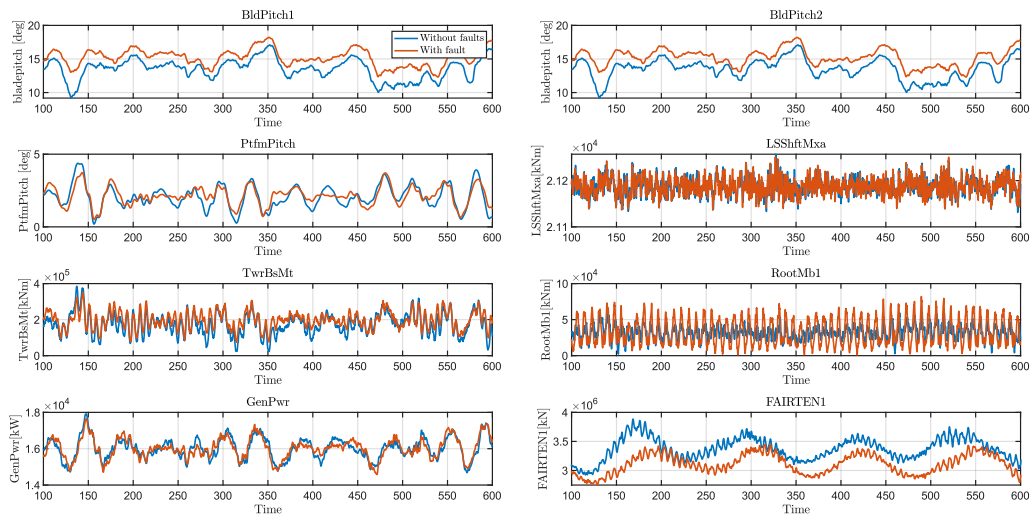
Figure 5.26: Main results for the simulation with wind speed=17 m/s
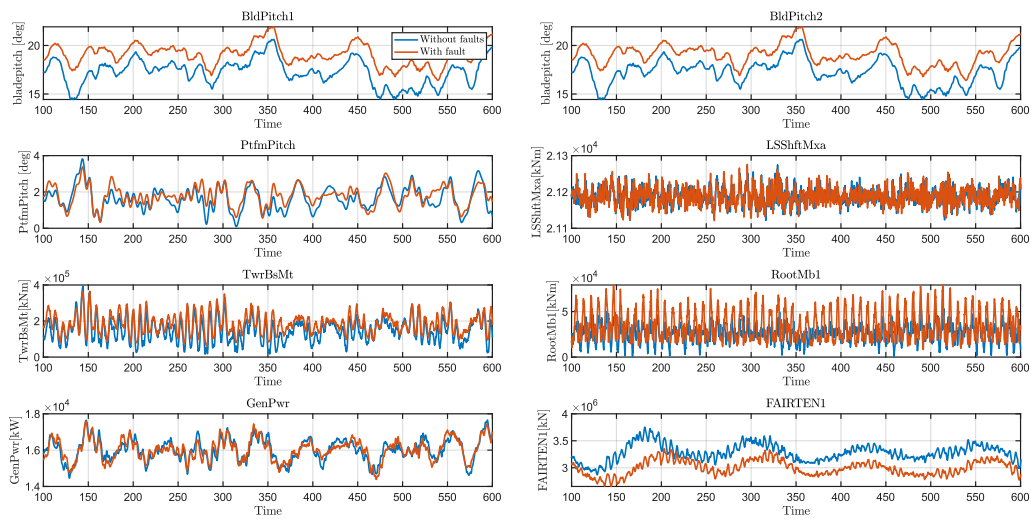


Figure 5.27: Main results for the simulation with wind speed=20 m/s

Figure 5.28: Main results for the simulation with wind speed=23 m/s

| | | Maximum | Minimum | Standard deviation |
|---|---|---|---|---|
| **BldPitch1** | *11 m/s* | 8.7480 9.2913 | 0.0000 0.0000 | 1.8201 2.2015 |
| | *14 m/s* | 13.1576 14.3419 | 4.0350 4.4066 | 1.9338 1.9701 |
| | *17 m/s* | 17.0932 18.2246 | 9.1779 12.3093 | 1.5491 1.2522 |
| | *20 m/s* | 20.6196 21.9221 | 14.4363 16.4092 | 1.3296 1.0815 |
| | *23 m/s* | 24.1368 25.4768 | 17.7800 19.9679 | 1.2130 1.0044 |
| **BldPitch2** | *11 m/s* | 8.7480 9.2913 | 0.0000 0.0000 | 1.8201 2.2015 |
| | *14 m/s* | 13.1576 14.3419 | 4.0350 4.4066 | 1.9338 1.9701 |
| | *17 m/s* | 17.0932 18.2246 | 9.1779 12.3093 | 1.5491 1.2522 |
| | *20 m/s* | 20.6196 21.9221 | 14.4363 16.4092 | 1.3296 1.0815 |
| | *23 m/s* | 24.1368 25.4768 | 17.7800 19.9679 | 1.2130 1.0044 |
| **PtfmPitch** | *11 m/s* | 5.5299 7.1693 | 1.3302 1.4586 | 0.7480 1.0175 |
| | *14 m/s* | 5.0145 5.9394 | 0.2663 -0.4576 | 1.0405 1.3943 |
| | *17 m/s* | 4.3746 3.7288 | 0.1953 0.5148 | 0.7983 0.6407 |
| | *20 m/s* | 3.8224 3.3803 | 0.0888 0.3286 | 0.6472 0.5530 |
| | *23 m/s* | 3.5466 3.1058 | -0.0360 0.1030 | 0.6059 0.5182 |

| | | | | | | |
|---|---|---|---|---|---|---|
| **LSShftMxa** | 11 m/s | 21235.0684 | 21237.5566 | 12516.4678 | 15984.2686 | 2196.6156 1061.3098 |
| | 14 m/s | 21248.9316 | 21253.2148 | 21144.0117 | 21128.1836 | 15.4488 17.0259 |
| | 17 m/s | 21257.1348 | 21251.2422 | 21131.3145 | 21136.2793 | 17.8012 17.9430 |
| | 20 m/s | 21274.6465 | 21275.9395 | 21121.9023 | 21121.0176 | 21.9140 22.6133 |
| | 23 m/s | 21286.2754 | 21285.9746 | 21096.2285 | 21100.9629 | 25.7781 26.5970 |
| **TwrBsFt** | 11 m/s | 4671.0334 | 5519.2682 | 1652.6445 | 1378.2306 | 530.1272 688.4096 |
| | 14 m/s | 4291.3070 | 4530.0832 | 584.7426 | 430.9804 | 710.9212 886.2246 |
| | 17 m/s | 4126.4401 | 3335.3329 | 159.1385 | 536.6510 | 641.8190 528.1356 |
| | 20 m/s | 4097.6110 | 3439.4332 | 8.8075 | 406.6685 | 699.0689 575.9358 |
| | 23 m/s | 4099.4283 | 3608.0028 | 17.8944 | 483.4250 | 716.0145 550.2715 |
| **TwrBsMt** | 11 m/s | 439663.4950 | 546981.4057 | 160851.9008 | 142699.4720 | 50389.7371 65003.1669 |
| | 14 m/s | 410534.2799 | 442123.5059 | 37353.1484 | 66462.6817 | 67464.2077 82221.9633 |
| | 17 m/s | 385227.0383 | 350382.1219 | 22809.7752 | 73818.1994 | 60124.0384 48330.5573 |
| | 20 m/s | 393777.4953 | 365289.5298 | 15975.1307 | 60503.7349 | 63780.3842 54294.3689 |
| | 23 m/s | 387754.4633 | 385618.8473 | 9597.3486 | 68494.1589 | 63965.3745 53002.1675 |
| **RootFb1** | 11 m/s | 1306.1672 | 1483.1501 | 483.5387 | 255.2342 | 131.5086 219.0457 |
| | 14 m/s | 1203.1547 | 1380.6387 | 338.6004 | 12.2481 | 144.9964 261.1318 |
| | 17 m/s | 1149.8011 | 1278.3797 | 158.8869 | 7.7392 | 155.2612 280.4531 |
| | 20 m/s | 1139.1564 | 1298.0748 | 125.9497 | 4.4158 | 167.0427 280.2869 |
| | 23 m/s | 1130.2712 | 1359.5541 | 35.9176 | 4.4940 | 178.6648 282.3827 |
| **RootMb1** | 11 m/s | 77515.0023 | 97185.4634 | 22052.1589 | 5918.3183 | 7757.4003 17942.9204 |
| | 14 m/s | 70196.3611 | 91053.6835 | 12196.1216 | 324.5338 | 8859.0997 20177.6903 |
| | 17 m/s | 60119.0209 | 82066.6849 | 2211.2142 | 870.7522 | 8997.9296 18064.3667 |
| | 20 m/s | 53329.1239 | 79238.9518 | 70.9733 | 8160.3095 | 9287.1560 15694.7128 |
| | 23 m/s | 50926.9743 | 88941.9090 | 159.2206 | 10831.9859 | 9302.4846 15299.1569 |
| **GenPwr** | 11 m/s | 15939.0459 | 17292.8926 | 8314.3545 | 10242.4570 | 1828.4364 1417.8694 |
| | 14 m/s | 17584.6094 | 18090.2168 | 13479.9824 | 14122.5879 | 746.1326 843.5500 |
| | 17 m/s | 17918.7012 | 17650.5918 | 14680.9307 | 14574.1631 | 593.7853 570.8757 |
| | 20 m/s | 17655.9375 | 17576.7773 | 14449.3174 | 14384.5391 | 620.8355 587.2358 |
| | 23 m/s | 17879.0840 | 17497.4199 | 14399.1465 | 14230.4873 | 664.7399 621.4981 |

| | | | | |
|---|---|---|---|---|
| | *11 m/s* | 4175905.7500 4141910.5000 | 3217655.2500 3310134.0000 | 204321.6746 176265.0456 |
| | *14 m/s* | 4221720.5000 3832708.7500 | 2994581.5000 2855926.2500 | 275044.0517 263620.3832 |
| **FAIRTEN1** | *17 m/s* | 3885722.2500 3450863.7500 | 2922031.0000 2749271.2500 | 191405.7774 168277.0976 |
| | *20 m/s* | 3753333.0000 3355037.5000 | 2869060.5000 2653766.5000 | 156043.5705 136297.2733 |
| | *23 m/s* | 3664181.0000 3309256.2500 | 2825870.2500 2560991.2500 | 155616.6418 131477.6956 |

Table 5.9: Comparison of results for "No fault" and "Extreme wind shear" models at different wind speeds

The exponent in the power law represents how quickly wind speeds change with height. A typical exponent for average conditions is around 0.1 to 0.2, but under extreme conditions, an exponent of 0.82 is unusually high and reflects severe wind shear. With wind speeds drastically increasing at higher heights, the turbine platform tilt forward or backward, causing the platform pitch to oscillate more intensely. The tower base moment show higher peaks and higher standard deviations, reflecting the added stress caused by the imbalance in forces on the rotor and tower. The low-speed shaft moment exhibit significant fluctuations, with moments of high torque followed by lower values, reflecting the uneven wind distribution across the rotor. The generator power show great variability, with severe peaks corresponding the rotor enter regions of very high wind speed. The fairlead tension show larger oscillations, with greater peaks reflecting the increased platform motion due to wind shear effects.

## 5.4.8   NREL 5-MW - Blade pitch angle fixed
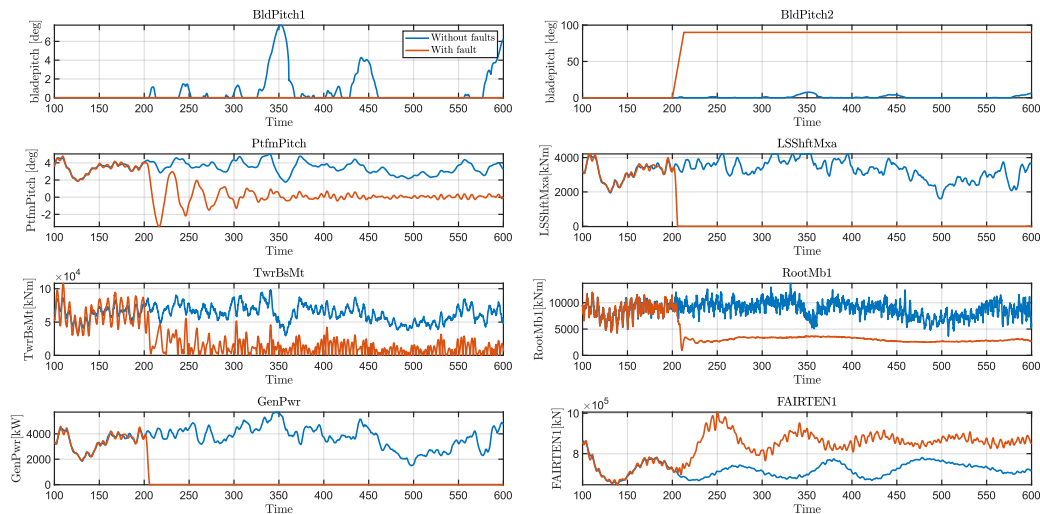


Figure 5.29: Main results for the simulation with wind speed=11 m/s

Figure 5.30: Main results for the simulation with wind speed=14 m/s



Figure 5.31: Main results for the simulation with wind speed=17 m/s

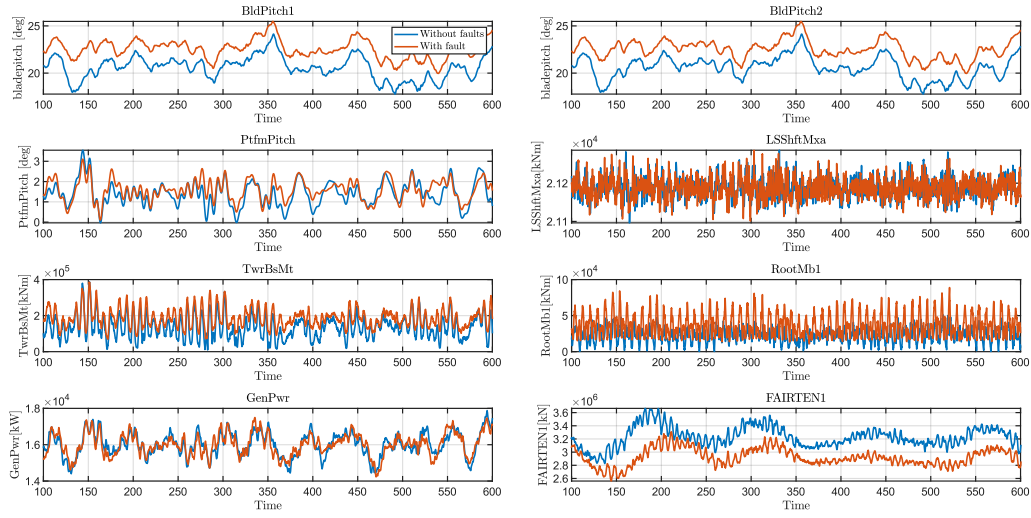Figure 5.32: Main results for the simulation with wind speed=20 m/s



Figure 5.33: Main results for the simulation with wind speed=23 m/s

|  |  | Maximum | Minimum | Standard deviation |
|---|---|---|---|---|
| **BldPitch1** | *11 m/s* | 7.7337 0.0000 | 0.0000 0.0000 | 1.6292 0.0000 |
|  | *14 m/s* | 12.9862 10.8648 | 4.8893 6.6884 | 1.7875 0.6469 |
|  | *17 m/s* | 16.8134 15.1299 | 9.9687 11.4942 | 1.4196 0.5018 |
|  | *20 m/s* | 20.2966 18.3512 | 13.3151 14.7027 | 1.3803 0.4707 |
|  | *23 m/s* | 23.4441 21.3980 | 16.8727 17.7199 | 1.3017 0.4683 |

| | | | | |
|---|---|---|---|---|
| **BldPitch2** | 11 m/s | 7.7337 90.1200 | 0.0000 0.0000 | 1.6292 36.3668 |
| | 14 m/s | 12.9862 90.0867 | 4.8893 6.6884 | 1.7875 32.5999 |
| | 17 m/s | 16.8134 90.1387 | 9.9687 11.4942 | 1.4196 30.8844 |
| | 20 m/s | 20.2966 90.1304 | 13.3151 14.7027 | 1.3803 29.6035 |
| | 23 m/s | 23.4441 90.0979 | 16.8727 17.7199 | 1.3017 28.3808 |
| **PtfmPitch** | 11 m/s | 5.0388 4.7766 | 1.7618 -3.4232 | 0.6910 1.5815 |
| | 14 m/s | 3.6948 3.2953 | 0.7062 -2.0259 | 0.5999 0.9584 |
| | 17 m/s | 3.2635 2.6430 | 0.5519 -1.5793 | 0.5401 0.7313 |
| | 20 m/s | 3.3573 2.7059 | 0.6213 -1.2955 | 0.5390 0.6803 |
| | 23 m/s | 3.3284 2.7995 | 0.5979 -0.8171 | 0.5838 0.6316 |
| **LSShftMxa** | 11 m/s | 4213.7808 4212.2773 | 1601.9858 0.0000 | 566.1913 1304.9779 |
| | 14 m/s | 4211.6919 3215.9282 | 1697.2799 0.0000 | 436.0191 1084.6779 |
| | 17 m/s | 4212.3101 3453.8152 | 1605.2422 0.0000 | 498.9332 1108.5363 |
| | 20 m/s | 4216.2866 3997.7979 | 1890.2089 0.0000 | 506.8362 1284.2888 |
| | 23 m/s | 4218.2505 4214.8979 | 2211.1274 0.0000 | 476.6071 1451.1988 |
| **TwrBsFt** | 11 m/s | 1424.7499 1591.9864 | 415.9612 0.3064 | 178.5721 330.8899 |
| | 14 m/s | 1020.1573 1121.4485 | 127.3911 1.0584 | 156.4776 217.4891 |
| | 17 m/s | 907.9630 984.8566 | 44.1264 0.3221 | 143.1379 190.9414 |
| | 20 m/s | 921.3069 976.8155 | 67.4168 0.7357 | 140.5216 188.5131 |
| | 23 m/s | 872.8709 911.0835 | 77.4743 2.6823 | 142.8111 190.4962 |
| **TwrBsMt** | 11 m/s | 98554.5302 108162.1278 | 29466.9708 20.1038 | 12195.7415 23576.0444 |
| | 14 m/s | 72929.7047 76714.3066 | 11958.6677 59.4851 | 10758.3919 15276.2384 |
| | 17 m/s | 65230.9368 69526.2512 | 5919.1659 74.7464 | 9807.1620 13332.6580 |
| | 20 m/s | 67861.9311 69463.2251 | 6659.3466 94.5946 | 9656.2835 13249.0447 |
| | 23 m/s | 65154.5332 67550.7725 | 5383.4557 163.8606 | 9880.7819 13361.8749 |
| **RootFb1** | 11 m/s | 382.7877 352.3939 | 110.5929 37.9426 | 40.7329 50.0907 |
| | 14 m/s | 332.9482 318.1394 | 60.3974 32.7440 | 41.0980 46.2977 |
| | 17 m/s | 314.0328 285.0737 | 28.3751 17.0282 | 43.4226 38.5069 |
| | 20 m/s | 322.7677 321.3745 | 8.0055 29.8975 | 47.9820 43.3671 |
| | 23 m/s | 329.3387 352.9254 | 3.5635 15.2518 | 50.0130 41.2281 |

| | | | | |
|---|---|---|---|---|
| **RootMb1** | 11 m/s | 13693.2582 12022.8982 | 3634.0756 937.8979 | 1470.4310 2417.1182 |
| | 14 m/s | 10277.0662 10661.1893 | 1281.6773 869.7051 | 1451.1332 1565.1009 |
| | 17 m/s | 9500.7451 9243.7831 | 133.0448 122.0905 | 1455.3694 1251.7506 |
| | 20 m/s | 9469.9502 9469.8962 | 33.7835 66.6909 | 1614.2181 1231.5282 |
| | 23 m/s | 9345.0019 10542.8426 | 33.2934 36.5860 | 1625.3458 1189.8088 |
| **GenPwr** | 11 m/s | 5714.9907 4591.3193 | 1488.8264 0.0000 | 872.6553 1405.5891 |
| | 14 m/s | 5752.6377 4220.2305 | 2006.4176 0.0000 | 641.5541 1379.1429 |
| | 17 m/s | 5889.0615 4601.4116 | 1868.4121 0.0000 | 744.0751 1409.5932 |
| | 20 m/s | 6067.3423 5377.2944 | 2162.1306 0.0000 | 794.5307 1631.7600 |
| | 23 m/s | 6118.3887 5776.4058 | 2499.7327 0.0000 | 795.8896 1840.5999 |
| **FAIRTEN1** | 11 m/s | 866677.0625 1005856.8750 | 650949.3125 646255.0625 | 36531.2117 71515.6476 |
| | 14 m/s | 837488.2500 944898.5000 | 712211.6250 720889.1250 | 23139.6672 43106.5181 |
| | 17 m/s | 832003.9375 940830.0625 | 749922.9375 754269.0625 | 15696.8977 35268.6500 |
| | 20 m/s | 833859.2500 928352.6875 | 755488.3750 759118.4375 | 14984.7952 33065.8044 |
| | 23 m/s | 834413.6250 928044.9375 | 763754.2500 759770.5625 | 14558.8480 32578.1898 |

Table 5.10: Comparison of results for "No fault" and "Pitched to feather" models at different wind speeds

## 5.4.9   NREL 5-MW - Offset in blade pitch angle
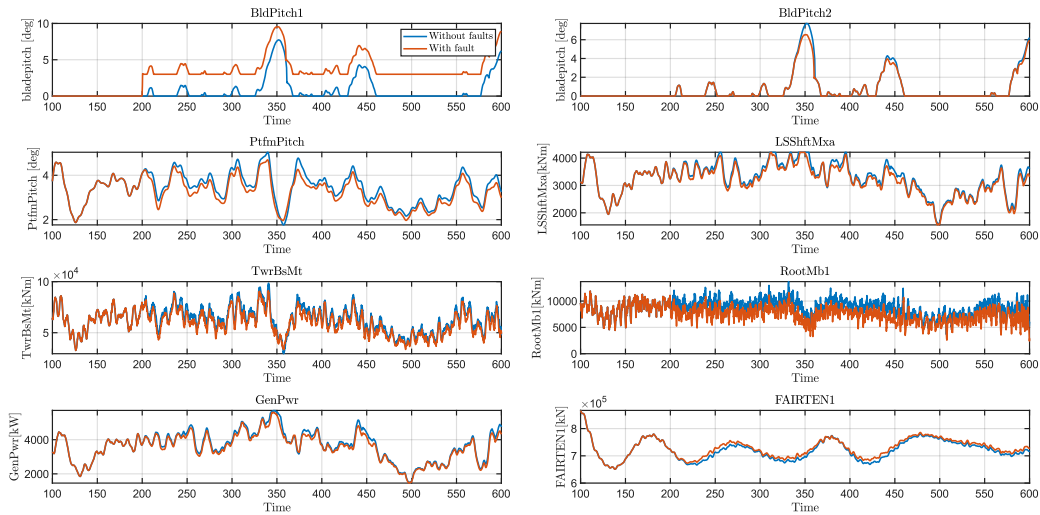


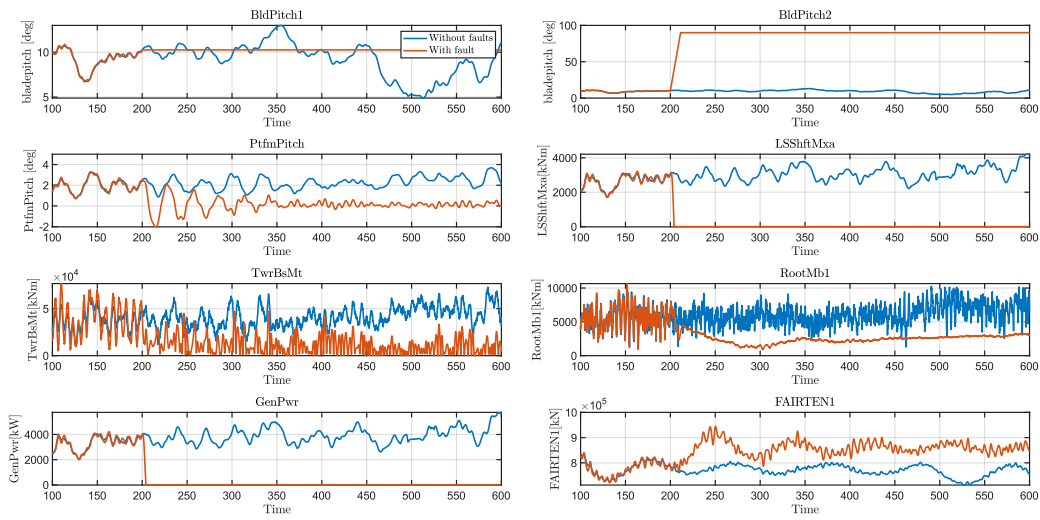Figure 5.34: Main results for the simulation with wind speed=11 m/s
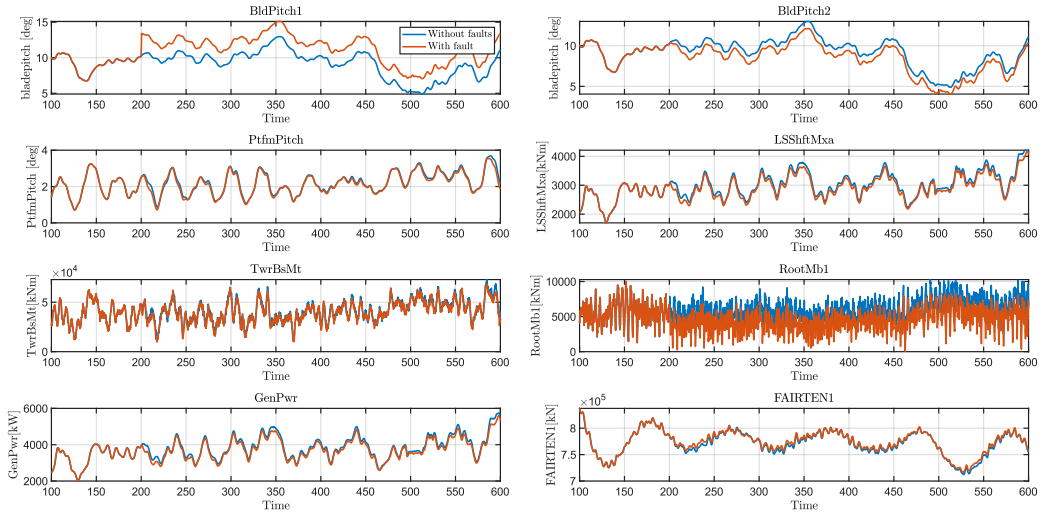
Figure 5.35: Main results for the simulation with wind speed=14 m/s
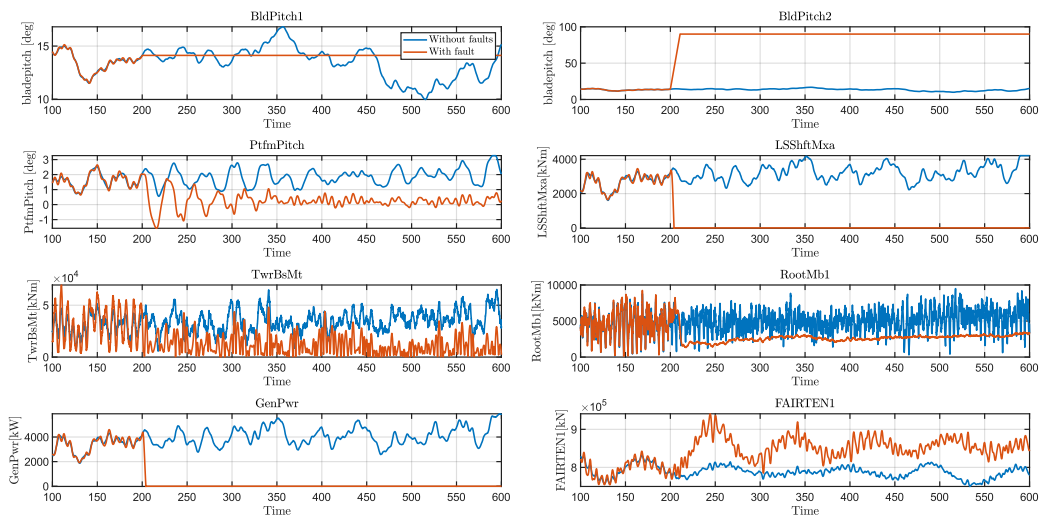


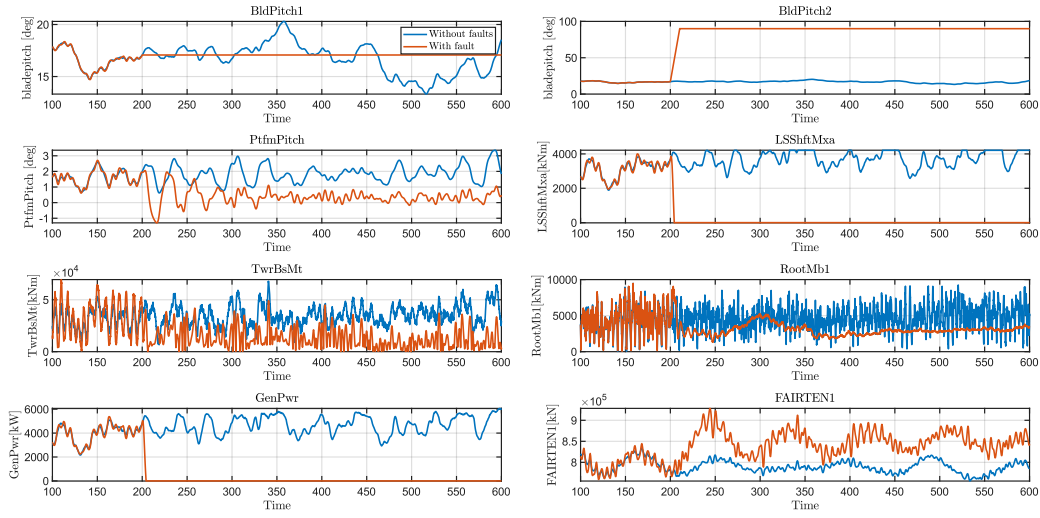Figure 5.36: Main results for the simulation with wind speed=17 m/s

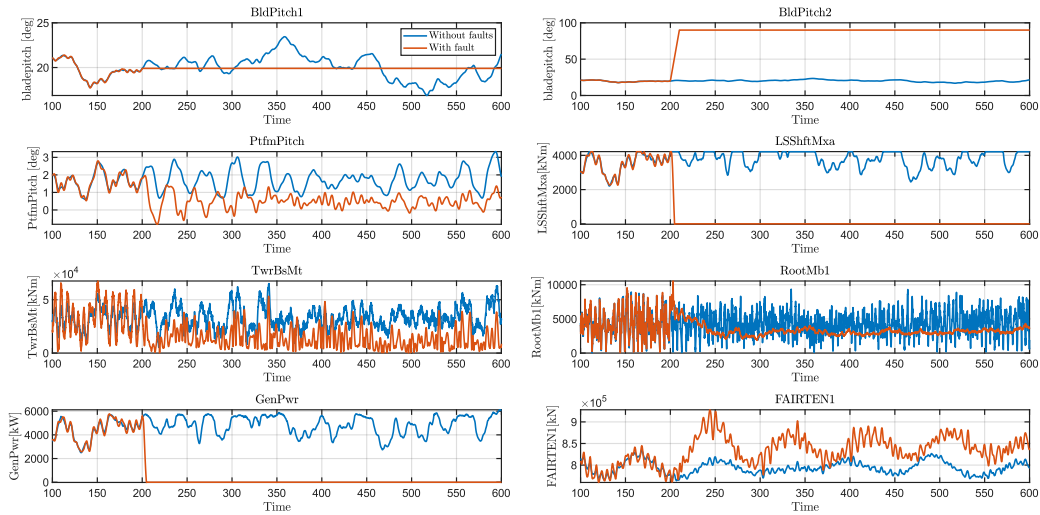Figure 5.37: Main results for the simulation with wind speed=20 m/s



Figure 5.38: Main results for the simulation with wind speed=23 m/s

| | | Maximum | Minimum | Standard deviation |
|---|---|---|---|---|
| **BldPitch1** | *11 m/s* | 7.7337 9.5444 | 0.0000 0.0000 | 1.6292 2.0933 |
| | *14 m/s* | 12.9862 15.1096 | 4.8893 6.7337 | 1.7875 1.9869 |
| | *17 m/s* | 16.8134 18.9915 | 9.9687 11.4990 | 1.4196 1.6777 |
| | *20 m/s* | 20.2966 22.3636 | 13.3151 14.7536 | 1.3803 1.6559 |
| | *23 m/s* | 23.4441 25.5461 | 16.8727 17.7724 | 1.3017 1.6498 |

| | | | | |
|---|---|---|---|---|
| **BldPitch2** | *11 m/s* | 7.7337 6.5444 | 0.0000 0.0000 | 1.6292 1.4523 |
| | *14 m/s* | 12.9862 12.1096 | 4.8893 4.0552 | 1.7875 1.8400 |
| | *17 m/s* | 16.8134 15.9915 | 9.9687 9.1306 | 1.4196 1.4707 |
| | *20 m/s* | 20.2966 19.3636 | 13.3151 12.3236 | 1.3803 1.4268 |
| | *23 m/s* | 23.4441 22.5461 | 16.8727 15.7551 | 1.3017 1.3464 |
| **PtfmPitch** | *11 m/s* | 5.0388 4.6951 | 1.7618 1.8715 | 0.6910 0.6490 |
| | *14 m/s* | 3.6948 3.5526 | 0.7062 0.7062 | 0.5999 0.5899 |
| | *17 m/s* | 3.2635 3.1570 | 0.5519 0.4256 | 0.5401 0.5239 |
| | *20 m/s* | 3.3573 3.3114 | 0.6213 0.5275 | 0.5390 0.5327 |
| | *23 m/s* | 3.3284 3.3494 | 0.5979 0.5979 | 0.5838 0.5662 |
| **LSShftMxa** | *11 m/s* | 4213.7808 4212.6768 | 1601.9858 1558.2601 | 566.1913 550.0191 |
| | *14 m/s* | 4211.6919 4177.7822 | 1697.2799 1697.2799 | 436.0191 409.0412 |
| | *17 m/s* | 4212.3101 4213.1821 | 1605.2422 1605.2422 | 498.9332 474.7107 |
| | *20 m/s* | 4216.2866 4214.1377 | 1890.2089 1890.2089 | 506.8362 508.0497 |
| | *23 m/s* | 4218.2505 4216.1455 | 2211.1274 2211.1274 | 476.6071 478.7357 |
| **TwrBsFt** | *11 m/s* | 1424.7499 1349.4170 | 415.9612 427.0758 | 178.5721 170.8631 |
| | *14 m/s* | 1020.1573 995.7056 | 127.3911 105.6751 | 156.4776 154.4287 |
| | *17 m/s* | 907.9630 865.2334 | 44.1264 20.9287 | 143.1379 140.4409 |
| | *20 m/s* | 921.3069 927.2086 | 67.4168 47.9981 | 140.5216 139.3982 |
| | *23 m/s* | 872.8709 909.7265 | 77.4743 52.8752 | 142.8111 141.0352 |
| **TwrBsMt** | *11 m/s* | 98554.5302 91291.9856 | 29466.9708 32613.9172 | 12195.7415 11667.5176 |
| | *14 m/s* | 72929.7047 67886.6925 | 11958.6677 9801.9606 | 10758.3919 10604.3680 |
| | *17 m/s* | 65230.9368 66279.2736 | 5919.1659 4943.2686 | 9807.1620 9866.0788 |
| | *20 m/s* | 67861.9311 64848.2282 | 6659.3466 1262.4753 | 9656.2835 9859.7732 |
| | *23 m/s* | 65154.5332 67054.8613 | 5383.4557 6338.9620 | 9880.7819 9866.2125 |
| **RootFb1** | *11 m/s* | 382.7877 344.5062 | 110.5929 82.5390 | 40.7329 42.2981 |
| | *14 m/s* | 332.9482 309.2643 | 60.3974 18.9716 | 41.0980 46.3148 |
| | *17 m/s* | 314.0328 287.7411 | 28.3751 3.9186 | 43.4226 48.7632 |
| | *20 m/s* | 322.7677 315.1324 | 8.0055 3.5333 | 47.9820 51.3005 |
| | *23 m/s* | 329.3387 314.4385 | 3.5635 2.2765 | 50.0130 52.9247 |

|  |  | | | |
|---|---|---|---|---|
| **RootMb1** | *11 m/s* | 13693.2582 11911.2691 | 3634.0756 2400.4635 | 1470.4310 1476.6026 |
|  | *14 m/s* | 10277.0662 10025.3718 | 1281.6773 61.0302 | 1451.1332 1530.3234 |
|  | *17 m/s* | 9500.7451 8787.8155 | 133.0448 44.7347 | 1455.3694 1448.0023 |
|  | *20 m/s* | 9469.9502 9469.9502 | 33.7835 33.7835 | 1614.2181 1490.1608 |
|  | *23 m/s* | 9345.0019 9074.5909 | 33.2934 24.0359 | 1625.3458 1439.2785 |
| **GenPwr** | *11 m/s* | 5714.9907 5604.1343 | 1488.8264 1459.6473 | 872.6553 827.1603 |
|  | *14 m/s* | 5752.6377 5605.0156 | 2006.4176 2006.4176 | 641.5541 600.6087 |
|  | *17 m/s* | 5889.0615 5830.9248 | 1868.4121 1868.4121 | 744.0751 708.6559 |
|  | *20 m/s* | 6067.3423 6018.5601 | 2162.1306 2162.1306 | 794.5307 790.9430 |
|  | *23 m/s* | 6118.3887 6103.1401 | 2499.7327 2499.7327 | 795.8896 795.0986 |
| **FAIRTEN1** | *11 m/s* | 866677.0625 866677.0625 | 650949.3125 650949.3125 | 36531.2117 34932.2990 |
|  | *14 m/s* | 837488.2500 837488.2500 | 712211.6250 716464.5000 | 23139.6672 22104.2629 |
|  | *17 m/s* | 832003.9375 832003.9375 | 749922.9375 753938.6875 | 15696.8977 15149.3801 |
|  | *20 m/s* | 833859.2500 833859.2500 | 755488.3750 760285.1875 | 14984.7952 14950.4052 |
|  | *23 m/s* | 834413.6250 834413.6250 | 763754.2500 764872.2500 | 14558.8480 14527.3062 |

Table 5.11: Comparison of results for "No fault" and "Offset" models at different wind speeds

## 5.4.10   NREL 5-MW - Precision degradation
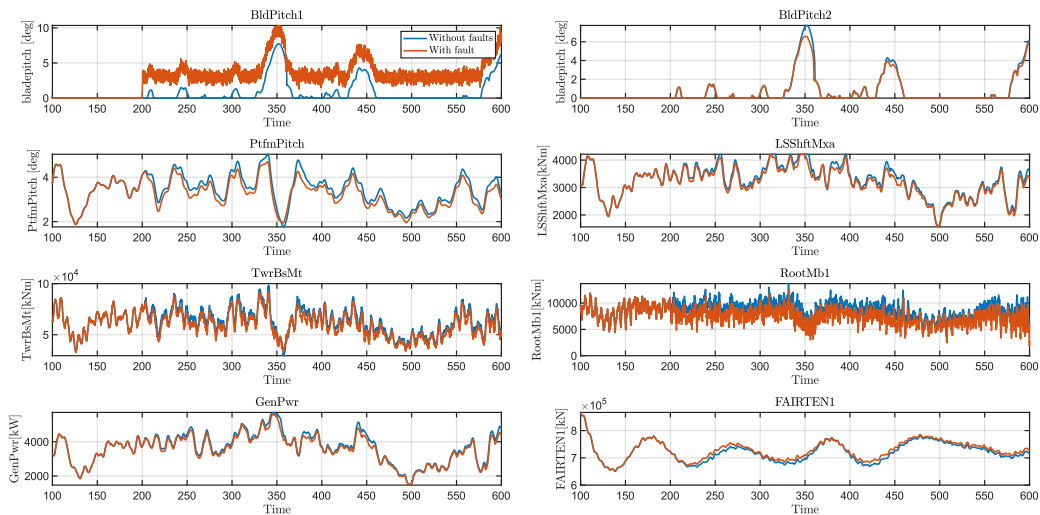


Figure 5.39: Main results for the simulation with wind speed=11 m/s
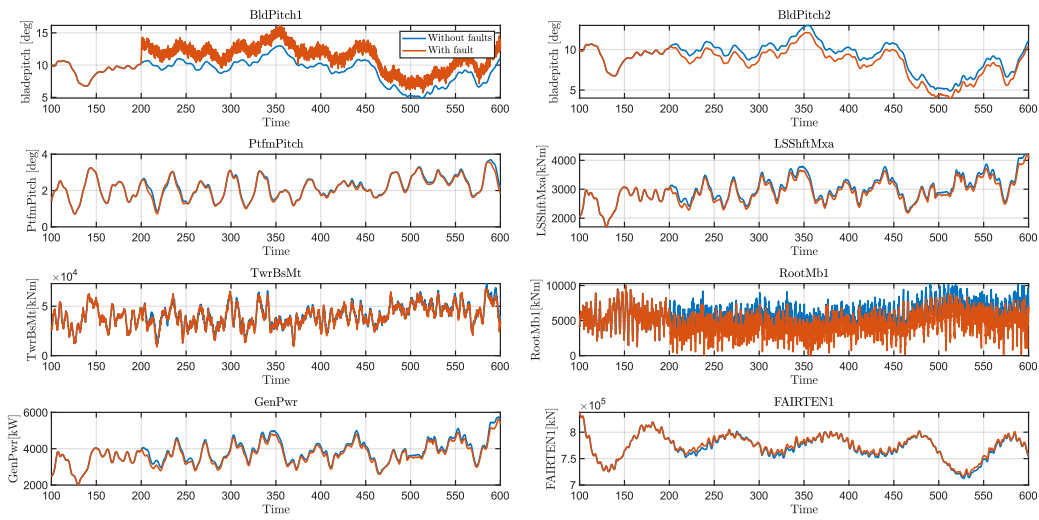
Figure 5.40: Main results for the simulation with wind speed=14 m/s
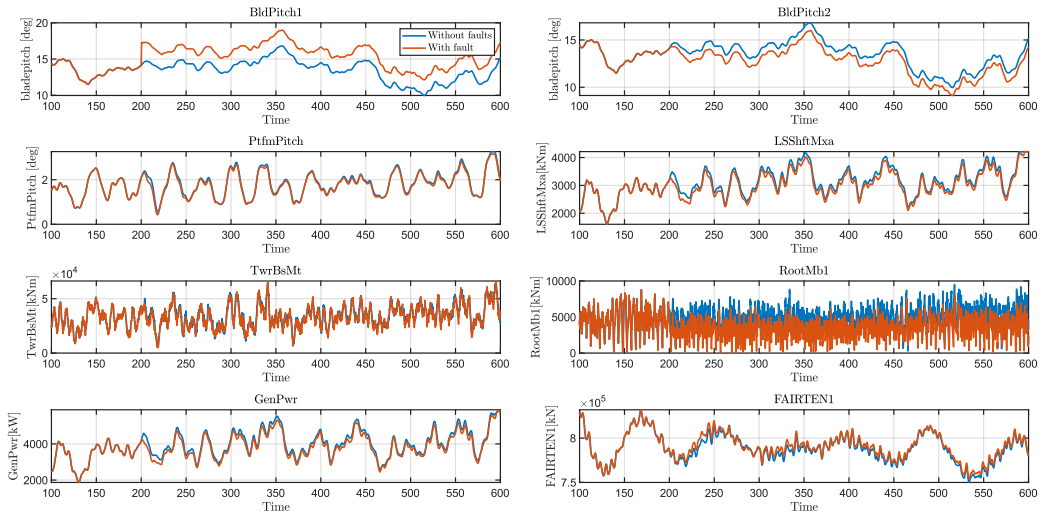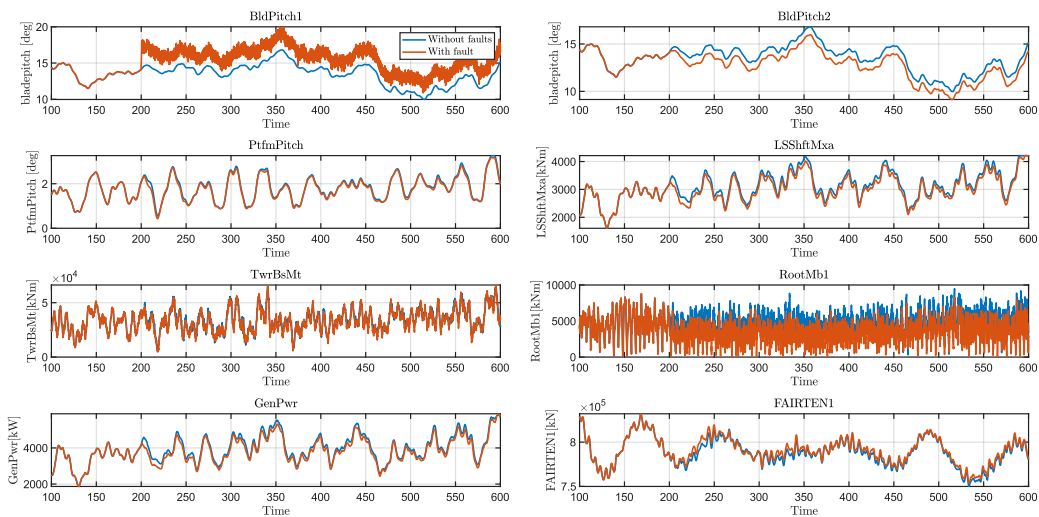


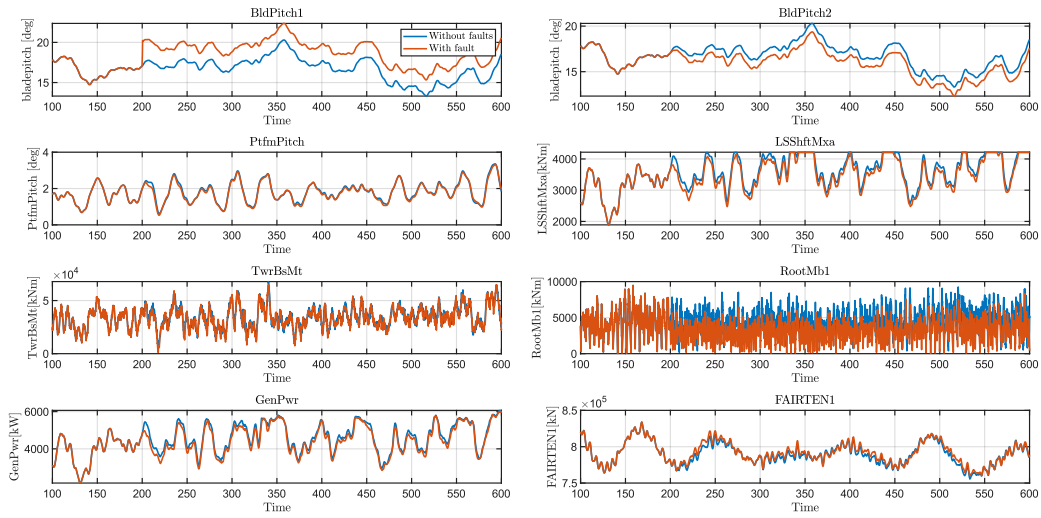Figure 5.41: Main results for the simulation with wind speed=17 m/s

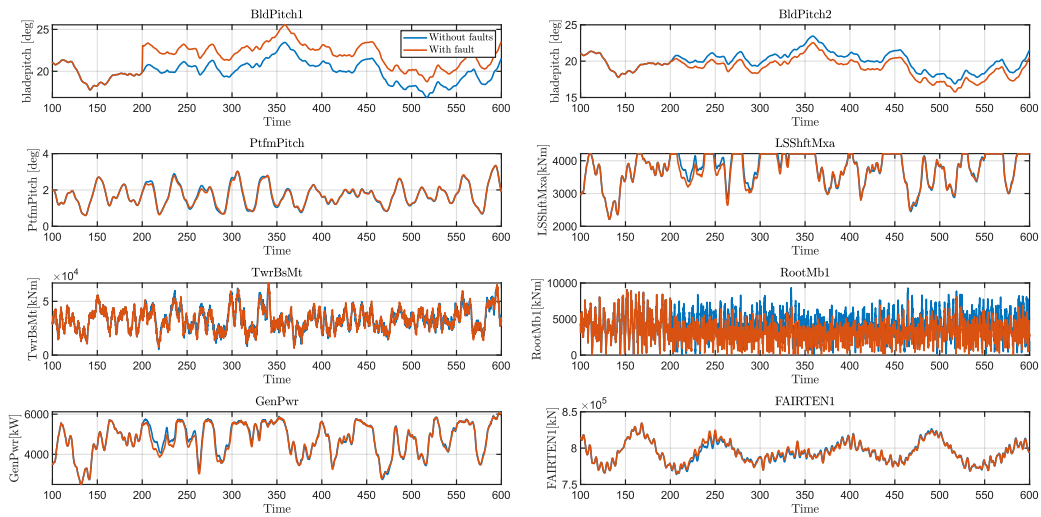Figure 5.42: Main results for the simulation with wind speed=20 m/s



Figure 5.43: Main results for the simulation with wind speed=23 m/s

|  |  | Maximum | Minimum | Standard deviation |
|---|---|---|---|---|
| **BldPitch1** | *11 m/s* | 7.7337 10.3449 | 0.0000 0.0000 | 1.6292 2.1231 |
|  | *14 m/s* | 12.9862 16.1582 | 4.8893 5.7452 | 1.7875 2.0268 |
|  | *17 m/s* | 16.8134 19.9824 | 9.9687 10.8671 | 1.4196 1.7232 |
|  | *20 m/s* | 20.2966 23.4442 | 13.3151 14.2742 | 1.3803 1.7022 |
|  | *23 m/s* | 23.4441 26.6828 | 16.8727 17.7579 | 1.3017 1.6963 |

84

| | | | | |
|---|---|---|---|---|
| **BldPitch2** | 11 m/s | 7.7337 6.5768 | 0.0000 0.0000 | 1.6292 1.4551 |
| | 14 m/s | 12.9862 12.0955 | 4.8893 4.0125 | 1.7875 1.8408 |
| | 17 m/s | 16.8134 15.9736 | 9.9687 9.1409 | 1.4196 1.4698 |
| | 20 m/s | 20.2966 19.3483 | 13.3151 12.3420 | 1.3803 1.4250 |
| | 23 m/s | 23.4441 22.5395 | 16.8727 15.7599 | 1.3017 1.3449 |
| **PtfmPitch** | 11 m/s | 5.0388 4.6979 | 1.7618 1.8715 | 0.6910 0.6515 |
| | 14 m/s | 3.6948 3.5687 | 0.7062 0.7062 | 0.5999 0.5935 |
| | 17 m/s | 3.2635 3.1736 | 0.5519 0.4314 | 0.5401 0.5279 |
| | 20 m/s | 3.3573 3.3131 | 0.6213 0.5187 | 0.5390 0.5375 |
| | 23 m/s | 3.3284 3.3593 | 0.5979 0.5979 | 0.5838 0.5699 |
| **LSShftMxa** | 11 m/s | 4213.7808 4212.5552 | 1601.9858 1563.9655 | 566.1913 549.5195 |
| | 14 m/s | 4211.6919 4198.8882 | 1697.2799 1697.2799 | 436.0191 410.6602 |
| | 17 m/s | 4212.3101 4212.5503 | 1605.2422 1605.2422 | 498.9332 475.7123 |
| | 20 m/s | 4216.2866 4215.6665 | 1890.2089 1890.2089 | 506.8362 509.2774 |
| | 23 m/s | 4218.2505 4217.3423 | 2211.1274 2211.1274 | 476.6071 479.3380 |
| **TwrBsFt** | 11 m/s | 1424.7499 1353.6564 | 415.9612 427.0758 | 178.5721 171.1941 |
| | 14 m/s | 1020.1573 999.8787 | 127.3911 100.3111 | 156.4776 154.9873 |
| | 17 m/s | 907.9630 871.2542 | 44.1264 20.3791 | 143.1379 141.0306 |
| | 20 m/s | 921.3069 929.8802 | 67.4168 44.7670 | 140.5216 140.0724 |
| | 23 m/s | 872.8709 908.9988 | 77.4743 46.3202 | 142.8111 141.6062 |
| **TwrBsMt** | 11 m/s | 98554.5302 91771.4047 | 29466.9708 32613.9172 | 12195.7415 11689.5772 |
| | 14 m/s | 72929.7047 67990.0463 | 11958.6677 8808.4065 | 10758.3919 10637.6598 |
| | 17 m/s | 65230.9368 66285.0779 | 5919.1659 4756.8863 | 9807.1620 9904.7171 |
| | 20 m/s | 67861.9311 65066.6366 | 6659.3466 933.3373 | 9656.2835 9903.8748 |
| | 23 m/s | 65154.5332 67364.3130 | 5383.4557 6028.2932 | 9880.7819 9907.7467 |
| **RootFb1** | 11 m/s | 382.7877 352.1890 | 110.5929 79.3384 | 40.7329 42.6682 |
| | 14 m/s | 332.9482 309.2643 | 60.3974 15.9112 | 41.0980 46.7811 |
| | 17 m/s | 314.0328 287.7411 | 28.3751 1.4128 | 43.4226 49.1853 |
| | 20 m/s | 322.7677 315.1324 | 8.0055 2.2727 | 47.9820 51.5649 |
| | 23 m/s | 329.3387 314.4385 | 3.5635 0.9683 | 50.0130 53.1684 |

| | | | | |
|---|---|---|---|---|
| **RootMb1** | *11 m/s* | 13693.2582 12485.5668 | 3634.0756 1875.7706 | 1470.4310 1499.0448 |
| | *14 m/s* | 10277.0662 10025.3718 | 1281.6773 66.7996 | 1451.1332 1560.5071 |
| | *17 m/s* | 9500.7451 8787.8155 | 133.0448 32.7924 | 1455.3694 1465.0340 |
| | *20 m/s* | 9469.9502 9469.9502 | 33.7835 20.6861 | 1614.2181 1503.1208 |
| | *23 m/s* | 9345.0019 9074.5909 | 33.2934 33.2934 | 1625.3458 1444.7165 |
| **GenPwr** | *11 m/s* | 5714.9907 5614.4434 | 1488.8264 1465.9092 | 872.6553 826.7517 |
| | *14 m/s* | 5752.6377 5641.7671 | 2006.4176 2006.4176 | 641.5541 603.1787 |
| | *17 m/s* | 5889.0615 5846.1074 | 1868.4121 1868.4121 | 744.0751 710.4426 |
| | *20 m/s* | 6067.3423 6032.5181 | 2162.1306 2162.1306 | 794.5307 793.0815 |
| | *23 m/s* | 6118.3887 6124.1045 | 2499.7327 2499.7327 | 795.8896 796.3909 |
| **FAIRTEN1** | *11 m/s* | 866677.0625 866677.0625 | 650949.3125 650949.3125 | 36531.2117 34925.9229 |
| | *14 m/s* | 837488.2500 837488.2500 | 712211.6250 716308.9375 | 23139.6672 22105.8591 |
| | *17 m/s* | 832003.9375 832003.9375 | 749922.9375 753771.1875 | 15696.8977 15164.3951 |
| | *20 m/s* | 833859.2500 833859.2500 | 755488.3750 760136.1250 | 14984.7952 14973.6752 |
| | *23 m/s* | 834413.6250 834413.6250 | 763754.2500 765005.6875 | 14558.8480 14559.5918 |

Table 5.12: Comparison of results for "No fault" and "Precision degradation" models at different wind speeds

## 5.4.11 NREL 5-MW - Disconnection from the grid
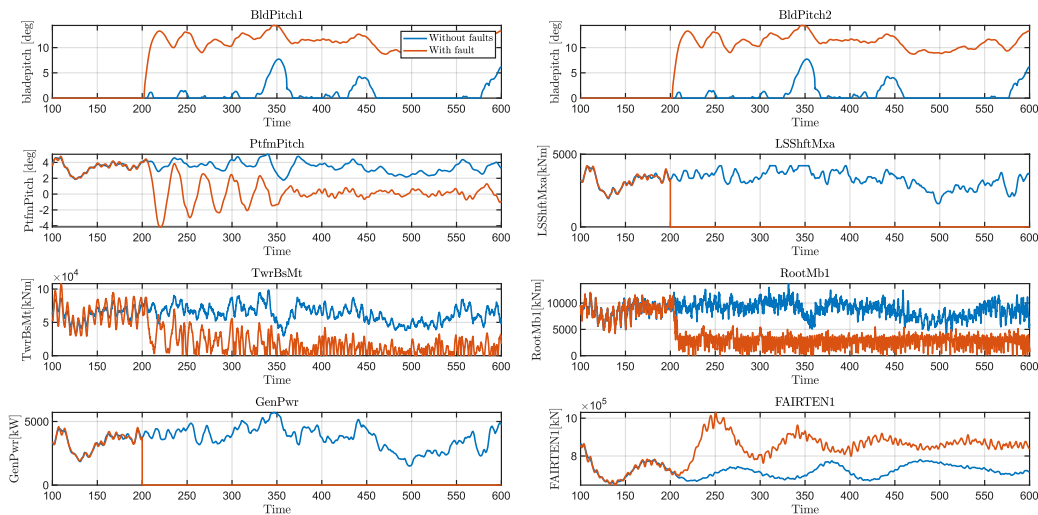


Figure 5.44: Main results for the simulation with wind speed=11 m/s

86
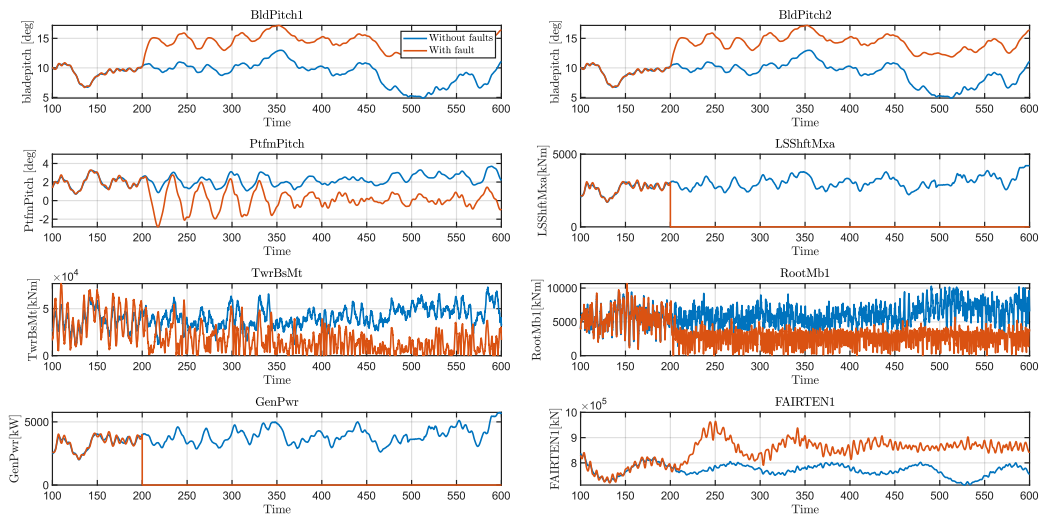
Figure 5.45: Main results for the simulation with wind speed=14 m/s
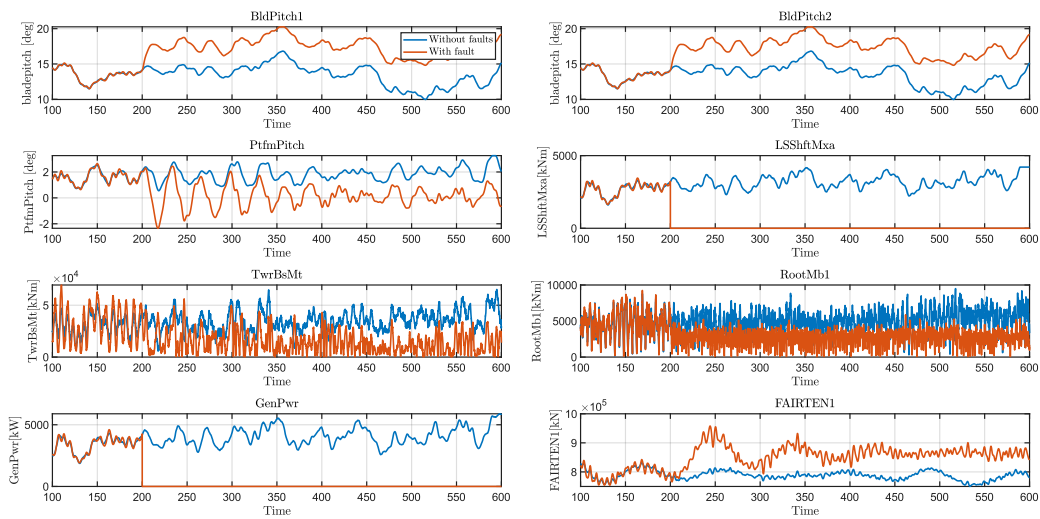


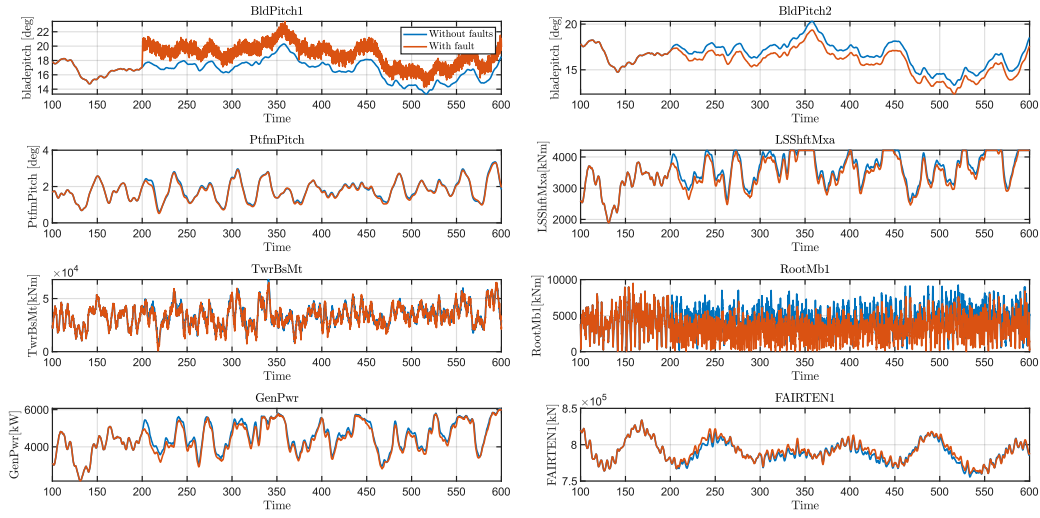Figure 5.46: Main results for the simulation with wind speed=17 m/s

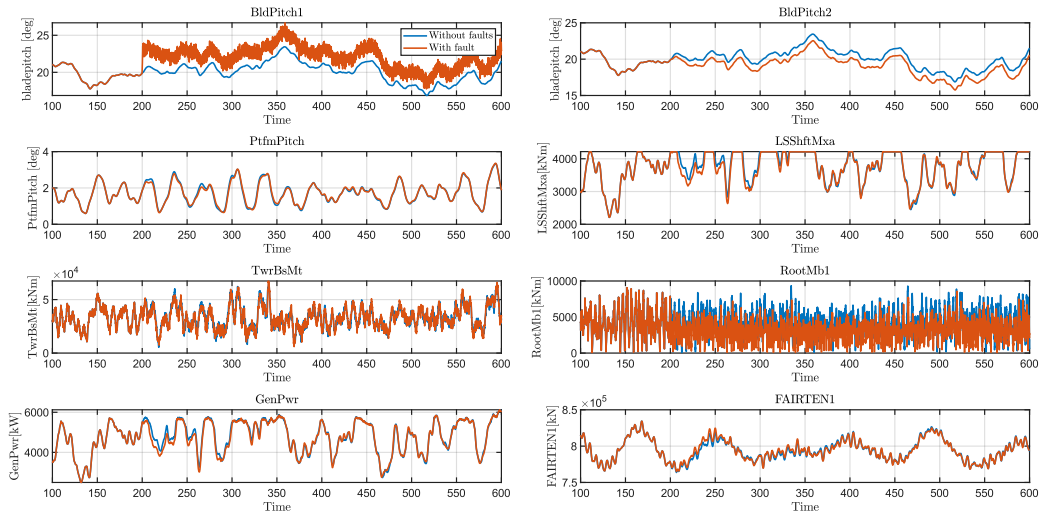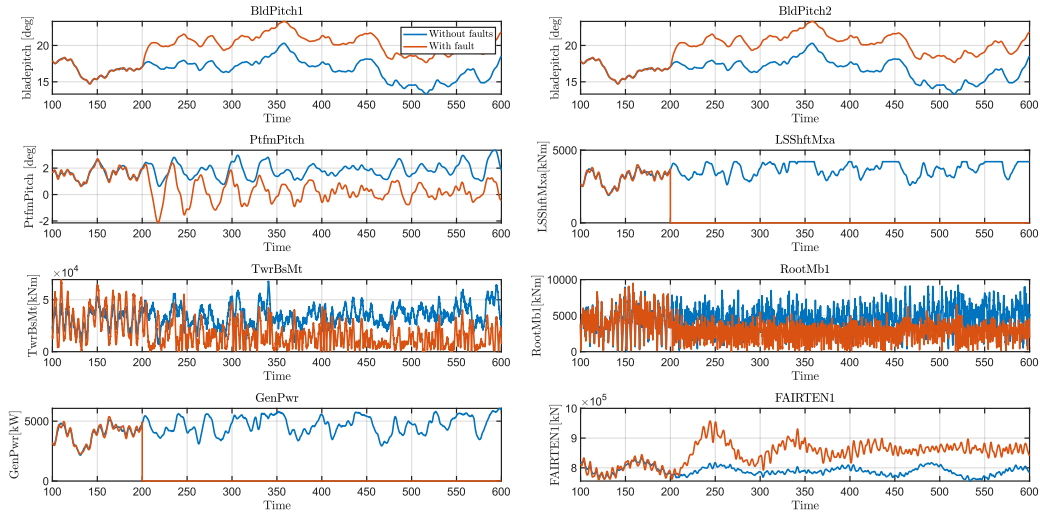Figure 5.47: Main results for the simulation with wind speed=20 m/s
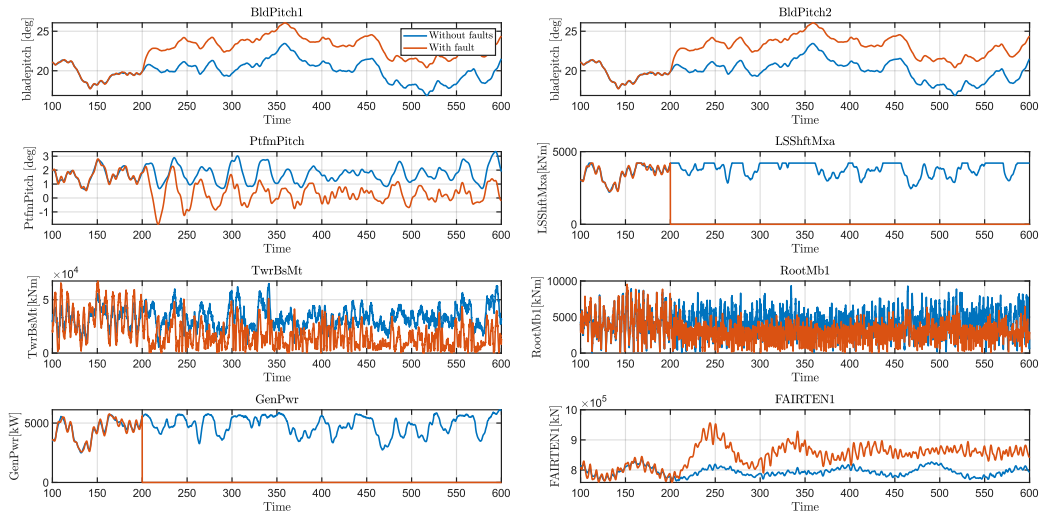


Figure 5.48: Main results for the simulation with wind speed=23 m/s

|  |  | Maximum | Minimum | Standard deviation |
|---|---|---|---|---|
| **BldPitch1** | *11 m/s* | 7.7337 14.3978 | 0.0000 0.0000 | 1.6292 4.6593 |
|  | *14 m/s* | 12.9862 17.1882 | 4.8893 6.6884 | 1.7875 2.3946 |
|  | *17 m/s* | 16.8134 20.2631 | 9.9687 11.4942 | 1.4196 1.9815 |
|  | *20 m/s* | 20.2966 23.3069 | 13.3151 14.7027 | 1.3803 1.9064 |
|  | *23 m/s* | 23.4441 26.0642 | 16.8727 17.7199 | 1.3017 1.8371 |

| | | | | |
|---|---|---|---|---|
| **BldPitch2** | 11 m/s | 7.7337 14.3978 | 0.0000 0.0000 | 1.6292 4.6593 |
| | 14 m/s | 12.9862 17.1882 | 4.8893 6.6884 | 1.7875 2.3946 |
| | 17 m/s | 16.8134 20.2631 | 9.9687 11.4942 | 1.4196 1.9815 |
| | 20 m/s | 20.2966 23.3069 | 13.3151 14.7027 | 1.3803 1.9064 |
| | 23 m/s | 23.4441 26.0642 | 16.8727 17.7199 | 1.3017 1.8371 |
| **PtfmPitch** | 11 m/s | 5.0388 4.7766 | 1.7618 -4.1496 | 0.6910 1.8105 |
| | 14 m/s | 3.6948 3.2953 | 0.7062 -2.8281 | 0.5999 1.2027 |
| | 17 m/s | 3.2635 2.6430 | 0.5519 -2.3472 | 0.5401 0.9762 |
| | 20 m/s | 3.3573 2.7059 | 0.6213 -2.1439 | 0.5390 0.9054 |
| | 23 m/s | 3.3284 2.7995 | 0.5979 -1.8878 | 0.5838 0.8495 |
| **LSShftMxa** | 11 m/s | 4213.7808 4212.2773 | 1601.9858 0.0000 | 566.1913 1286.3145 |
| | 14 m/s | 4211.6919 3215.9282 | 1697.2799 0.0000 | 436.0191 1071.0637 |
| | 17 m/s | 4212.3101 3453.8152 | 1605.2422 0.0000 | 498.9332 1093.3027 |
| | 20 m/s | 4216.2866 3997.7979 | 1890.2089 0.0000 | 506.8362 1267.2459 |
| | 23 m/s | 4218.2505 4214.8979 | 2211.1274 0.0000 | 476.6071 1431.9172 |
| **TwrBsFt** | 11 m/s | 1424.7499 1591.9864 | 415.9612 0.9475 | 178.5721 338.7937 |
| | 14 m/s | 1020.1573 1121.4485 | 127.3911 1.0965 | 156.4776 224.2046 |
| | 17 m/s | 907.9630 984.8566 | 44.1264 1.1327 | 143.1379 195.2427 |
| | 20 m/s | 921.3069 976.8155 | 67.4168 0.9104 | 140.5216 191.2916 |
| | 23 m/s | 872.8709 911.0835 | 77.4743 0.5857 | 142.8111 189.9894 |
| **TwrBsMt** | 11 m/s | 98554.5302 108162.1278 | 29466.9708 60.6728 | 12195.7415 23955.1785 |
| | 14 m/s | 72929.7047 76714.3066 | 11958.6677 42.6858 | 10758.3919 15695.1336 |
| | 17 m/s | 65230.9368 69526.2512 | 5919.1659 36.2620 | 9807.1620 13701.4748 |
| | 20 m/s | 67861.9311 69463.2251 | 6659.3466 107.1728 | 9656.2835 13663.9982 |
| | 23 m/s | 65154.5332 67550.7725 | 5383.4557 42.7418 | 9880.7819 13732.8950 |
| **RootFb1** | 11 m/s | 382.7877 352.3939 | 110.5929 0.2631 | 40.7329 68.3175 |
| | 14 m/s | 332.9482 318.1394 | 60.3974 0.2314 | 41.0980 53.0473 |
| | 17 m/s | 314.0328 285.0737 | 28.3751 0.8237 | 43.4226 50.5954 |
| | 20 m/s | 322.7677 321.3745 | 8.0055 1.0447 | 47.9820 51.0178 |
| | 23 m/s | 329.3387 312.8454 | 3.5635 1.0059 | 50.0130 52.8404 |

| | | | | |
|---|---|---|---|---|
| **RootMb1** | *11 m/s* | 13693.2582 12022.8982 | 3634.0756 13.9674 | 1470.4310 2653.2135 |
| | *14 m/s* | 10277.0662 10661.1893 | 1281.6773 6.1261 | 1451.1332 1634.4366 |
| | *17 m/s* | 9500.7451 9243.7831 | 133.0448 39.9910 | 1455.3694 1385.8231 |
| | *20 m/s* | 9469.9502 9469.8962 | 33.7835 51.4006 | 1614.2181 1371.5703 |
| | *23 m/s* | 9345.0019 9548.9121 | 33.2934 33.9433 | 1625.3458 1387.1014 |
| **GenPwr** | *11 m/s* | 5714.9907 4591.3193 | 1488.8264 0.0000 | 872.6553 1384.1114 |
| | *14 m/s* | 5752.6377 4220.2305 | 2006.4176 0.0000 | 641.5541 1363.2580 |
| | *17 m/s* | 5889.0615 4601.4116 | 1868.4121 0.0000 | 744.0751 1391.5160 |
| | *20 m/s* | 6067.3423 5377.2944 | 2162.1306 0.0000 | 794.5307 1611.8748 |
| | *23 m/s* | 6118.3887 5776.4058 | 2499.7327 0.0000 | 795.8896 1818.4646 |
| **FAIRTEN1** | *11 m/s* | 866677.0625 1030515.3750 | 650949.3125 646255.0625 | 36531.2117 75871.8190 |
| | *14 m/s* | 837488.2500 964404.7500 | 712211.6250 720889.1250 | 23139.6672 46542.6699 |
| | *17 m/s* | 832003.9375 958008.0625 | 749922.9375 754269.0625 | 15696.8977 38638.1953 |
| | *20 m/s* | 833859.2500 957714.6875 | 755488.3750 759118.4375 | 14984.7952 37885.1726 |
| | *23 m/s* | 834413.6250 956435.3125 | 763754.2500 758681.5625 | 14558.8480 37513.0350 |

Table 5.13: Comparison of results for "No fault" and "Disconnection from the grid" models at different wind speeds

## 5.4.12  NREL 5-MW - Shutdown of the wind turbine
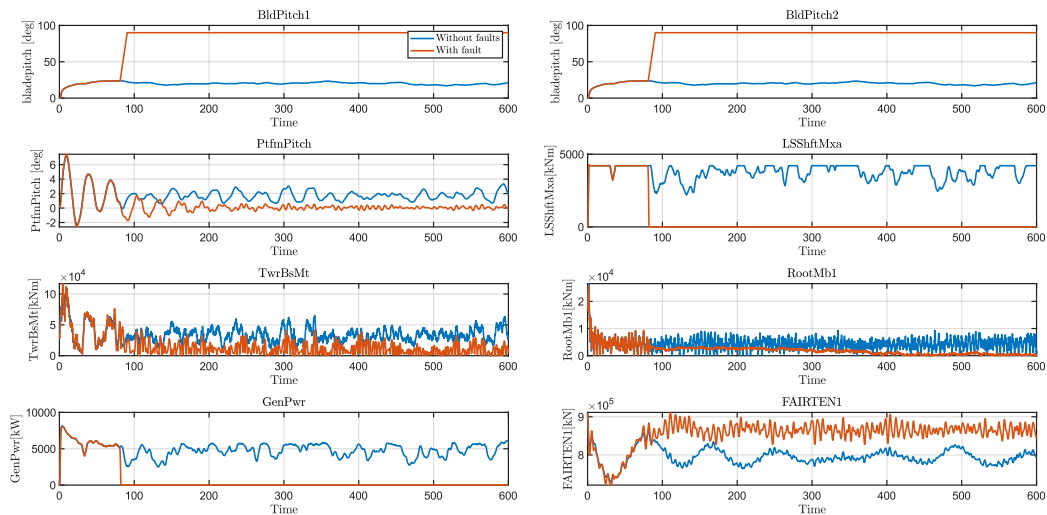


Figure 5.49: Main results for the simulation with wind speed=23 m/s

|  |  |  | **Maximum** | **Minimum** | **Standard deviation** |
|---|---|---|---|---|---|
| **BldPitch1** | *23 m/s* |  | 23.8331 90.1151 | 16.8727 22.7574 | 1.5421 16.0312 |
| **BldPitch2** | *23 m/s* |  | 23.8331 90.1151 | 16.8727 22.7574 | 1.5421 16.0312 |
| **PtfmPitch** | *23 m/s* |  | 3.8723 3.8078 | -0.3857 -1.7345 | 0.6842 0.6650 |
| **LSShftMxa** | *23 m/s* |  | 4218.2505 4210.2378 | 2211.1274 0.0000 | 498.4028 975.8849 |
| **TwrBsFt** | *23 m/s* |  | 872.8709 1090.0373 | 77.4743 1.0917 | 149.8684 160.9906 |
| **TwrBsMt** | *23 m/s* |  | 65154.5332 76535.0577 | 5383.4557 15.2331 | 10252.0743 11060.2042 |
| **RootFb1** | *23 m/s* |  | 348.0517 362.9699 | 3.5635 2.1776 | 51.4776 54.6468 |
| **RootMb1** | *23 m/s* |  | 9345.0019 9373.6623 | 33.2934 6.6297 | 1640.3475 1242.8283 |
| **GenPwr** | *23 m/s* |  | 6118.3887 6013.4097 | 2499.7327 0.0000 | 826.6266 1272.3662 |
| **FAIRTEN1** | *23 m/s* |  | 864778.8125 911473.4375 | 763754.2500 764216.5000 | 18072.7832 18010.0808 |

Table 5.14: Comparison of results for "No fault" and "Shutdown" model at 23m/s wind speed

## 5.4.13   NREL 5-MW - Extreme wind and waves conditions in shutdown state
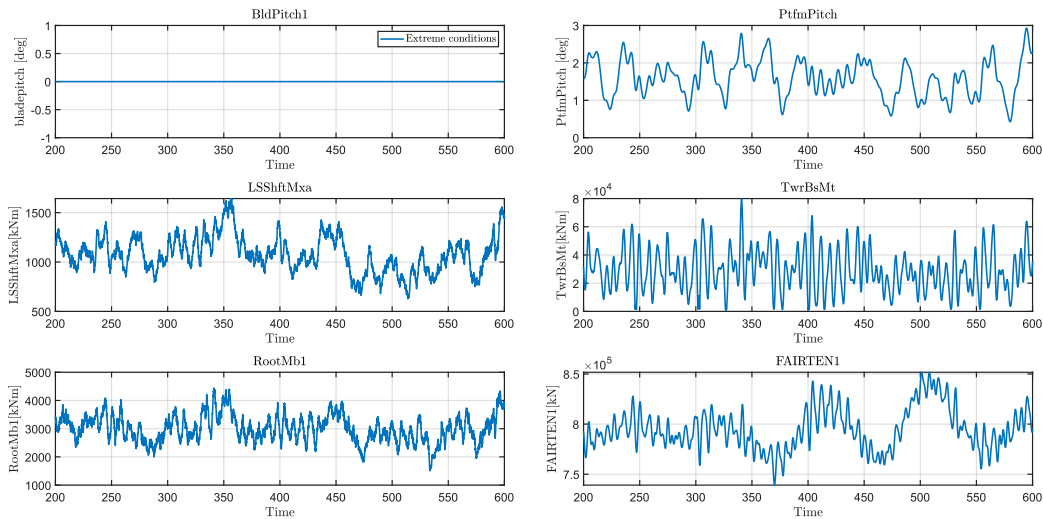


Figure 5.50: Main results for the simulation with extreme weather conditions

| | | Maximum | Minimum | Standard deviation |
|---|---|---|---|---|
| **BldPitch1** | *26.14 m/s* | 23.4441 0.0000 | 16.8727 0.0000 | 1.3017 0.0000 |
| **PtfmPitch** | *26.14 m/s* | 3.3284 2.9303 | 0.5979 0.4275 | 0.5838 0.4978 |
| **LSShftMxa** | *26.14 m/s* | 4218.2505 1642.3967 | 2211.1274 627.3432 | 476.6071 177.1466 |
| **TwrBsMt** | *26.14 m/s* | 65154.5332 79860.5899 | 5383.4557 868.6112 | 9880.7819 14830.1695 |
| **RootMb1** | *26.14 m/s* | 9345.0019 4444.3346 | 33.2934 1507.0628 | 1625.3458 471.7534 |
| **FAIRTEN1** | *26.14 m/s* | 834413.6250 851695.1900 | 763754.2500 739160.1200 | 14558.8480 19836.7368 |

Table 5.15: Comparison of results for "No fault" model at 23 m/s and "Extreme wind condition" case

## 5.4.14 NREL 5-MW - Extreme wind shear
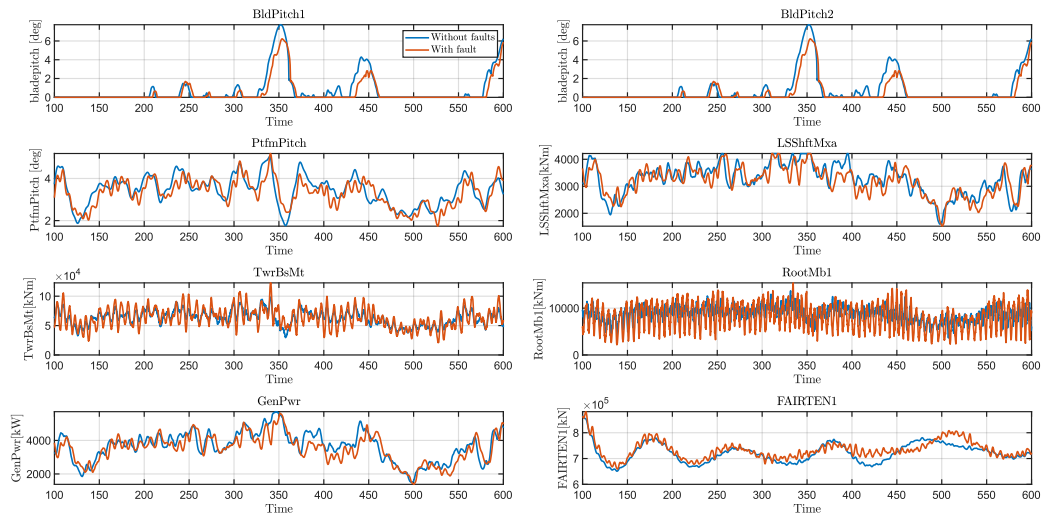


Figure 5.51: Main results for the simulation with wind speed=11 m/s
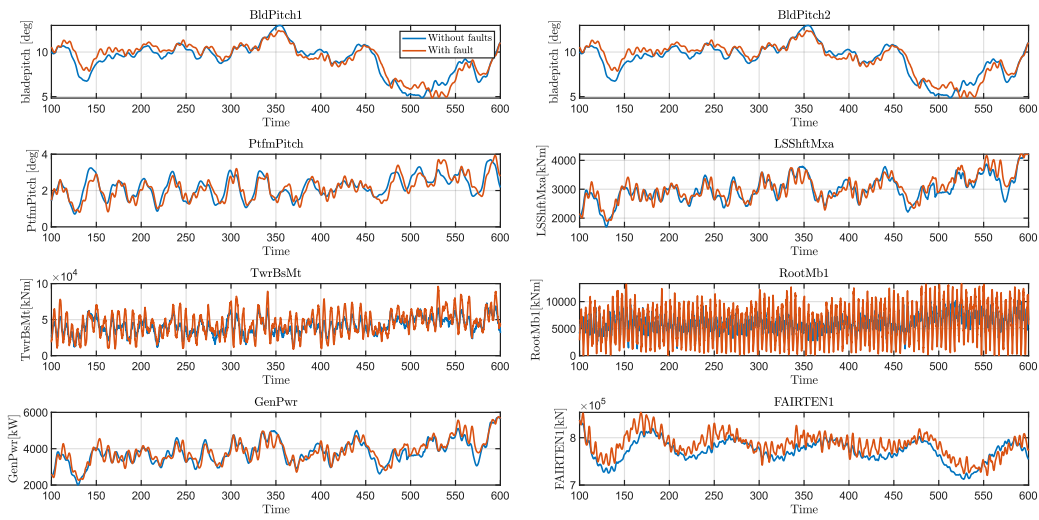
Figure 5.52: Main results for the simulation with wind speed=14 m/s
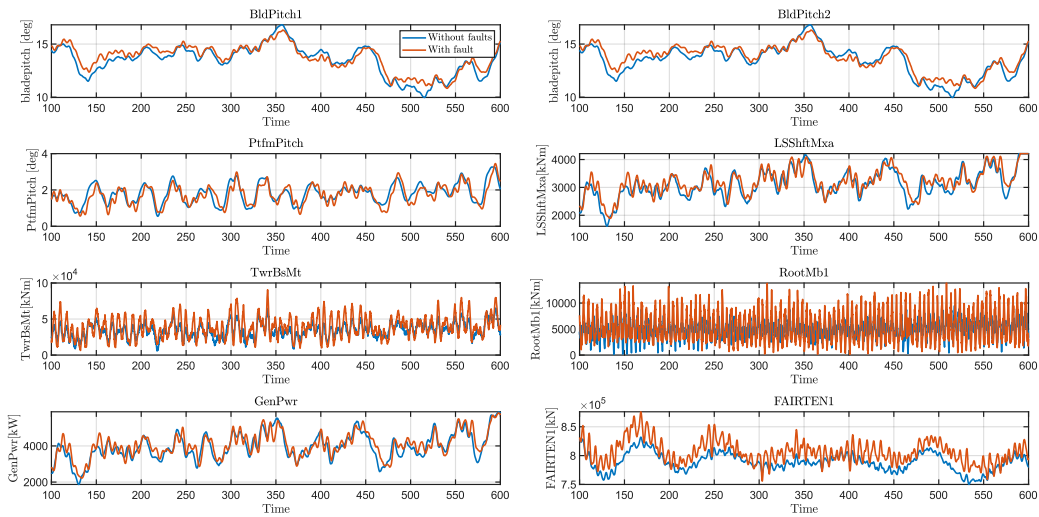


Figure 5.53: Main results for the simulation with wind speed=17 m/s
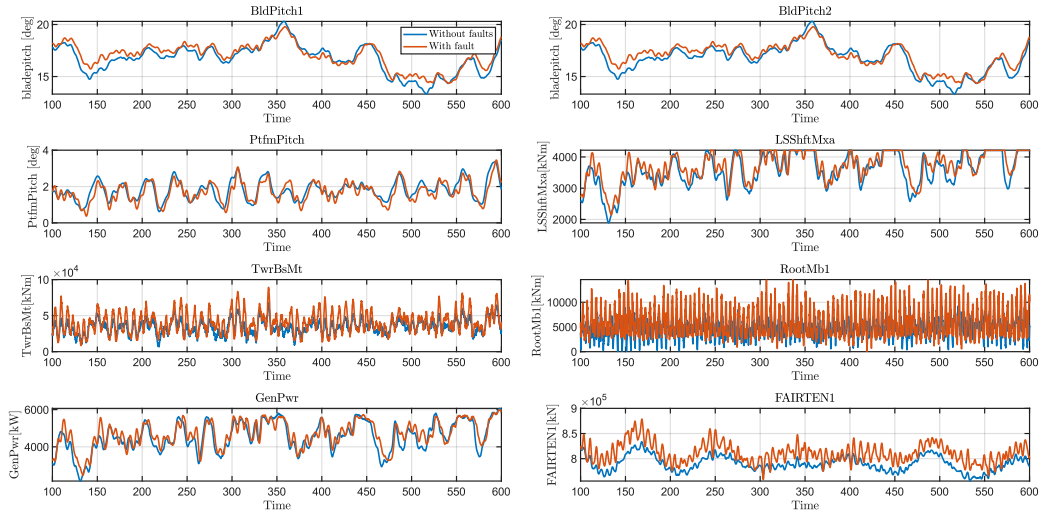
Figure 5.54: Main results for the simulation with wind speed=20 m/s
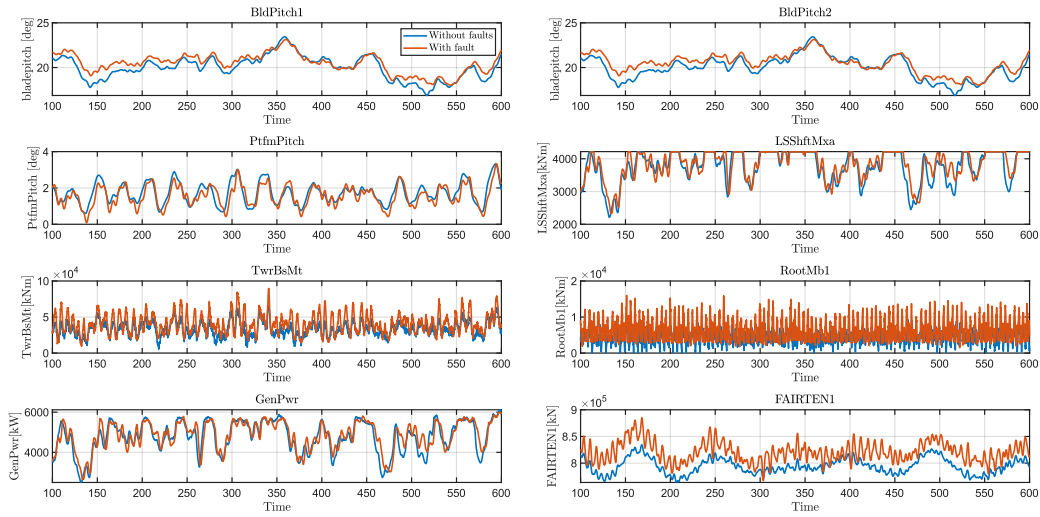


Figure 5.55: Main results for the simulation with wind speed=23 m/s

|  |  | Maximum | Minimum | Standard deviation |
|---|---|---|---|---|
| **BldPitch1** | *11 m/s* | 9.2256 8.9717 | 0.0000 0.0000 | 2.5229 2.3450 |
|  | *14 m/s* | 14.3606 14.3448 | 4.8893 4.8398 | 2.0682 2.0470 |
|  | *17 m/s* | 17.6678 18.1103 | 9.9687 10.8318 | 1.6978 1.5689 |
|  | *20 m/s* | 20.7524 21.3042 | 13.3151 14.3539 | 1.6460 1.5282 |
|  | *23 m/s* | 23.8331 24.4424 | 16.8727 18.0341 | 1.5421 1.3848 |

| | | | | |
|---|---|---|---|---|
| **BldPitch2** | *11 m/s* | 9.2256 8.9717 | 0.0000 0.0000 | 2.5229 2.3450 |
| | *14 m/s* | 14.3606 14.3448 | 4.8893 4.8398 | 2.0682 2.0470 |
| | *17 m/s* | 17.6678 18.1103 | 9.9687 10.8318 | 1.6978 1.5689 |
| | *20 m/s* | 20.7524 21.3042 | 13.3151 14.3539 | 1.6460 1.5282 |
| | *23 m/s* | 23.8331 24.4424 | 16.8727 18.0341 | 1.5421 1.3848 |
| **PtfmPitch** | *11 m/s* | 5.0388 5.1854 | 1.6078 1.7349 | 0.7467 0.6735 |
| | *14 m/s* | 3.6948 3.9349 | 0.7062 0.6548 | 0.6149 0.6434 |
| | *17 m/s* | 3.2635 3.4522 | 0.4495 0.0493 | 0.5686 0.5884 |
| | *20 m/s* | 3.3573 3.4580 | 0.2947 -0.5582 | 0.5934 0.6524 |
| | *23 m/s* | 3.8723 4.0197 | -0.3857 -1.2436 | 0.6842 0.7466 |
| **LSShftMxa** | *11 m/s* | 4213.7808 4213.1846 | 1601.9858 1523.5116 | 556.2625 530.9482 |
| | *14 m/s* | 4211.6919 4212.8384 | 1697.2799 1877.8866 | 453.0584 458.5381 |
| | *17 m/s* | 4212.3101 4212.1479 | 1605.2422 1870.9087 | 516.8414 478.7378 |
| | *20 m/s* | 4216.2866 4216.2012 | 1890.2089 2144.1982 | 528.7405 470.0671 |
| | *23 m/s* | 4218.2505 4217.0093 | 2211.1274 2256.3655 | 498.4028 453.1622 |
| **TwrBsFt** | *11 m/s* | 1424.7499 1712.2748 | 252.6196 105.8491 | 193.3247 260.8917 |
| | *14 m/s* | 1020.1573 1314.4989 | 113.7624 60.0506 | 162.0302 242.6310 |
| | *17 m/s* | 907.9630 1171.9590 | 44.1264 63.3744 | 146.8464 209.5677 |
| | *20 m/s* | 921.3069 1134.8276 | 67.4168 79.4508 | 145.2480 198.6958 |
| | *23 m/s* | 872.8709 1123.2391 | 77.4743 79.9638 | 149.8684 182.7724 |
| **TwrBsMt** | *11 m/s* | 98554.5302 122644.2305 | 18789.8490 13640.1263 | 13158.2512 17321.8904 |
| | *14 m/s* | 72929.7047 96106.2070 | 10193.9136 8995.6911 | 11102.3178 16499.7514 |
| | *17 m/s* | 65230.9368 90588.9828 | 5919.1659 6356.4820 | 10009.2883 14784.2665 |
| | *20 m/s* | 67861.9311 89256.4328 | 6659.3466 8441.4026 | 9896.0522 14332.0710 |
| | *23 m/s* | 65154.5332 89698.9173 | 5383.4557 9423.3542 | 10252.0743 13774.4993 |
| **RootFb1** | *11 m/s* | 382.7877 415.7586 | 110.5929 26.7604 | 42.6908 65.5259 |
| | *14 m/s* | 332.9482 359.3512 | 60.3974 0.9016 | 42.0780 78.6064 |
| | *17 m/s* | 314.0328 386.0436 | 28.3751 1.3933 | 44.6238 79.9483 |
| | *20 m/s* | 334.8356 421.8507 | 8.0055 1.0565 | 48.8017 86.4996 |
| | *23 m/s* | 348.0517 457.3241 | 3.5635 2.2170 | 51.4776 87.9132 |

|  |  |  |  |  |
| --- | --- | --- | --- | --- |
| **RootMb1** | *11 m/s* | 13693.2582 15393.8242 | 3250.3789 40.1702 | 1604.6003 2783.6162 |
|  | *14 m/s* | 10277.0662 13333.8857 | 581.7467 18.9050 | 1496.7184 3181.9643 |
|  | *17 m/s* | 9500.7451 13855.2283 | 133.0448 112.2452 | 1490.8834 2843.0727 |
|  | *20 m/s* | 9469.9502 14593.9680 | 33.7835 78.0093 | 1619.7085 2906.8207 |
|  | *23 m/s* | 9345.0019 16009.6627 | 33.2934 1472.9326 | 1640.3475 2841.6026 |
| **GenPwr** | *11 m/s* | 5893.3906 5836.0488 | 1488.8264 1380.1672 | 865.7339 855.7443 |
|  | *14 m/s* | 5752.6377 5768.1895 | 2006.4176 2210.5496 | 669.5198 666.1047 |
|  | *17 m/s* | 5889.0615 5833.6582 | 1868.4121 2158.6714 | 770.3626 717.5608 |
|  | *20 m/s* | 6067.3423 5992.4634 | 2162.1306 2445.2952 | 825.3953 746.3965 |
|  | *23 m/s* | 6118.3887 6084.5293 | 2499.7327 2482.7312 | 826.6266 753.5090 |
| **FAIRTEN1** | *11 m/s* | 887759.8125 896269.2500 | 632474.8125 638649.0000 | 47346.8738 44114.8390 |
|  | *14 m/s* | 906589.2500 927897.8125 | 712211.6250 720405.0625 | 33816.1680 33143.4134 |
|  | *17 m/s* | 884163.1875 911095.2500 | 749922.9375 755606.3750 | 22697.7387 24180.6959 |
|  | *20 m/s* | 869873.6250 897805.1250 | 755488.3750 758602.5625 | 19808.3300 22018.5117 |
|  | *23 m/s* | 864778.8125 896544.4375 | 763754.2500 766921.5625 | 18072.7832 20424.7954 |

Table 5.16: Comparison of results for "No fault" and "Extreme wind shear" models at different wind speeds

# Chapter 6

# Conclusions

In this study, we analyzed the performance of the IEA 15-MW Offshore Reference Wind Turbine under different fault conditions and extreme environmental scenarios. The results were examined using plots and tables that highlighted key performance metrics such as blade pitch angles, generator power output, tower base forces, platform motions, and blade root moments. Each scenario provided insights into how the turbine behaves under specific conditions, and this was compared with the behavior of the NREL 5 MW turbine to assess the scalability of the faults and environmental impacts.

## 6.1 Comparative Analysis of Fault Cases for the 15 MW Turbine

### 6.1.1 Blade Pitch Angle Fixed

In this fault scenario, where one blade's pitch angle remains fixed while the other two blades are pitched to feather by the control system, the results indicate severe imbalance in aerodynamic loads. As seen in the plots, this leads to significant fluctuations in generator power output. For example, at wind speeds of 23 m/s, there are visible spikes in platform pitch motion with standard deviations increasing from normal conditions by approximately 50%, reflecting increased instability (Table 5.3).

This imbalance also causes higher torque variations on the low-speed shaft, which increases the mechanical stress on the drivetrain. At 20 m/s and 23 m/s, the drivetrain's torque variations spiked by 15% compared to normal operational values. Tower base moments and root blade moments increase, signaling an important risk of fatigue failure.

### 6.1.2 Offset in Blade Pitch Angle

Introducing an offset in the blade pitch angle results in reduced generated power. The imbalance in rotor forces is reflected in higher shear forces at the tower base,

as well as higher bending moments in the blades (Tables 5.4). At 20 m/s, the tower base forces increase by about 10%, and the blade root moments experience significant peaks due to this imbalance. The turbine's performances are compromised, particularly at wind speeds above 17 m/s, where power generation efficiency decreases by 5

### 6.1.3 Precision Degradation

In this scenario, precision degradation in blade pitch control introduces slight fluctuations in aerodynamic loads, leading to variability in mechanical stresses. These changes are not as severe as other fault scenarios, but they still present long-term risks. For example, the results show a 3% increase in standard deviation for tower base moments at 23 m/s, indicating a potential source of fatigue over time (Table 5.5). The platform's stability remains almost intact, with minor fluctuations in pitch motion.

### 6.1.4 Disconnection from the Grid

The grid disconnection fault results in an immediate and significant drop in power generation, which is clearly visible in the power output plots at all wind speeds (Figures from 5.17 to 5.21. The turbine experiences rapid changes in torque and structural loads. The low-speed shaft torque oscillations are particularly relevant, with fluctuations of up to 30% in some wind conditions, indicating the importance of grid stability for minimizing mechanical stress on the turbine components (Table 5.6).

### 6.1.5 Extreme Wind and Wave Conditions in Shutdown State

Even in a shutdown state, extreme environmental conditions continue to exert huge mechanical loads on the turbine. The results put in evidence very high maximum values for blade root moments, where moments exceed 9,000 kNm (Table 5.8). Platform heave and pitch motions are also more pronounced, reflecting the difficulty in maintaining structural stability in such conditions. This scenario underscores the importance of designing turbines to withstand extreme offshore environments.

### 6.1.6 Extreme Wind Shear

The presence of extreme wind shear introduces substantial aerodynamic load asymmetries, particularly affecting the upper portions of the blades. The results show that blade root moments and tower base forces increase by approximately 20% compared to normal wind profiles (Table 5.9). The platform pitch and heave motions are unpredictable, making it difficult for the turbine to be stable under these conditions.

## 6.2 Comparative Analysis of IEA 15-MW and NREL 5-MW Turbines

In the comparison between the 15MW and 5MW turbines, it's possible to notice key differences in terms of mechanical loads, platform stability, and control system performance under the different fault scenarios.

**Mechanical Loads:** The 15MW turbine is subjected to higher structural loads due to its larger size and capacity. For example, the tower base moment for the 15MW turbine under extreme wind conditions reaches 300000 kNm, while the 5MW turbine peaks at approximately 65000 kN (Table 5.15). However, when normalized for turbine size, the 15MW turbine shows better load distribution, reflecting improved structural resilience. The maximum values for parameters such as blade root moment (RootMb1), tower base moment (TwrBsMt), and low-speed shaft torque (LSShftMxa) are consistently higher for the 15MW turbine compared to the 5MW. For example, in the blade pitch angle fixed scenario at 23 m/s wind speed, the blade root moment for the 15MW turbine exceeds 53,722 kNm, while the 5MW turbine sees a maximum moment of 9,345 kNm. The minimum values in both turbines reflect moments when the turbines are either in a fault state or experiencing reduced operational loads. In grid disconnection scenarios for example, the generator power drops to zero in both turbines. However, the residual mechanical loads in the 15MW turbine are still higher than those in the 5MW due to the larger inertia and forces acting on its structure.

**Platform Stability:** The 15MW turbine shows more pronounced platform motions under fault scenarios. For instance, in the precision degradation scenario, the standard deviation of platform pitch motions for the 15MW turbine is 20% higher than that of the 5MW turbine (Table 5.12). A confirm of this behaviour is in the extreme wind and wave conditions, where the 15MW turbine's platform pitch variability reaches 0.586 degrees, compared to the 5MW turbine's 0.497 degree.

**Control System Impact:** The control systems of both turbines are challenged by blade pitch faults, but the 15MW turbine reduced more significantly its efficiency. For example, in the blade pitch angle fixed scenario, the power output of the 15MW turbine has a standard deviation of GenPwr increased by approximately 8%, compared to a 5% increase for the 5MW turbine under similar conditions(Tables 5.3 and (5.10).

## 6.3 Identification of Worst-Case Scenarios

The identification of worst case scenarios is based on an overview of the key parameters, making a comparison between the values of maximum, minimum and standard deviation. Both turbines demonstrate similar trends in response to fault scenarios, but the 15MW turbine consistently shows higher values.

**Extreme Wind and Wave Conditions in Shutdown State:** for the 15MW turbine, the most significant worst-case scenario arises in extreme wind and wave

conditions with the turbine in a shutdown state. In this situation, even though the turbine is not generating power, the aerodynamic and hydrodynamic forces on the system are huge. As a key variable, it's possible to consider the maximum tower base moment that reaches an extraordinary value of 387,754 kNm, far exceeding any other fault scenario. Also blade root moment shows alarming peaks, exceeding 10,000 kNm. These extreme values are driven by the combination of turbulent wind profiles and wave actions. About the stability, the platform pitch shows a maximum pitch angle of 0.586 degrees, with significant variability as indicated by the standard deviation.

**Blade Pitch Angle Fixed:** the second major worst-case scenario for the 15MW turbine involves a blade pitch angle fixed fault; the low-speed shaft torque underlines significant fluctuations under this fault scenario. At wind speeds of 23 m/s, torque peaks 15% above nominal operational values, which indicates a huge risk to the drivetrain and gearbox, particularly over extended operational periods. The blade root moments become highly asymmetric and this imbalance leads to large oscillations in rotor thrust and a severe increase in tower base forces, as reflected by a 20% increase in the standard deviation of these loads compared to normal operating conditions, as can be seen in the table 5.3.

**Grid disconnection:** in the grid disconnection scenario, the turbine experiences a sharp power loss, but the aerodynamic forces remain at their peak due to high wind speeds. The grid disconnection leads to rapid and extreme torque oscillations in the drivetrain, with torque peaking at 30% above nominal levels shortly after the disconnection, as can be seen in the plot 5.21. In the 5MW system, in a similar way to 15MW, the loads are important although the peak is lower at around 65,154 kNm. The low-speed shaft torque sees large oscillations, with fluctuations of up to 25% in some wind conditions, leading to significant stress on the drivetrain. Although the loads are lower than in the 15MW turbine, they still represent a critical scenario for turbine durability.

**Extreme wind shear:** for the 5MW turbine, the extreme wind shear scenario presents one of the worst-case situations, as the uneven wind profile significantly disturbs the aerodynamic balance. The blade root forces increase by 20%, similar to the 15MW turbine, but the overall magnitude is lower, peaking at around 65,154 kNm. The platform also experiences significant pitch, reaching 0.497 degrees in some cases.

## 6.4   Overview

This thesis has investigated the complex behavior of floating offshore wind turbines under many fault conditions, utilizing advanced simulation techniques. By modeling two reference turbines the IEA 15 MW and NREL 5 MW turbines this research has demonstrated how different failure scenarios impact the overall dynamic response and energy generation of offshore wind systems.

Through extensive simulations using OpenFAST, combined with fault implementations in Simulink, the study captured the interactions between environmental forces

and turbine control systems. It was found that faults in key components, such as the blade pitch system and electrical disconnections, can lead to significant mechanical stresses and performance drops and that the results underscore the critical role of robust control strategies and fault detection mechanisms in ensuring the reliability and efficiency of floating wind turbines.

The comparative analysis between the two turbines highlighted the distinctions in fault resilience and response, studying different turbine sizes and configurations. Additionally, this work has quantified the potential energy loss due to faults, emphasizing the need for optimized turbine designs that account for real-world operational challenges.

## 6.5   Recommendations for Future Work

Although this thesis provides a comprehensive analysis of fault scenarios in floating offshore wind turbines using OpenFAST and Simulink, several areas remain open for further investigation. Below are recommendations for future work:

**Gearbox Failures:** Gearbox faults, which are one of the most frequent causes of downtime in wind turbines, were not modeled in this thesis. Future research should focus on simulating various gearbox faults, such as gear tooth cracking, bearing failures, or lubrication degradation. The complexity of simulating these faults accurately may require coupling Simulink with more advanced tools like finite element analysis (FEA) or multibody dynamics simulation (MBS) to address the mechanical nuances of gearbox components effectively.

**Drivetrain Faults:** This thesis focused primarily on electrical and blade pitch faults. The expansion of this study to include drivetrain faults, such as shaft misalignment or excessive vibrations, is fundamental. Drivetrain faults can significantly impact gearbox reliability, and their interactions with other components under varying wind and wave conditions could reveal insights that are critical for offshore turbine design. These studies would require more detailed mechanical and fatigue modeling beyond the use of Simulink.

**Electrical Failures:** Electrical systems failures are critical too, but this thesis did not address certain types of them. Future research should investigate electrical failures, such as short circuits in generator windings or voltage drops in the power grid, which can cause significant mechanical and operational stress on wind turbines, as seen in the literature review in chapter 2 [16]. These scenarios, which involve high transient loads and dynamic interactions between electrical and mechanical systems, were not feasible to model in Simulink. More specialized tools, maybe modeling electrical networks, would be required to accurately analyze these fault conditions.

**Long-Term Fatigue and Structural Analysis:** The current work focused on short-term, transient fault conditions, but future work should explore the long-term fatigue of structural components, especially the blades and drivetrain. Turbines experience constant mechanical loads, which over time lead to wear and material

degradation. Simulating long-term wear requires integrating advanced fatigue analysis tools with OpenFAST and Simulink for more accurate lifetime predictions.

**Advanced Environmental Interactions:** This thesis modeled extreme wind and wave conditions based on data from a specific site, but further case studies could explore additional environmental challenges for example underwater currents. These factors can introduce new fault cases that were not considered, requiring more sophisticated environmental modeling and simulations to assess their impacts.

**Comparative Studies on New Turbine Types:** Future work should explore a wider range of turbine designs, maybe including other floating platforms like Tension Leg Platforms (TLPs). Such comparative studies could help determine how different designs respond to similar fault conditions and environmental loads. These scenarios may also require more sophisticated modeling tools beyond Simulink.

# Bibliography

[1] Global wind report 2023, 2023.

[2] Wind EUROPE. Wind energy in europe: 2022 statistics and the outlook for 2023-2027, 2023.

[3] IEA. Offshore wind outlook 2019, 2019.

[4] Authors. Title of the report, Year. Technical report.

[5] National Renewable Energy Laboratory (NREL). Title of the document, 2010.

[6] Massimo Sirigu. MOST – Hydrodynamics and control system, 2022.

[7] Massimo Sirigu, Emilio Faraggiana, Alberto Ghigo, Ermando Petracca, G. Mattiazzo, and G. Bracco. *Development of a simplified blade root fatigue analysis for floating offshore wind turbines*, pages 935–941. 10 2022.

[8] Evwind. what is wind energy? `https://www.evwind.es/about-wind-energy/what-is-wind-energy`.

[9] GWEC. Gwec report floating offshore wind. a global opportunity, 2022.

[10] Jesús María Pinar Pérez, Fausto Pedro García Márquez, Andrew Tobias, and Mayorkinos Papaelias. Wind turbine reliability analysis. *Renewable and Sustainable Energy Reviews*, 23:463–472, 2013.

[11] Braam H Zaaijer M B Rademakers, L W.M.M. and G J.W. Van Bussel. Assessment and optimisation of operation and maintenance of offshore wind turbines, Jun 2003.

[12] Yerai Peña Sanchez, Markel Penalba, and Vincenzo Nava. *Faulty wind farm simulation: An estimation/control-oriented model*, pages 679–685. 10 2022.

[13] Yoon Hyeok Bae and Moo-Hyun Kim. Influence of failed blade-pitch-control system to fowt by aero-elastic-control-floater-mooring coupled dynamic analysis. *Ocean Systems Engineering*, 3, 12 2013.

[14] Erin E. Bachynski, Mahmoud Etemaddar, Marit Irene Kvittem, Chenyu Luan, and Torgeir Moan. Dynamic analysis of floating wind turbines during pitch actuator fault, grid loss, and shutdown. *Energy Procedia*, 35:210–222, 2013.

[15] Erin Bachynski-Polić, Mahmoud Etemaddar, Marit Irene Kvittem, Chenyu Luan, and Torgeir Moan. Dynamic analysis of floating wind turbines during

pitch actuator fault, grid loss, and shutdown. *Energy Procedia*, 35:210–222, 12 2013.

[16] Laurenz Roth, Julian Röder, Jens Brimmers, Dennis Bosse, Christian Brecher, and Georg Jacobs. Investigation on the impact of electrical faults on the loads and exposures of wind turbine gears. *Forschung im Ingenieurwesen*, 87:1–13, 03 2023.

[17] A. Morató, S. Sriramula, N. Krishnan, and J. Nichols. Ultimate loads and response analysis of a monopile supported offshore wind turbine using fully coupled simulation. *Renewable Energy*, 101:126–143, 2017.

[18] Autore o autori. Titolo del rapporto, anno. Rapporto tecnico.

[19] J Jonkman, S Butterfield, W Musial, and G Scott. Definition of a 5-mw reference wind turbine for offshore system development.

[20] Behzad Golparvar, Petros Papadopoulos, Ahmed Aziz Ezzat, and Ruo-Qian Wang. A surrogate-model-based approach for estimating the first and second-order moments of offshore wind power. *Applied Energy*, 299:117286, 2021.

[21] Gordon M. Stewart and Matthew A. Lackner. The impact of passive tuned mass dampers and wind–wave misalignment on offshore wind turbine loads. *Engineering Structures*, 73:54–61, 2014.

[22] Matthew A. Lackner and Mario A. Rotea. Passive structural control of offshore wind turbines. *Wind Energy*, 14(3):373–388.

[23] H. Namik and K. Stol. Individual blade pitch control of floating offshore wind turbines. *Wind Energy*, 13(1):74–85.

[24] Bonnie J Jonkman. Turbsim user's guide. Technical report, National Renewable Energy Lab.(NREL), Golden, CO (United States), 2006.

[25] International Electrotechnical Commission et al. Wind energy generation systems-part 1: Design requirements. *International Electrotechnical Commission: Geneva, Switzerland*, 2019.

[26] Aitor Saenz-Aguirre, Alain Ulazia, Gabriel Ibarra-Berastegui, and Jon Saenz. Extension and improvement of synchronous linear generator based point absorber operation in high wave excitation scenarios. *Ocean Engineering*, 239:109844, 2021.

[27] N. J. Abbas, D. S. Zalkind, L. Pao, and A. Wright. A reference open-source controller for fixed and floating offshore wind turbines. *Wind Energy Science*, 7(1):53–73, 2022.

[28] Christopher Jung and Dirk Schindler. The role of the power law exponent in wind energy assessment: A global analysis. *International Journal of Energy Research*, 45, 01 2021.

[29] M. Debnath, P. Doubrawa, M. Optis, P. Hawbecker, and N. Bodini. Extreme

wind shear events in us offshore wind energy areas and the role of induced stratification. *Wind Energy Science*, 6(4):1043–1059, 2021.